STUDY OF COLOUR CONFINEMENT MODEL FOR QCD

BY

VINODKUMAR P.C.

A THESIS SUBMITTED

TO

GUJARAT UNIVERSITY

FOR

THE DEGREE OF

DOCTOR OF PHILOSOPHY

PHYSICAL RESEARCH LABORATORY

AHMEDABAD

MARCH 1988

CERTIFICATE

I hereby declare that the work presented in this thesis is original and has not formed the basis of the award of any degree or diploma by any University or Institution.

Vinodkumar P.C.
Author

Certified by:

S.B. Khadkikar
(Professor-in-Charge)

Place : Ahmedabad

Date : March 7, 1988

Dedicated to

My Parents

ACKNOWLEDGEMENT

I am greatly indebted to Professor S.B. Khadkikar for his invaluable guidance, inspiration and encouragement throughout the course of this work. During this period, I learnt a great deal from him, through educative discussions. I am extremely grateful to him for going through the manuscript of the thesis and for his valuable suggestions.

I am grateful to Professor K.H. Bhatt for his sincere encouragement in the early phase of this work. I am also grateful to Professor V.B. Sheorey for the helpful discussions that I had with him during the last phase of this work. I extend my sincere thanks to Professor J.C. Parikh, Professor A.C. Das and Dr. V.K.B. Kota for their interest in this work.

I would like to take this opportunity to thank all the members of the theory group for providing a very congenial atmosphere for research.

I also extend my thanks to all my friends and colleagues for their ever helping attitude. It is a pleasure to thank Mr. Vijaykumar K.B. and Dr. Subramanian K.P. for the careful and critical reading of the manuscript. I am thankful to Mr. Krishnakumar V. for helping me in plotting some graphs.

I acknowledge with gratitude the co-operation extended to me by the PRL administrative staff. I extend my sincere thanks to the staff of the Library for their kind co-operation and help.

I thank Mr. T.P. Muraleedharan and Mr. V.T. Viswanathan for fast and careful typing of the manuscript. I thank Mr. S.C. Bhavsar for the drafting of the figures.

I am grateful to Professor S. Krishnaswami and Mr. Rangarajan for allowing me to use the printer.

I am very thankful to Mrs. Vasundhara Khadkikar for her motherly affection and love towards me.

I am extremely fortunate to have come across Shri Padmanabhan and his family members, Mrs. Veena Padman, Miss Priya Padman and Mr. Nitin Padman. During those agonizing moments of anxiety and despair their presence, love, encouragement and inspiration have always come to my rescue. I owe immensely to them for all that they have bestowed on me.

Finally I am greatly indebted to my parents for their constant encouragement and advice.

"Circumstantial evidence is the best evidence there is, Paul. You just have to interpret it properly"

- Erle Stanley Gardner

"We seek him here, We seek him there, Those Frenchies seek him everywhere. Is he in heaven? Is he in hell?
That demmed, elusive Pimpernel?

- Baroness Orczy

ABSTRACT

The existence of colour singlet bound state of gluons called the glueball is an unique prediction of quantum chromo dynamics. Their theoretical as well as the experimental study is very crucial to the validity of this theory. Confinement of colour is an empirical result of QCD. There are confinement models for quarks to predict various properties of hadrons. Similar confinement schemes are extended for the confinement of gluons for the study of glueballs. This study aims at formulating a unified confinement basis for both quarks and gluons. Two different schemes for the confinement of coloured gluons are studied. A probable link from the basic theory of QCD to these phenomenological descriptions is obtained heuristically. The gluons in this phenomenology are considered as quasi-Maxwellian fields. This reduction from the nonlinear theory to a linear theory is the basis of all phenomenological confinement models.

In the first case a colour current confinement model (CCM) is formulated. In this formalism the nonlinear current of the gluon field is approximated to a colour super current in analogy with Ginzberg-Landau's theory of super conductivity. A particular choice of this gluon super current led to a consistent confinement scheme for the gluons in a general frame of Lorentz gauge with a secondary

gauge condition named as oscillator gauge. The two transverse modes of the confined gluons are obtained in this gauge. The gluon fields are second quantized and their energies are calculated in terms of the model parameter.

An alternate confinement scheme for the gluons is the dielectric confinement model (DCM). An inhomogeneous non-local dielectric function is obtained from the CCM by treating the CCM current as a self-induced polarization current. As the dynamical dependence is neglected the CCM dielectric function reduces to that of a simple inhomogeneous dielectric medium. Similar function is also obtained from the analogy of the Dirac Spinor equations, in the case of a confinement potential with Lorentz scalar plus vector part, with the Maxwell´s equation for a dielectric medium written in spin notations. Then a confinement model of the coloured gluons in a harmonically varying asympotically free dielectric medium is studied. In the choice of the gauge, we met with the difficulty which is similar to the bag model boundary conditions. With a restricted confinement boundary the confined gluon modes are obtained in the usual Coulomb gauge. These fields are quantized and the energies of the gluons in this model are expressed in terms of a single model parameter.

The lowest gluon modes obtained in both the schemes are characterized by $\ell = 0$, $J^{PC} = 1^{--}$ (E=gluon) and $\ell = 1$, $J^{PC} = 1^{+-}$ (M-gluon). However, their energy expressions in the two schemes are quite different. Coupling these lowest gluon modes colour singlet di-gluon and tri-gluon low-lying glueball states are constructed and their energies are calculated. The lightest glueballs are expected to have mass ranging from 1-3 GeV and have spin parities 0^{++}, 0^{-+} and 2^{++}. Experimental status of such states as the glueball candidates is discussed. Using a di-gluon glueball candidate the model parameter in both the schemes are fixed and the energies of all other glueball states are predicted. The spurious motion of the centre of the multi-gluon state is exactly taken into account in both the cases and the glueball energy states are corrected for the zeropoint motion. The resulting values for the di-gluon and tri-gluon systems are compared with the experimental candidates and similar naive bag model results.

The success of the CCM scheme for the gluons provided a harmonious confinement basis for treating both quarks and gluons together. the essential requirement here is then to obtain the confined gluon propagator. A translationally invariant ansatz has been made to develop the theory further. We obtained closed analytical expression for the relevant propagator. It is different from the usual oscillator Green's function which is not translationally invariant. We generalize this derivation for m-dimensional case. This closed analytical expression for the propagator has wider applications in the development of the bound state perturbation theory involving quarks and gluons.

CONTENTS

LIST OF TABLES

FIGURE CAPTIONS

Figure 5.1 : Asymptotic Behaviour of the Confined Gluon Propagator

a) ($\lambda = 0$)

b) ($\lambda = 1$)

c) ($\lambda = 2$)

d) ($R \to 0$)

GENERAL INTRODUCTION

In recent years, the understanding of the most fundamental interactions among elementary particles has undergone substantial changes in its experimental as well as theoretical aspects. As it stands today, the leptons ($e, \mu, \tau, \nu_e, \nu_\mu, \nu_\tau$) and quarks (u,d,s,c,b,t) are the most fundamental constituents of matter. The hadrons, i.e. the baryons and mesons are composites[1-3] and they are made up of three quarks and quark-antiquark pairs respectively. The electromagnetic, weak and strong interactions can be understood by knowing the exact dynamics of these leptons and quarks. Leptons carry integral electric charges, i.e. 0 or + e, where as the quarks carry fractional electric charges, i.e. 1/3 or 2/3 e (see Table 1.1) [4]. Leptons undergo electromagnetic and weak interactions while quarks undergo strong interactions also. But unlike the leptons, quarks are not found free in nature. The experimental evidences are that they are permanently confined objects[5,6]. This leads to the confinement theory [7-9], which will be discussed in subsequent chapters.

The difficulty in the simple quark model for baryons [1,10] led to the introduction of a new degree of freedom for quarks. This is called the colour degree of freedom of the quarks [7,8]. Accordingly by the Pauli's principle, to construct a completely antisymmetric wavefunction for the baryons, each quark must exist in three colours. The theory describing the dynamics of this colour is called the Quantum Chromo Dynamics (QCD) [11,12].

Like the photon in Quantum Electrodynamics (QED) gluons are the gauge bosons in QCD [9]. But QCD is a non-abelian gauge theory [11,12] unlike QED which is abelian. The salient features of QCD are: (1) Colour-colour interactions are very weak at very high momentum transfers or at very short distances (asymptotic freedom) [13], and (2) these interactions grow strong at low momentum transfer or at very large distances (infra red slavery) [14]. The latter presumably is giving rise to confinement [15]. While the QCD (Yang-Mills) theory is shown to exhibit asymptotic freedom, the confinement is more of an empirical necessity, i.e., only colour singlet states are seen free. The gluons which are the quanta of the colour field carry colour charges and they interact among themselves. One of the evidences for QCD is then the existence of glueballs which are the colour singlet bound states of multigluons [16]. Thus the study of glueballs and their experimental confirmation is very crucial to the validity of quantum chromodynamics. Since these coloured gluons are many in number (SU3-colour octet) the coupled nonlinear equations obeyed by them are too complex to solve. Hence to understand the nature of glueball states, the strong interactions and the properties of hadrons from their microscopic structure, one has to go for phenomenological models incorporating confinement. This is the spirit in which various models like bag models [17-19], potential models [20-22], etc., for confinement are developed to study various aspects of hadrons and its properties. One of the very successful models is the relativistic confinement potential model for quarks using Lorentz scalar plus vector harmonic oscillator potential (RHM) [23], for the predictions of the diverse aspects of hadronic properties. Successes of this simple model (RHM) motivated us to look for a similar confinement model for the QCD colour fields (i.e., gluons) for the prediction of the glueball states and thus to formulate a unified harmonic confinement basis for both quarks and gluons.

The gauge theory of fundamental interactions of elementary particles is reviewed in the first chapter. QED is described to illustrate the abelian gauge theory and the QCD is described to illustrate the nonabelian gauge theory. The general properties of QCD and some of the phenomenological colour confinement model for QCD are discussed in chapter two.

New confinement models for the coloured gluons motivated from the RHM for quarks [23] are proposed in chapter three. A Colour Confinement Model (CCM) and a Dielectric Confinement Model (DCM) for the gluons satisfying the 'quasi-Maxwellian' type of field equations are developed.

We construct in the fourth chapter the colour singlet multi-gluon glueball states using the confined gluon modes in both CCM and DCM. We discuss, in this chapter, the experimental status of such exotic states and their identification as glueball candidates. We calculate the low-lying di-gluon and tri-gluon glueball energies by fitting some of the experimental candidates for glueballs. The spurious motion of the centre of a multi-gluon state is taken into account as in the case of RHM and the results are presented in this chapter.

Having developed a harmonic theory for the confinement of gluons for the study of glueballs, in chapter five, we calculate the confined gluon propagator corresponding to the CCM gluons for the future application of the unified confinement theory of quarks and gluons. We are able to obtain an analytical closed expression for the m-dimensional harmonic oscillator propagator in a translationally invariant ansatz.

In the last chapter the conclusions and future applications of this study are discussed.

CHAPTER I

A REVIEW OF GAUGE THEORY FOR FUNDAMENTAL INTERACTIONS

1.1. Introduction

In this chapter, a general description of fundamental interaction among the elementary particles is reviewed. The gauge theory of fundamental interaction is discussed in little detail. The Quantum Electro Dynamics (QED) and QCD are described as examples of abelian and non-abelian gauge theory respectively.

Classically, interaction at a distance is commonly described in terms of a potential or field due to one particle acting on another. In quantum field theory, it is viewed in terms of the exchange of specific quanta associated with the particular type of interaction[24,25]. For example, charged particles in QED interact through the exchange of virtual photons. Similarly, the coloured quarks interact through the exchange of virtual coloured photons called gluons. Thus QCD is the theory describing the dynamics of quarks and gluons. And now it is well established that QCD is the underlying theory for strong interactions[26,27]. The theory describing the weak interactions among quarks is then called the Quantum Flavour

Dynamics (QFD) [27].

1.2. Gauge Principle and Gauge Fields

A natural way to reveal the secrets of nature is the correct identification of various symmetries in nature. And the existence of a symmetry implies that some variable is unmeasureable and the corresponding conjugate variable is conserved. Each symmetry is followed by some invariance and that implies some conservation laws. For example, the translational invariance means that we cannot determine the absolute position in space and the total momentum is conserved. Generalizing this concept that physical measurements are relative, Weyl [29] proposed that absolute magnitude or norm of a physical vector is also not absolute but should depend on space time points. A new connection would then be necessary in order to relate the length of vectors at different positions. This idea became known as scale or gauge invariance. With the development of quantum mechanics the Weyl´s original gauge theory was given a new meaning by realising that the phase of a wave function could be a new local variable. Thus the gauge transformation was reinterpreted as a change in the phase of the wave function [30].

1.2.1. Global and Local Gauge Invariance:

The inspection of the Lagrangian for a charge particle shows that it is invariant under the phase transformation,

$$\psi(x) \longrightarrow \psi'(x) = e^{i\alpha}\psi(x)$$

where α is a constant. This phase invariance implies that the phase is unmeasureable, it has no physical meaning and can be chosen arbitrarily. If we choose this as a constant, ie fix for all space and time, then we call this as a global gauge invariance [31]. But if α could make space time dependent i.e. locally varying and then to construct a locally gauge invariant theory automatically brings in new fields which are called gauge fields [31]. The gauge fields can mediate both long range and short range interactions. They are massless (for long range) when the Lagrangian and the vacuum state are invariant under a given symmetry group [32]. Introduction of a mass term can only shorten the range of the interaction due to gauge field. However, such a term violates gauge invariance. If the Lagrangian is invariant, while the vacuum state is non invariant (i.e. spontaneous symmetry break down) the gauge fields acquire mass thus can mediate the short range interactions such as weak interaction [33-35]. And the theory remains renormalizable [36].

For a local gauge transformation the wave function of the matter field transforms as

$$\psi(x) \rightarrow \psi'(x) = e^{i\alpha(x)}\psi(x) \quad . \tag{1.2.1}$$

And the gauge principle insists the invariance of the matter Lagrangian, under this transformation. For example, for a Dirac particle

$$\mathcal{L} = i\bar{\Psi}\gamma_\mu\partial_\mu\Psi - m\bar{\Psi}\Psi \quad . \tag{1.2.2}$$

Thus under local phase transformation,

$$\mathcal{L} \rightarrow \mathcal{L}' = i\bar{\Psi}'\gamma_\mu\partial_\mu\Psi' - m\bar{\Psi}'\Psi' \tag{1.2.3}$$

$$= \mathcal{L} - \bar{\Psi}\gamma_\mu(\partial_\mu\alpha(x))\Psi \tag{1.2.4}$$

Thus here $\mathcal{L}' \neq \mathcal{L}$ i.e. the Lagrangian is no longer invariant under such local phase transformations. To restore this invariance a new field say A_μ is introduced to cancel this unwanted extra term. These newly introduced fields are called the gauge fields [35,37]. These gauge fields are added to the derivative terms to define a new derivative such that it transforms as

$$\mathcal{D}_\mu\Psi \rightarrow \mathcal{D}'_\mu\Psi' = e^{i\alpha(x)}\mathcal{D}_\mu\Psi \tag{1.2.5}$$

Thus defining

$$\mathcal{D}_\mu = \partial_\mu - iqA_\mu \tag{1.2.6}$$

and

$$\mathcal{D}'_\mu = \partial_\mu - iq A'_\mu$$

(1.2.7)

Where $A_\mu \to A'_\mu$ so as to cancel the extra term which breaks the invariance. Thus the new Lagrangian which is invariant under local phase transformation can be written as

$$\mathcal{L} = i\bar{\Psi}\gamma_\mu \mathcal{D}_\mu \Psi - m\bar{\Psi}\Psi$$

(1.2.8)

The invariance of this Lagrangian can be verified as

$$\mathcal{L}' = i\bar{\Psi}\gamma_\mu(\partial_\mu - iq A'_\mu)\Psi - \bar{\Psi}\gamma_\mu(\partial_\mu \alpha(x))\Psi - m\bar{\Psi}\Psi$$

(1.2.9)

Thus for the invariance of (1.2.8)

$$A_\mu \to A'_\mu = A_\mu + \frac{1}{q}\partial_\mu \alpha(x)$$

(1.2.10)

Substituting back in (1.2.9)

$$\mathcal{L}' = i\bar{\Psi}\gamma_\mu(\partial_\mu - iq A_\mu - i\partial_\mu \alpha(x))\Psi - \bar{\Psi}\gamma_\mu \partial_\mu \alpha(x)\Psi - m\bar{\Psi}\Psi \quad (1.2.11)$$

$$= i\bar{\Psi}\gamma_\mu \mathcal{D}_\mu \Psi - m\bar{\Psi}\Psi .$$

(1.2.12)

Hence the local invariant Lagrangian is obtained by replacing the ordinary derivative by another derivative called the covariant derivative. The new gauge field A_μ is interacting with Dirac field exactly the same way as the photon field interacting with matter i.e. the additional term in the new Lagrangian in this case is nothing but the interaction of the matter field with an external 'electromagnetic' field of the form $J_\mu A^\mu$ where J_μ is the matter current. Thus the mere requirement of local phase invariance has generated an interaction term between the matter field and the gauge field. This is the essence of the gauge principle for generating the dynamical theories [35,37].

1.2.2. Gauge Group:

The family of phase transformations $U(\alpha) = e^{i\alpha}$ where the single parameter α depends on space and time form a unitary abelian group U(1). Abelian just records the property that the group multiplication is commutative,

$$\text{i.e.} \qquad U(\alpha_1)\,U(\alpha_2) = U(\alpha_2)\,U(\alpha_1) . \tag{1.2.13}$$

But in general the family of such transformation exists which transforms the field such that

$$\delta \psi_i(x) = T_{ij}^{k}\, \alpha_k(x)\, \psi_j(x) \tag{1.2.14}$$

The group of such local transformations is called the local or gauge group [35]. Depending upon the dimension of such groups say U(N) the number of the gauge fields need to introduce are (N^2). As the matter fields transforms as (1.2.14) the gauge fields also transforms as [30]

$$\delta A_{\mu}^{k} = f^{lmk} A_{\mu}^{k} \alpha^{l}(x) + \partial_{\mu} \alpha^{k}(x) \tag{1.2.15}$$

And the general covariant derivative D_{μ} becomes

$$\mathcal{D}_{\mu} \psi_i = \partial_{\mu} \psi_i - q T_{ij}^{k} \psi_j A_{\mu}^{k} . \tag{1.2.16}$$

For the dynamics of the gauge field one has to add a separate term to the matter Lagrangian involving its derivatives. And each term in the Lagrangian must also be gauge invariant. Such terms are expressed in terms of the covariant derivative D_{μ} .

Let us define a hermetian quantity

$$F_{\mu\nu} = -i \left[\mathcal{D}_{\mu} , \mathcal{D}_{\nu} \right] \tag{1.2.17}$$

$$= \partial_{\mu} A_{\nu} - \partial_{\nu} A_{\mu} + iq \left[A_{\mu} , A_{\nu} \right] . \tag{1.2.18}$$

In a general gauge group U(N)

$$F_{\mu\nu} = F_{\mu\nu}^{l} T^{l} \quad (1.2.19)$$

where

$$F_{\mu\nu}^{l} = \partial_{\mu} A_{\nu}^{l} - \partial_{\nu} A_{\mu}^{l} + iq A_{\mu}^{m} A_{\nu}^{n} [T^{m}, T^{n}] \quad (1.2.20)$$

and T^{l} is the corresponding transformation matrix. Now the simplest gauge invariant term which is bilinear in its field with a minimum coupling is given by

$$\mathcal{L}_{g} = -\frac{1}{4} \, Tr. \, F_{\mu\nu} F^{\mu\nu} \quad (1.2.21)$$

Thus the full gauge invariant Lagrangian now becomes,

$$\mathcal{L} = i \bar{\Psi} \gamma_{\mu} \partial_{\mu} \Psi - m \bar{\Psi} \Psi + \mathcal{L}_{g} \, . \quad (1.2.22)$$

Thus the gauge theory provides a complete knowledge about the dynamics of matter, gauge field and its interactions [35].

1.2.3. Geometrical Description of Gauge Theory:

The geometrical picture provides a common area for discussing electromagnetic, the strong and weak nuclear forces, and gravity. It depends only on very general properties of gauge principle. Any particle or system which carries an internal quantum number like charge, isospin, colour etc. is considered to have a direction in its internal symmetry space. In this picture a particle is identified with its space time co-ordinate and the orientation in its internal space. Thus as the particle moves through space time, it traces out a path in its internal space above the space time trajectory [30]. In order to compare this internal space directions at different space time points we need, to define a connection. This connection must be capable of relating all possible directions and orientations in the internal space to each other. The set of all such rotations form a symmetry group, and the group transformations lead to a connection which will be identified with a gauge potential field.

A general form of a local symmetry transformation from an arbitrary group can then be written as [30]

$$U\Psi = \exp\left[-iq\sum_k \theta^k(x) T^k\right]\Psi \tag{1.2.23}$$

Here q is a general coupling constant for the gauge group. For example (q = e) the electric charge for the electromagnetic U(1) gauge group, T^k's are the generators of the internal symmetry group and satisfy the commutation relations

$$[T^i, T^j] = i C^{ijk} T^k . \tag{1.2.24}$$

C^{ijk} are called the structure constants pertaining to the Lie group defined by the commutation relations. Let a particle's wavefunction be split into external and internal parts corresponding to the space time co-ordinate and the internal space co-ordinate as:

$$\psi(x) = \sum_{\alpha} \psi_{\alpha}(x) u_{\alpha} \tag{1.2.25}$$

Here u_α form a set of basis vectors in the internal space, $\psi_\alpha(x)$ is a component of $\psi(x)$ in the basis of u_α. And they transform like

$$\psi_{\beta} = U_{\beta\alpha} \psi_{\alpha} \tag{1.2.26}$$

When this particle moves from x to x + dx through an external potential field, $\psi(x)$ changes by

$$d\psi = \psi(x+dx) - \psi(x)$$

$$= \sum_{\alpha} (\partial_\mu \psi_\alpha) dx^\mu u_\alpha + \psi_\alpha du_\alpha \tag{1.2.27}$$

The du_α can be calculated from an infinitesimal internal rotation associated with an external displacement dx. Thus from eqn (1.2.23)

$$U(dx) = exp\left[-iq \sum_{k} d\theta^k T^k\right] \tag{1.2.28}$$

where $d\theta^k = \partial_\mu \theta^k dx^\mu$ which rotates the internal basis by an infinitesimal amount du_α.

$$U(dx) u_\alpha = u_\alpha + du_\alpha \tag{1.2.29}$$

$$= \left[\delta_{\alpha\beta} - iq \sum_{k} \partial_\mu \theta^k dx^\mu T^k_{\alpha\beta}\right] u_\beta \tag{1.2.30}$$

Thus

$$du_\alpha = iq\sum_k \partial_\mu \theta^k T^k_{\alpha\beta} u_\beta \, dx^\mu . \tag{1.2.31}$$

Now defining a new connection

$$(A_\mu)_{\alpha\beta} = \sum_k \partial_\mu \theta^k T^k_{\alpha\beta} . \tag{1.2.32}$$

Such that eqn. (1.2.27) becomes

$$d\Psi = \sum_{\alpha,\beta} \left[\partial_\mu \Psi_\alpha \delta_{\alpha\beta} - iq(A_\mu)_{\alpha\beta}\Psi_\alpha\right] dx^\mu u_\beta . \tag{1.2.33}$$

Thus defining

$$\mathcal{D}_\mu \Psi_\alpha = \sum_\beta \left[\delta_{\alpha\beta}\partial_\mu - iq(A_\mu)_{\alpha\beta}\right]\Psi_\beta . \tag{1.2.34}$$

This new derivative is called the gauge covariant derivative [30] which describes the changes in both external and internal parts of $\Psi(x)$. For electromagnetic U(1) gauge group the internal space is one dimensional so that eqn. (1.2.34) reduces to

$$\mathcal{D}_\mu \Psi = (\partial_\mu - iqA_\mu)\Psi \tag{1.2.35}$$

and A_μ transforms as

$$A'_\mu = UA_\mu U^{-1} - \frac{i}{q}(\partial_\mu U)U^{-1} . \tag{1.2.36}$$

The field tensor $F_{\mu\nu}$ also can be derived geometrically using Stoke's theorem. For example in classical electrodynamics the line integral over the potential A; $\oint(A.dx)$ can be interpreted geometrically as the net change in the internal directions of a test particle which has been moved around a closed path. This expression therefore is a phase change of the particle's wave function. Consider a test particle moving with a successive displacements dx and dy around a closed path. And the net change in its internal direction in a two different path can be calculated [30].

The gauge transformation for the displacement $x \rightarrow x + dx$ along path (1) can be written as

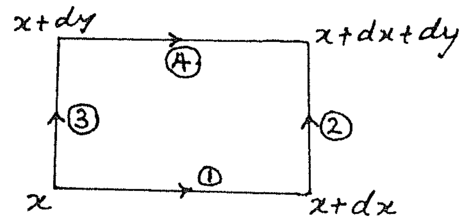

$$U_x(dx) = 1 - iqA_\mu(x)\,dx^\mu \tag{1.2.37}$$

Then along path (2) i.e. $x + dx \rightarrow x + dx + dy$

$$U_{x+dx}(dy) = 1 - iq\,A_\mu(x+dx)\,dy^\nu . \tag{1.2.38}$$

Using the Taylor expansion and keeping only lower order terms in dx and dy. One gets

$$\begin{aligned} U_{x+dx}(dy)\,U_x(dx) = {} & 1 - iqA_\mu(x)\,dx^\mu - iqA_\nu(x)\,dy^\nu \\ & - q^2 A_\nu(x)\,A_\mu(x)\,dy^\nu dx^\mu \\ & - iq\,\partial_\mu A_\nu(x)\,dy^\nu dx^\mu . \end{aligned} \tag{1.2.39}$$

Similarly for the path (3) and (4),

$$U_{x+dy}(dx)\,U_x(dy) = 1 - iqA_\nu(x)dy^\nu - iq\,A_\mu(x)dx^\mu$$

$$- q^2 A_\mu(x) A_\nu(x)\, dx^\mu dy^\nu$$
$$- iq\, \partial_\nu A_\mu(x)\, dx^\mu dy^\nu . \qquad (1.2.40)$$

Thus the net change in its internal orientation;

$$U(dy)\,U(dx) - U(dx)\,U(dy)$$
$$= -iq \left\{ \partial_\mu A_\nu - \partial_\nu A_\mu + iq [A_\mu, A_\nu] \right\} dx^\mu dy^\nu$$

(1.2.41)

Where A_μ and A_ν (x) do not commute because they are different combinations of the internal group generators T^k. Thus the derivatives $\partial_\mu A_\nu$ and $\partial_\nu A_\mu$ are also not equal in general. Thus the gauge transformation for the two different paths does not produce the same phase. Now comparing with the Stokes theorem, dx dy is the surface area enclosed by the path, then one identifies the non abelian version of the field tensor defined as [30,31]

$$F_{\mu\nu} = \partial_\mu A_\nu - \partial_\nu A_\mu + iq [A_\mu, A_\nu] . \qquad (1.2.42)$$

1.3. Abelian Gauge Fields

Here the quantum electro dynamics is discussed to illustrate the abelian gauge theory. In the case of abelian fields, the gauge group generators commute each other. Consequently, the last term in eqn. (1.2.42) vanishes. Thus for an abelian case the field tensor is simply,

$$F_{\mu\nu} = \partial_\mu A_\nu - \partial_\nu A_\mu \qquad (1.3.1)$$

The components of this gauge field tensor can be identified as the usual electric and magnetic fields in the Maxwell's electromagnetic theory. The time components are the electric fields and the space components are the magnetic fields [38]. Then the QED Lagrangian density is now written as

$$\mathcal{L}_{QED} = i\bar{\Psi}\gamma_\mu(\partial_\mu - ieA_\mu)\Psi - m\bar{\Psi}\Psi - \frac{1}{4}F_{\mu\nu}F^{\mu\nu} \tag{1.3.2}$$

where the electric charge e here is the gauge coupling constant. By the variational principle the equations of motion for the photon field A_μ and the charge field Ψ are obtained as,

$$\partial_\mu F_{\mu\nu} = -eJ_\nu = -e\bar{\Psi}\gamma_\nu\Psi \tag{1.3.3}$$

and

$$\gamma_\mu(\partial_\mu - ieA_\mu)\Psi + m\Psi = 0 . \tag{1.3.4}$$

The canonical momentum conjugate to the potential A_μ is given by

$$\Pi_\mu = \frac{\partial\mathcal{L}}{\partial(\partial_0 A_\mu)} = F_{0\mu} . \tag{1.3.5}$$

Since $F_{\mu\nu}$ is anti-symmetric,

$$\Pi_0 = 0 . \tag{1.3.6}$$

This constraint on Π_0 require another constraint on its conjugate variable A_0 such that the fundamental commutation relations between them at equal times do not have any problem. The constraint on π_0 is called the primary constraint, and then A_0 becomes a dependent variable. Considering now only the pure gauge fields, the corresponding Hamiltonian density is given by

$$\mathcal{H} = \pi^{\mu} \partial_0 A_{\mu} - \mathcal{L} \tag{1.3.7}$$

and

$$H = \int d^3x \left[\frac{1}{4} F_{ij} F^{ij} - \frac{1}{2} \pi_i \pi^i + A_0 \partial_i \pi^i \right] \tag{1.3.8}$$

The fact that $\pi_0 = 0$ means that the change of variable from velocity $\partial_0 A_{\mu}$ to momentum π_{μ} is singular. And the definition of H is not unique [39]. Consider now the change in π_0 i.e. from the Hamiltonian

$$\dot{\pi}_0 = -\partial_i \pi^i \tag{1.3.9}$$

But π_0 is zero for all times by the canonical procedure, hence we obtain another constraint,

$$\partial_i \pi^i = 0 \tag{1.3.10}$$

This is called the secondary constraint [40]. Now there are more constraints on momenta. And it looks like one is mapping four velocities into two independent π's. To consider this arbitrariness an extra term is added to H.

Thus the new Hamiltonian becomes

$$H_{New} = \int d^3x \left[\frac{1}{4} F_{ij} F^{ij} - \frac{1}{2} \pi^i \pi_i + G \partial_i \pi^i \right] \tag{1.3.11}$$

where A_0 term in (1.3.8) is also absorbed in G. The time variation of any physical quantity now contains this arbitrary element due to the $\partial_i \pi^i$ term. But a true physical quantity should not be arbitrary in its time variation. Thus the physical quantity must not depend on the variable conjugate to $\partial_i \pi^i$. In other words a physical quantity must be defined only on some surface in the (A_i , π_i) plane; which is characterized by a condition, say,

$$g(A_i, \pi_i) = 0 \tag{1.3.12}$$

provided the change of variable between g and the variable conjugate to $\partial_i \pi^i$ is non singular [39], i.e.,

$$\det \left| [g, \partial_i \pi^i] \right| \neq 0 \tag{1.3.13}$$

i.e., Jacobian for the transformation is non zero. Thus $\partial_i \pi^i$ generates a gauge transformation and g must be able to fix the gauge. There are various choices for g. Since the theory is gauge invariant, any choice of the gauge should lead to the same physical results.

a) Coulomb gauge:

It is defined by taking

$$g = \partial_i A^i \tag{1.3.14}$$

and this satisfies the criterion to be a good gauge (eqn. 1.3.13)), and $\partial_i \pi^i = 0$ is the codition whose conjugate is given by equation (1.3.14). Thus these conditions give the transversality conditions on $\underset{\sim}{A}$ ′s and $\underset{\sim}{\pi}$ ′s such that

$$\partial_i \pi^{iT} = \partial_i A^{iT} = 0 \tag{1.3.15}$$

where

$$A_i = A_i^L + A_i^T \tag{1.3.16}$$

and

$$\pi_i = \pi_i^L + \pi_i^T \tag{1.3.17}$$

Then the coulomb gauge reads

$$A_i^L = 0 \tag{1.3.18}$$

and the constraint (1.3.10) leads to

$$\pi_i^L = 0 \quad . \tag{1.3.19}$$

Thus in this gauge the Hamiltonian is a function of the independent variables A^T and π^T alone:

$$H = \int d^3x \left[\tfrac{1}{4} \epsilon_{ijk} \partial_j A_k^T \epsilon_{ijk} \partial_j A_k^T + \tfrac{1}{2} \pi_i^T \pi^{iT} \right]. \tag{1.3.20}$$

Thus the quantization procedure in the coulomb gauge can be carried out directly using the canonical formalism.

b) Arnowitt-Fickler gauge:

The other choice of the gauge is

$$g = A_3 = 0 .$$
(1.3.21)

This is called the Arnowitt-Fickler gauge [39]. Here also the determinant condition for the Jacobian is satisfied. This choice gives π_3 in terms of π_1 and π_2 . Thus from (1.3.10)

$$\pi_3(x,y,z,t) = -\int_{-\infty}^{z} dz'\left(\partial_1\pi^1 + \partial_2\pi^2\right)$$
(1.3.22)

where the system is now described in terms of the canonical variables A_1, A_2, π_1 and π_2. The Hamiltonian becomes,

$$H = \frac{1}{2}\int d^3x\left[B_3^2 + B_1^2 + B_2^2 + \pi_1^2 + \pi_2^2 + \pi_3^2(\pi_1,\pi_2)\right]$$
(1.3.23)

where

$$\begin{aligned} B_1 &= -\partial_3 A_2 \\ B_2 &= \partial_3 A_1 \\ B_3 &= \partial_1 A_2 - \partial_2 A_1 . \end{aligned}$$
(1.3.24)

It is now easy to do the quantization procedure.

1.4. Non Abelian Gauge Fields

In 1954 C.N. Yang and R. Mills constructed a field theory for the strong interactions [41] just like the electromagnetic theory, which is exactly gauge invariant. They postulated the local gauge group as SU(2)-isotopic spin group. A new isotopic spin potential was therefore postulated by them in analogy with electromagnetic potential. However the greater complexity of the SU(2) compared to U(1) makes the Yang Mill's potential quite different from that of the electromagnetic. The most general form of the Yang-Mill's potential is a linear combination of the generators of the SU(2) group similar to the angular momentum operators. Thus

$$A_\mu = \sum_i A_\mu^i L_i \qquad (1.4.1)$$

This explicitly displays the dual act of Yang-Mills potential as both the field in space time and an operator in the isotopic spin. The potential has three charge components corresponding to the three independent 'angular momentum' components. In this description a neutron is transformed into a proton by absorbing a unit of isospin from the Yang Mill's gauge field A_μ. This shows the Yang Mill's gauge field A_μ must itself carry an 'electric charge' unlike the electromagnetic potential. However, the gauge invariance demands them to be massless. Thus the short range nuclear force could not be explained by this. But Yang Mills theory established a foundation for the modern gauge theory and provides a new insight into the newly discovered internal quantum numbers to determine the fundamental form of the interactions. As a result of the subsequent developments in particle physics [42] especially the introduction of quarks [1,8] and its colour degrees of freedom, the Yang Mill's theory was revived to describe the SU(3) colour dynamics [26]. In this SU(3) local gauge symmetry the gauge potential A_μ carries eight charges corresponding to the three colours for quarks and this field is represented as

$$A_\mu = A_\mu^l T^l \tag{1.4.2}$$

and then the field tensor derived earlier becomes,

$$F_{\mu\nu} = F_{\mu\nu}^l T^l$$

where T^l are the generators of SU(3) group and are related to the Gell Mann λ-matrices as [43]

$$T^l = \frac{1}{2}\lambda^l \tag{1.4.3}$$

and they are given as

$$\lambda_1 = \begin{pmatrix} 0 & 1 & 0 \\ 1 & 0 & 0 \\ 0 & 0 & 0 \end{pmatrix}, \quad \lambda_2 = \begin{pmatrix} 0 & -i & 0 \\ i & 0 & 0 \\ 0 & 0 & 0 \end{pmatrix}$$

$$\lambda_3 = \begin{pmatrix} 1 & 0 & 0 \\ 0 & -1 & 0 \\ 0 & 0 & 0 \end{pmatrix}; \quad \lambda_4 = \begin{pmatrix} 0 & 0 & 1 \\ 0 & 0 & 0 \\ 1 & 0 & 0 \end{pmatrix}$$

$$\lambda_5 = \begin{pmatrix} 0 & 0 & -i \\ 0 & 0 & 0 \\ i & 0 & 0 \end{pmatrix}; \quad \lambda_6 = \begin{pmatrix} 0 & 0 & 0 \\ 0 & 0 & 1 \\ 0 & 1 & 0 \end{pmatrix}$$

$$\lambda_7 = \begin{pmatrix} 0 & 0 & 0 \\ 0 & 0 & -i \\ 0 & i & 0 \end{pmatrix}; \quad \lambda_8 = \begin{pmatrix} 1 & 0 & 0 \\ 0 & 1 & 0 \\ 0 & 0 & -2 \end{pmatrix}\frac{1}{\sqrt{3}} \tag{1.4.4}$$

and they satisfy the commutation relation

$$[T^l, T^m] = i f^{lmn} T^n . \tag{1.4.5}$$

Then the colour field tensor

$$F^l_{\mu\nu} = \partial_\mu A^l_\nu - \partial_\nu A^l_\mu - g f^{lmn} A^m_\mu A^n_\nu \tag{1.4.6}$$

where f^{lmn} is the fine structure constant. From the expression for $F^l_{\mu\nu}$, it is evident that these colour gauge fields interact among themselves. Thus this theory becomes a non linear field theory unlike the electromagnetic U(1) gauge theory. The colour electric and colour magnetic field component of this field tensor can be obtained as

$$\underset{\sim}{E}^l = -\frac{\partial \underset{\sim}{A}^l}{\partial t} - \underset{\sim}{\nabla} A^l_0 - g f^{lmn} A^m_0 \underset{\sim}{A}^n \tag{1.4.7}$$

$$\underset{\sim}{B}^l = \underset{\sim}{\nabla} \times \underset{\sim}{A}^l - g f^{lmn} \underset{\sim}{A}^m \times \underset{\sim}{A}^n \tag{1.4.8}$$

Because of these non linear interactions of Yang-Mills potentials among themselves the quantum chromodynamics become almost impossible to solve exactly [43]. Also the dynamics of these fields possesses peculiar properties compared to the electro magnetic case. Like in QED the gauge potential corresponds to the photon, here in QCD, these non linear gauge potential corresponds to 'colour photons' called gluons. And the coloured quarks interact through the exchange of these coloured gluons. The interactions of these colour gluons among themselves are the ones which cause the theory to become nonlinear unlike the QED.

Quantization :

As in the abelian case, the Lagrangian for the colour fields can be written as

$$\mathcal{L}_{QCD} = -\frac{1}{2} \mathrm{Tr}\, F_{\mu\nu} F^{\mu\nu}. \tag{1.4.9}$$

It does not contain the time derivative of the fourth component of the colour field A^{l}_{μ}; thus the corresponding momenta

$$\pi_0^{\,l} = 0 \quad . \tag{1.4.10}$$

And in the canonical quantization procedure we identify A^{l}_{μ} and its conjugate $\pi_{\mu}^{\,l}$ as operators and postulates the commutation relations between them. Apart from the primary constraint given by equation (1.4.10), the equation of motion provides one more constraint on the canonical momenta, i.e.

$$(\mathcal{D}_i \pi^i)^l = \partial_i \pi^i_l + g f^{lmn} A^m_i \pi^{in} = 0 \tag{1.4.11}$$

where the Hamiltonian H is given as

$$H = \int d^3x \, \tfrac{1}{2}\left[\pi^l_i \pi^{il} + B^l_i B^{il} + 2A^m_0 (\mathcal{D}_i \pi^i)^m\right]. \tag{1.4.12}$$

As in the abelian case it can be seen that this extra term in the Hamiltonian generates the gauge transformation [39] with gauge parameter A^m_0. Thus for A_i^l and π_i^l to be physical quantity, it must satisfy the two conditions;

$$(\mathcal{D}_i \pi^i)^l = 0 \tag{1.4.13}$$

and

$$\{ f_{phy}, (\mathcal{D}_i \pi^i)^l \}_{P.B} = 0 \tag{1.4.14}$$

that is to say the physical quantity must not depend on the variable that is conjugate to $(\mathcal{D}_i \pi^i)^l$. These conditions restrict the functional space spanned by A_i^l and π_i^l to a functional space spanned by A_1^l, A_2^l and π_1^l, π_2^l in an appropriately chosen basis. This sub space is in another way written as [39]

$$g^{l}(A_i^m, \pi_i^n) = 0 \qquad (1.4.15)$$

which is the gauge choice. The necessary condition for it to be a desirable gauge is that

$$\det \left| \{ g^m, (\mathcal{D}_i \pi^i)^n \} \right| \neq 0 \qquad (1.4.16)$$

Consider a canonical transformation

$$(A_i^l, \pi_i^l) \rightarrow (\tilde{A}_j^l, \tilde{\pi}_j^l) \qquad (1.4.17)$$

and let

$$A_3^l = g^l(A_i, \pi_i) \qquad (1.4.18)$$

then the constraint 1.4.15 reads

$$\det \left| \frac{\delta \mathcal{D}_i \tilde{\pi}^i}{\delta \tilde{\pi}_3} \right| \neq 0 \qquad (1.4.19)$$

Thus for $g^l = A_3^l = 0$ then to make sense of the commutation relations between A_3^l and π_3^l is that to express $\tilde{\pi}_3^l = \tilde{\pi}_3^l(\tilde{\pi}_1^l, \tilde{\pi}_2^l)$ and then the Hamiltonian becomes

$$H = \frac{1}{2} \int d^3x \left[\tilde{\pi}_T^l \tilde{\pi}_T^l + \left(\tilde{\pi}_3^l (\tilde{\pi}_T, \tilde{A}_T) \right)^2 + \tilde{B}^l \cdot \tilde{B}^l \right]. \qquad (1.4.20)$$

The choice of the usual Coulomb gauge,

$$\partial_i A_i^l = 0 \qquad (1.4.21)$$

is shown to be not a well defined gauge for the Yang-Mill's theories[44]. It does not allow for an unambiguous extraction of the independent canonical variables. That is the contraint on the gauge condition here shows

$$\det\{\partial_i A_i^l, (D_i \pi^i)^m\}_{P.B} = \det\{\partial_i \partial_i^i \delta^{lm} - g f^{lmn} A_i^n\}$$

(1.4.22)

which has no nontrivial zero eigenvalues. Gribov pointed out that there exist nontrivial solutions to the operator equation [39]

$$(\partial_i \partial^i \delta^{lm} + f^{lmn} A_i^n \partial_i) f^m = 0$$

(1.4.23)

This is known as the Gribov ambiguity [37,39]. Whereas in the axial gauge choice

$$n_i A_i^l = 0$$

(1.4.24)

there is no Gribov problem [39]. But the Hamiltonian here becomes messy. It is still not clear that the Gribov ambiguity is really there in the case of the Coulomb gauge for the Yang-Mill's fields. According to I. Singer [39] if one does the quantization through the path integral methods then the Gribov problem is endemic to the Yang-Mill's fields and its cause lies in the fact that it is not possible to get away with the same gauge condition over all of space-time points. However, in the perturbative evaluation of the Yang-Mill's path integral one ignores the Gribov problem.

In the gauge theories the four vector massless gauge field A_μ actually represents only two independent dynamical degrees of freedom [37]. The canonical commutation relations between these transverse fields have to be formulated so that they are consistent with their constraints. But in such formulations one sacrifies the Lorentz covariance. A physically sensible theory is recovered only after restricting the admissible states to those satisfying the Lorentz gauge

$$\partial_\mu A^\mu \,|\mathrm{physical}\rangle = 0 \; . \tag{1.4.25}$$

The key point in all these formulations is that one must remove the redundant degrees of freedom (resulting from gauge invariance) of the theory by some acceptable gauge fixing conditions. A consistent implementation of such constraints for non abelian theories is highly nontrivial. These difficulties for the quantization of gauge theories was dealt by Feynman (1963) [45], Dewitt (1967) [46], Faddeev and Popov (1967) [47], Mandelstam (1968) [48], t´Hooft (1971) [36].

Table 1.1. List of leptons and quarks

Leptons			Quarks		
Flavour	Charge in units of e	Mass MeV	Flavour	Charge units of e	Mass MeV
	-1	0.511	d	-1/3	350
	0	0	u	+2/3	350
	-1	105.6	s	-1/3	550
	0	0	c	+2/3	1800
	-1	1870	b	-1/3	4500
	0	0	t	+2/3	50000

CHAPTER II

PROPERTIES AND PHENOMENOLOGICAL MODELS OF QCD

2.1. Introduction

In this chapter the salient features of QCD are described from the theoretical as well as experimental points of view. The two major properties i.e., (1) asymptotic freedom and (2) confinement property, are discussed in sections 2.2 and 2.3 respectively. The chiral symmetry is very briefly mentioned in section 2.4 since its detailed discussion is not relevant for the further development of the thesis. Finally the various properties are summarised and listed in comparison with QED in section 2.5.

The rest of the chapter is devoted to explain the pros and cons of some of the popular phenomenological models of QCD in explaining the properties of hadrons. Bag models, potential models, soliton models, etc. for the quark confinement in section 2.6 and their extension for the confinement of gluons are discussed in section 2.7. This chapter provides the philosophy behind phenomenological confinement models for studying the bound states of quarks as well as gluons in QCD.

2.2. Asymptotic Freedom

The Bjorken scaling observed in deep inelastic lepton-hadron scattering [49,50] clearly suggests that the theory of strong interaction should be asymptotically free; i.e. the quarks interact very weakly at very short distances or at very high momentum transfer [11,51]. Yang-Mill´s free field theory exhibits this property and hence the Yang-Mill´s theory becomes the theory for the quantum chromodynamics and the quantum chromodynamics becomes the best candidate for the theory of strong interactions [26,27]. The fact that the quarks exist in colour triplet state [7,8] the symmetry involved here is the SU(3) colour symmetry.

The renormalization of the non-abelian Yang-Mill´s fields shows that the strong interaction running coupling constant $\alpha_s(Q^2)$ as [37] is given by

$$\alpha_s(Q^2) = \frac{4\pi}{(11-\frac{2}{3}n_f)\ln\frac{Q^2}{\Lambda^2}} . \tag{2.2.1}$$

From this expression one can see that for small momenta, $\alpha_s(Q^2)$ increases and even diverges when the momentum transfer squared $Q^2 = \Lambda^2$. Here Λ is the fundamental momentum scale of the theory called the QCD scale parameter and n_f is the number of quark flavours. As Q^2 increases $\alpha_s(Q^2)$ decreases when $n_f < 17$, i.e. the quarks interact very weakly at very high momentum transfer or at very short distances. This is the meaning of asymptotic freedom. This expression is derived perturbatively and it may fail in large coupling regimes in infra red.. As compared to QED derivations, here the factor 11, coming out of the pure gluonic nonlinear contributions, dominates and it gives the increase of $\alpha_s(Q^2)$ at low momentum regimes making the theory nonperturbative. In QED the decrease of effective coupling constant at long distance is associated with the dielectric screening by the cloud of virtual electron-positron pairs. But here for non-abelian case one has to understand the increase of the coupling constant at long distance as antiscreening due to the virtual gauge particles carrying the colour charge. Thus the asymptotic freedom means the Yang-Mill's vacuum antishields the charges. That is, it acts as a colour dielectric medium with a dielectric constant

$$\epsilon < 1 . \tag{2.2.2}$$

The relativistic invariance of the vacuum gives the magnetic permiability

$$\mu > 1 . \tag{2.2.3}$$

so that

$$\mu \epsilon = 1 . \tag{2.2.4}$$

Thus the Yang-Mill's vacuum acts like a colour paramagnetic medium. This dielectric picture of the QCD vacuum is the basis of the dielectric confinement schemes [52,53].

Although QCD is asymptotically free it is still difficult to use perturbation theory for many of the high energy processes because the quarks and gluons are not found as physically asymptotic states like electrons or photons in QED. Also because of the increasing trend of the coupling constant, the higher order terms cannot be neglected. However the perturbative QCD results hold better in high energy deep inelastic scattering processes. When n_f becomes $\geqslant 17$, the vacuum polarization might produce very heavy fermion pairs that change the QCD vacuum from dielectric to paraelectric (i.e., screening instead of antiscreening) at a length scale $< 10^{-14}$ cms. In the 10^{-14}-10^{-15} cm region, one can ignore such ultra heavies and in the present energy range QCD possesses the asymptotic freedom. So far there are only six flavours of quarks (see Table 1.1).

2.3. Confinement

The increase in the effective coupling shows that the quarks interact very strongly as they move apart. This is supported by the experimental result that no free quarks or gluons are seen or detected in any of the brilliant efforts made to discover them [5,54]. Thus the empirical requirement is that only colour neutral objects are asymptotically free in nature. That is to say the coloured objects are permanently confined inside the hadrons. But it

13568

is not at all clear how confinement can be proven from the Yang-Mill's theory for the long distances. And it cannot be explained within the frame work of perturbation theory as its breaks in this regime. Thus whether confinement occurs or not can only be known through non perturbative calculations. That is to say the contributions from the higher and higher orders of colour interactions between the quarks and gluons become more and more important (see figure 2.1).

A general approach to this problem is the KLN theorem, named after the classic work of Kinoshita [55] and of Lee and Nauenberg [56] originally done for QED but later adapted to QCD [43]. This theorem applies to the cross section, which is finite at lowest order, and becomes divergent when higher orders are included. Unlike in QED, in QCD two types of divergences are to be taken into account. One is the emission of soft gluons by coloured quarks and second due to the decay of massless gluons into hard massless particles. The main problem in QCD is associated with these kinds of divergences. According to KLN theorem, any transition probability in a theory involving massless particles is finite, provided summation over all degenerate states is performed. Thus the initial and final degenerate states to be considered here are the collections of the infinite set of massless colinear quanta of gluons. Though the confinement can be understood as a result of the nonlinear interactions of the exchanged gluons among themselves. A qualitative way of understanding the confinement mechanism is the squeezing of colour electric flux due to the nonlinear interactions of the colour fields between the quarks making the quark permanently bound. A possible method to study this long distance property is the formalism of lattice gauge theory for QCD proposed by Wilson in 1974 [57]. For a heavy system of quark-antiquark separated by a distance R, the confinement means, the energy of the system grows without bound, i.e.,

$$E(R) \rightarrow \infty \quad \text{as} \quad R \rightarrow \infty . \tag{2.3.1}$$

And if there is no confinement one expect

$$E(R) \rightarrow 2m \quad \text{as} \quad R \rightarrow \infty \tag{2.3.2}$$

where m is the quark mass. Using the Wilson loop [57] it is possible to study the question of colour confinement in a pure gluon theory without quark fields. In this descretised theory even though the results seem to lead towards confinement, it doesn't show that the Yang-Mill's theory possesses this property [58,59], since the two Lagrangians are different in the long range regimes. And the strong coupling result is obtained without the non-abelian nature of the theory. The problem is that the strong and weak coupling regimes may be separated by one or more discontinuous phase transitions. In the abelian case it has been proved whereas similar analytic proof that QCD does not undergo a phase transition at some finite coupling has not been obtained so far. Thus as it stands today the origin of the confinement is still a mystery. Hence it seems imperative to incorporate confinement in the models for dynamics of quarks and gluons and then study the properties of hadrons and glueballs.

2.4. Chiral Symmetry

Another property that QCD might possess is the chiral invariance of the QCD Lagrangian [60,61] in the limit when quark masses become negligible and when the partial conservation of axial current (PCAC) is assumed. But in the quark models the quarks acquire an effective constituent mass and it breaks this invariance. It is implemented then in the Goldstone mode with pions as massless particles[60]. Thus one must assume the dynamics such that the QCD vacuum breaks the chiral symmetry. This is a difficult dynamical problem which is not completely settled and the discussion of this is beyond the scope of the thesis.

2.5. QED and QCD - A Comparison

Here all the properties of QCD are summarised in comparison with that of QED.

Q E D	Q C D

1. The charged particles (electrons) and photons exist as asymptotic free states in nature.	1. Quarks and gluons do not axist as asymptotic free states in nature (i.e. they are permanently confined objects).
2. They do not carry colour charges.	2. They carry colour charges.
3. It is a U(1) gauge theory.	3. It is SU(3) colour gauge theory.
4. The gauge field i.e. photon does not carry any charge.	4. The gauge field i.e. gluons carry colour charges.
5. Photons do not interact themselves	5. Gluons interact among themselves
6. It is an abelian gauge theory.	6. It is a non-abelian gauge theory.
7. The electric flux lines spread out (see fig.2.2a)	7. The colour electric squeeze to form narrow flux tubes (see fig.2.2b).
8. The Coulomb potential persists to large separation giving rise to a potential $V(r) = q/r$	8. The gluon fragmentation and recombination contribute to generate non-Coulombic potential form (linear or oscillator) with no ionization of quarks

	occurring. V(r) = ar or br^2.
9. The running coupling constant increases at short distances (ultra-violet divergences).	9. The running coupling constant increases at long distances (infra red slavery).
10. QED vacuum is perfect diamagnetic i.e. $\epsilon > 1$ and $\mu < 1$	10. QCD vacuum is perfect dielectric i.e., $\epsilon < 1$ and $\mu > 1$.

2.6 Phenomenological Models of QCD

It is now well known that QCD is the underlying theory for strong interactions [26,27]. This non-abelian gauge theory describes the dynamics of coloured quarks and gluons [7,8]. In the absence of a satisfactory proof for the colour confinement and the empirical fact that only colour neutrals are seen free, sensible physical results will be obtained by considering the coloured quarks and gluons as permanently confined objects [15]. Hence to understand the properties of physical observables like hadrons (bound states of quarks and or quark-antiquarks) and glueballs (bound states of pure gluons - a unique prediction of QCD) [62] one has to go for phenomenological models incorporating the confinement. This section describes some of the successful phenomenological models i.e., bag model, potential model and colour dielectric model for confinement.

2.6.1. Bag Model:

It is the simplest form of the confinement, where the hadrons are considered as a spherical bag of finite radius equal to that of the hadron size. The quarks and gluons are freely moving inside the bag. This naive model was introduced by Bogolioubov in 1967 [63]. But such a bag is unstable due to the pressure exerted by the freely moving quarks and gluons at the surface of the bag. To compensate this internal pressure, in the MIT bag model, an external pressure is introduced to prevent the expansion [17]. The bag 'potential' acts on the mass of the quark or gluon which becomes very heavy at the surface of the bag and hence cannot escape.

The Lagrangian density for such a bag can be written as [64]

$$\mathcal{L} = \left\{ \frac{1}{2}\left[\bar{q}\,\gamma^{\mu}\partial_{\mu}q - \partial_{\mu}\bar{q}\,\gamma^{\mu}q\right] - B \right\}\theta_{V}(r) - \frac{1}{2}\bar{q}q\,\Delta S \tag{2.6.1}$$

where

$$\theta_{V} = \theta(R-r) \tag{2.6.2}$$

and $\theta_V = 1$ inside the bag $r \leq R$ and $\theta_V = 0$ outside the bag $r > R$. $\Delta_S = \delta(R-r)$ is the surface delta function. B is the inward vacuum pressure at the surface to balance the outward pressure of the quarks inside. This pressure is isotropic only in the ground state. In the excited state the bag would be deformed. In this simplest model the nonlinear confinement effects of QCD are imposed through a boundary condition

$$n_\mu \bar{q} \gamma_\mu q = 0 \tag{2.6.3}$$

i.e. the normal component of the quark current at the bag surface is equal to zero. These are the basic features of the bag model. The Hamiltonian of the N quark system in the bag may be deduced from the Lagrangian. For the massless quarks in the ground state, the mass of the N-quark system is obtained as [64]

$$M(R) = \frac{2.04\,N}{R} + \frac{4\pi}{3} R^3 B . \tag{2.6.4}$$

If one takes into account the one gluon exchange interaction between the quarks, perturbatively, it gives the mass of the baryon where N=3 as

$$M(R) = \frac{3 \times 2.04}{R} + \frac{4\pi}{3} R^3 B \mp \frac{3 \times 0.117\,\alpha_s}{R} + \frac{Z_0}{R} . \tag{2.6.5}$$

Here the first term is just the kinetic energy of the three quarks in a sperical bag of radius R. The second term may be interpreted as the extra energy required to keep the bag stable, the third term is the hyperfine interaction due to the one gluon exchange between the quarks. The last term is supposed to take care of all effects which are difficult to calculate - like centre of mass correction, zero point energy, colour magnetic self-energy, etc. For the equilibrium radius R = R_h

$$\left.\frac{\partial M(R)}{\partial R}\right|_{R=R_h} = 0 \tag{2.6.6}$$

gives the hadron mass

$$M_h = \frac{16}{3}\pi B R_h^3 = \frac{4}{3}\frac{a_h}{R_h} \tag{2.6.7}$$

where

$$a_h = \left(2{\cdot}04 \pm 0{\cdot}117\alpha_s + \frac{z_0}{N}\right)N \tag{2.6.8}$$

and N is the number of quarks constituting the hadron. Thus for the nucleonic case,

$$M_N = \frac{16}{3}\pi B R_N^3 = \frac{4}{3}\frac{a_N}{R_N} \,. \tag{2.6.9}$$

Incorporating the mass of the strange quarks and taking

$$B^{1/4} = 145 \text{ MeV}, \quad z_0 = -1{\cdot}84$$
$$\alpha_s = 2{\cdot}2 \quad \text{and} \quad m_s = 279 \text{ MeV} \tag{2.6.10}$$

This model could fit the masses of the lowest baryon octet and decuplet as well as the lowest meson octets reasonably well except the pion mass [65,66].

Though bag model gives beautiful description of the hadronic systems, there is no derivation of such models from the fundamental theory of QCD. But there are qualitative arguments for the bag formation. One among them is the formation of bubbles in the QCD vacuum. These bubbles may then be called 'bags' [17]. Such bubbles are accounted for the antiscreening property of the QCD vacuum. A detailed descussion on this topic is given by Lee [43]. He has shown a bag like state as solitons in a relativistic, local field theory containing just quarks and a phenomenological spin zero field σ which depends upon the polarizability of the medium. The coupling of this field with the quarks restricts the motion of the quark inside the hadron. This description is known as the soliton model. Inside the soliton the σ field is zero and the quarks are free. This enables one to do the expansion of any physical observables like hadron mass in terms of the quark gluon coupling 'g'. The mass relation upto the order of g^2 is [43]

$$M = \frac{NC_r}{R} + \frac{4\pi}{3} R^3 P + 4\pi R^2 S \tag{2.6.11}$$

where $C_r = C_0 + O(g^2)$ is a constant independent of N, the number of quarks and/or antiquarks inside the hadron, P is the pressure energy per unit volume and S is the surface energy due to the surface tension per unit surface. The first term is the thermodynamical energy of the bubble which prevents the collapsing of the bubble. The second term is the pressure energy and the last is the surface energy term. The above mass expression is not far from the bag model mass formula. In the case of MIT bag [17] the surface energy term was missing and for the SLAC bag model [67] the pressure energy term was missing. Thus the soliton structure of the hadrons in the QCD vacuum provides a physical basis for all possible bag like models.

Eventhough the phenomenology of bag models are successful in explaining the properties of low-lying hadrons, there are a couple of serious drawbacks in this model. The unnatural sharp boundary of the bag makes the physics at the boundary or surface of the bag more complicated and is least understood from the basic theory. The other problem is the size of the bag - it is too big. For R = 1.1 fm the bags would already touch each other at normal nuclear density. The calculation of the excited state is rather difficult in this model. The spurious motion of the centre of confinement is very difficult to eliminate. And finally it does not preserve the chiral symmetry But an attempt has been made to regain the chiral symmetry by diffusing the bag surface using pion clouds surrounding it. Here the pions are treated as a fundamental Goldstone boson. This leads to the phenomenology of cloudy bag model. The details of this model are given elsewhere [68].

2.6.2. Potential Models:

Another very popular confinement scheme is the potential model. Here one assumes a nonrelativistic confinement potential of the type, in general,

$$V(r) = \frac{a}{r} + br \text{ or } ar^2 . \tag{2.6.12}$$

The constituent mass of the quarks here is taken as one-third of the hadronic mass. The nonrelativistic potential models give a better description for the heavier quark systems [20,21,64]. But the results are not reliable in the case of lighter quarks (i.e. for u,d and s). Since the average kinetic energy of these quarks is larger than their masses, the better description of the hadrons (with u,d and s quarks) will be obtained from its relativistic treatment.

The potential in which a Dirac particle is moving can, in general, have two forms. They are the Lorentz scalar like the bag 'potential' and Lorentz vector analogous to the bag pressure. The Dirac equation with a general potential is written as [69]

$$\left[\underset{\sim}{\alpha} \cdot \underset{\sim}{p} + \beta(m + S(r)) + V(r)\right]\Psi = i\frac{\partial \Psi}{\partial t} \tag{2.6.13}$$

where S(r) is the scalar potential and V(r) is the fourth component of the vector potential . This can be rewritten in a covariant form as

$$\left[i\gamma^{\mu}\partial_{\mu} + \gamma^{0}V - (m+S)\right]\Psi = 0 \tag{2.6.14}$$

where

$$\underset{\sim}{\alpha} = \begin{pmatrix} 0 & \underset{\sim}{\sigma} \\ \underset{\sim}{\sigma} & 0 \end{pmatrix} ; \quad \beta = \gamma^{0} = \begin{pmatrix} I & 0 \\ 0 & -I \end{pmatrix}$$

and

$$\underset{\sim}{\gamma} = \begin{pmatrix} 0 & \underset{\sim}{\sigma} \\ -\underset{\sim}{\sigma} & 0 \end{pmatrix} . \tag{2.6.15}$$

In these models the scalar part is associated with the mass and its effective mass (i.e. m+S) grows as it moves away from each other and finally, leads to its confinement. In a pure vector potential case one would have the problem of Klein paradox [70]. It is because, when the potential becomes too strong, the Dirac theory starts accommodating solutions with $E < mc^2$ which are oscillatory and can penetrate the potential barrier, providing a finite probability of free quarks outside the confinement boundary. This will be prevented by the scalar part of the potential. Another qualitative argument for scalar plus vector potential is that it provides a consistent picture for the bound states for both mesons (q-$\bar{q}$ systems) and the baryons (3q systems) [71]. The pure vector potential would produce only q-$\bar{q}$ bound states whereas the scalar potential provides an attractive force for both $q\bar{q}$ and qq states. Since there is no di-quark states, the qq interaction must be weaker. This is provided by the repulsive nature of the vector potential. Again the three pair interaction of the quarks in the baryons makes it more strong. Thus for the confinement of quarks, a scalar plus vector potential is the more appropriate choice. The choice of such a potential in the relativistic scheme for the quark confinement has been eminently successful in the predictions of the hadronic properties [23]. In this relativistic harmonic oscillator potential model (RHM) [23] both the Lorentz scalar and Lorentz vector parts are taken as oscillator type. Thus the confinement potential in RHM is

$$V(r) = (1+\beta)\alpha^2 r^2 + M \, . \tag{2.6.16}$$

The corresponding Lagrangian density can be written as

$$\mathcal{L}_{RHM} = \bar{\Psi} \gamma^{\mu} \partial_{\mu} \Psi - \bar{\Psi}\left[\tfrac{1}{2}(1+\beta)\alpha^2 r^2 + M\right]\Psi \tag{2.6.17}$$

and the energy expression obtained as [23]

$$E_n = \left[M^2 + (2n+1)\Omega_n\right]^{1/2} \tag{2.6.18}$$

where the size parameter

$$\Omega_n = (E_n + M)^{1/2} \alpha \, . \tag{2.6.19}$$

Here $n \geqslant 1$.

The total energy or mass of the hadron is then obtained by adding individual contributions of the quarks but for the spurious centre of mass motion. This model is found to be very successful in explaining very diverse aspects of hadron spectroscopy, magnetic moments, nucleon polarizability, nucleon-antinucleon annihilation, etc. [23,72,73]. Success of this model is closely linked with the accounting for the spurious centre of motion. The results are in better agreement with the experimental results than any of the bag model or nonrelativistic oscillator potential model results.

2.6.3. Colour Dielectric Model:

In a QCD vacuum the gluons can produce virtual $q\bar{q}$ pairs, leading to the screening of the interaction and should make it diamagnetic as in the case of QED. However, since the gluons carry colour charges unlike the photon in QED, they can cause colour magnetisation of the medium and make the medium paramagnetic. This effect overcomes the diamagnetic property of the $q\bar{q}$ pairs. Thus for the QCD vacuum the colour magnetic permeability $\mu_c > 1$. Then it follows, from the Lorentz invariance , the colour dielectric constant $\epsilon_c < 1$. That is to say the colour electric interaction between the charged objects becomes stronger for larger distances. Thus the medium shows an antiscreening property. So, as briefly mentioned in the earlier sections, as $r \to 0$, μ_c and $\epsilon_c \to 1$ and the interaction becomes weaker showing asymptotic freedom. At the same time, for large r, $\mu_c \gg 1$ or $\epsilon_c \ll 1$ giving rise to the confinement of colour charge. It has been shown by T.D. Lee [52] for a medium whose dielectric constant is less than unity (ϵ < 1), the work required to separate two charges to infinity is infinite. Thus the colour dielectric picture gives a better physical understanding for the colour confinement. Accordingly, in a bag picture hadrons are embedded in a QCD vacuum where $\mu_c = \infty$ and $\epsilon_c = 0$, while inside the hadron $\mu_c = \epsilon_c = 1$. Consequently the colour fields are completely confined within the hadron. Following this, Nielson and Patkos [53] have made an attempt to derive a colour dielectric model from QCD. They suggest the following effective Lagrangian [53] :

$$\mathcal{L} = K\left[\bar{\Psi}\gamma_\mu\left(\frac{i}{2}\overleftrightarrow{\partial}^\mu + \frac{B^\mu}{K}\right)\right]\Psi - m_q\bar{\Psi}\Psi - \frac{1}{4g}K^4 F_{\mu\nu}F^{\mu\nu} + \mathcal{L}(K)$$

(2.6.20)

where K and B^μ are related to averages of the original gauge fields. The field tensor $F^{\mu\nu}$ is

$$F^{\mu\nu} = \partial^\mu\left(\frac{B^\nu}{K}\right) - \partial^\nu\left(\frac{B^\mu}{K}\right) - i\left[\frac{B^\mu}{K}, \frac{B^\nu}{K}\right].$$

(2.6.21)

Here one can identify K^4 with the colour dielectric constant,

$$\epsilon = K^4 . \tag{2.6.22}$$

By the manifestation of the confinement through the vanishing of ϵ in the vacuum, gives

$$\langle K \rangle_{vac} = 0 . \tag{2.6.23}$$

Thus the dielectric model provides a mechanism to construct models which lead to confinement without explicitly introducing a bag. Hence the problems associated with a sharp, non-dynamical bag would be eliminated [74].

For systems wihout the colour octet fields, the Lagrangian reduces to [74]

$$\mathcal{L} = \frac{i}{2} K(x) (\bar{\Psi} \overleftrightarrow{\partial\!\!\!/} \Psi) - m_q \bar{\Psi} \Psi + \mathcal{L}(K). \tag{2.6.24}$$

Here the field canonically conjugate to Ψ is not $i\Psi^+$ but iK Ψ^+. In an effective mean field theory, one introduces a field χ related to K and m_q as

$$\chi = \frac{\alpha}{m_q} K \tag{2.6.25}$$

such that

$$\mathcal{L} = \frac{i}{2} \bar{\Psi} \overleftrightarrow{\partial\!\!\!/} \Psi - \frac{\alpha \bar{\Psi} \Psi}{\chi} + \mathcal{L}(\chi) . \tag{2.6.26}$$

Here now the χ field is considered as a dynamical field[61,74]. An attempt has been made to connect this field with a colour and chiral singlets 0^{++} glueball field coupled to quarks [74,75].

Now if one compares this Lagrangian with the Lagrangian corresponding to the RHM without the $\mathcal{L}(\chi)$ part, the χ function would be equivalent to

$$\chi(r) = \frac{\alpha}{m_q} K(r) = \frac{2\alpha}{(1+\beta)\alpha^2 r^2 + 2m_q} . \tag{2.6.27}$$

Thus

$$K(r) \simeq \frac{m_q}{b^2 r^2 + m_q} \tag{2.6.28}$$

Thus as $r \to 0$; $K(r) \to 1$ and as $r \to \infty$, $K(r) \to 0$. Hence the colour dielectric model provides some physical arguments for both the bag models and potential models.

2.7. Confinement Models for Gluons

Confinement of coloured particles implies the confinement of gluons also. There exist confinement schemes for gluons similar to that of quarks [22,76,77]. For example, a dielectric bag model [78] provides the confinement of gluons by assuming $\epsilon = 1$ inside the bag and $\epsilon = 0$ outside the bag surface. Inside this bag, gluons are free and are described by the Maxwell´s equations. Here the gluon field confinement is implemented by the boundary conditions [78]

$$\hat{n} \cdot \underset{\sim}{E} = 0$$
$$\hat{n} \times \underset{\sim}{B} = 0 \tag{2.7.1}$$

at the surface, where E and B are the gluon electric and magnetic fields respectively. The two transverse cavity eigenmodes are obtained in multipole form in terms of the spherical Bessel functions [78]. The transverse magnetic (TM) eigenmode satisfies

$$\underset{\sim}{r} \cdot \underset{\sim}{B}^{TM} = 0 \ . \tag{2.7.2}$$

The frequency and the spin parity of the lowest TM mode in units of the cavity radius, given by

$$X_0(TM) = 4 \cdot 49 \ ; \ J^P = 1^- \ . \tag{2.7.3}$$

And the transverse electric (TE) eigenmode satisfies

$$\underset{\sim}{r} \cdot \underset{\sim}{E}^{TE} = 0 \ . \tag{2.7.4}$$

The frequency and the spin parity of the lowest TE mode is given as

$$X_0(TE) = 2 \cdot 74 \ ; \ J^P = 1^+ \ . \tag{2.7.5}$$

Using these spherical eigenmodes, the gluon potential A_μ is expanded and second quantized form of the Hamiltonian is written in terms of the frequency of the eigenmodes [78]. A naive calculation of the gluonium (glueball spectrum) is also produced by them. It should be noted that not only these models suffer from the difficulties of bag models but the implementation of gauge condition is not satisfactory.

There are also other models, like potential models for the gluon confinement and have predicted the glueball spectra. In these models they assume the gluons as massive and the motion of the gluons inside the glueball is described by a nonrelativistic Schrodinger equation [79].

In the next chapter, new relativistic confinement schemes [80] for the massless gluons will be discussed in the light of the success of the relativistic harmonic oscillator scalar plus vector potential (RHM) for quarks in the description of hadronic properties [23]. The formulation of this scheme aims at a unified confinement theory for the study of quark-gluon bound systems.

FEYN MAN DIAGRAMS IN QED AND QCD

a)

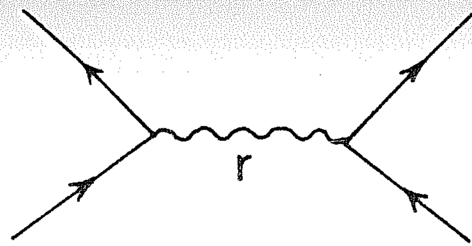

b)

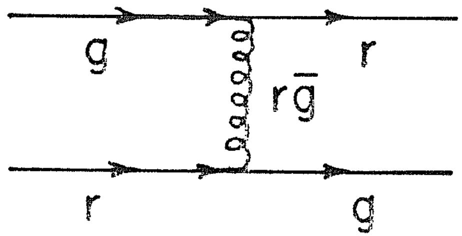

f)

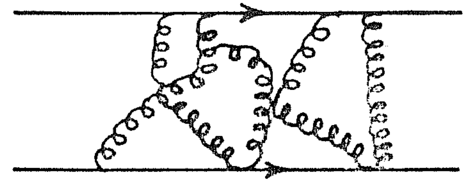

c)

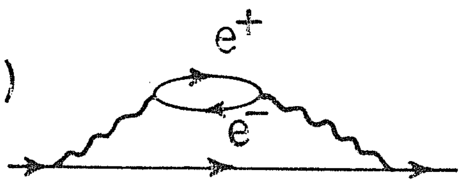

d)

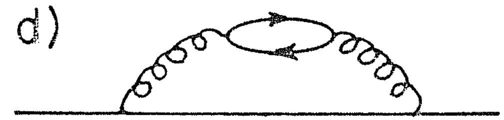

e)

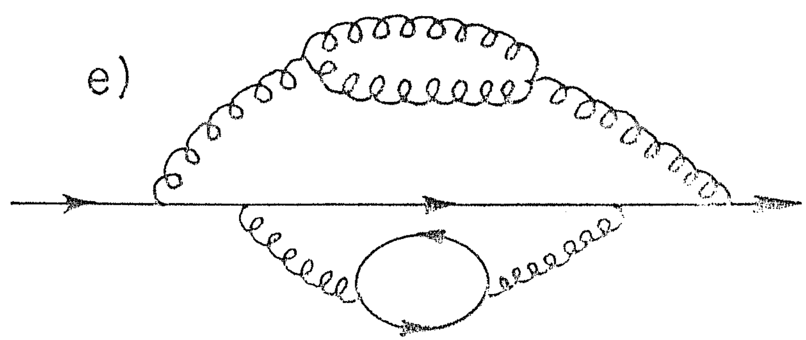

Fig. 2·1

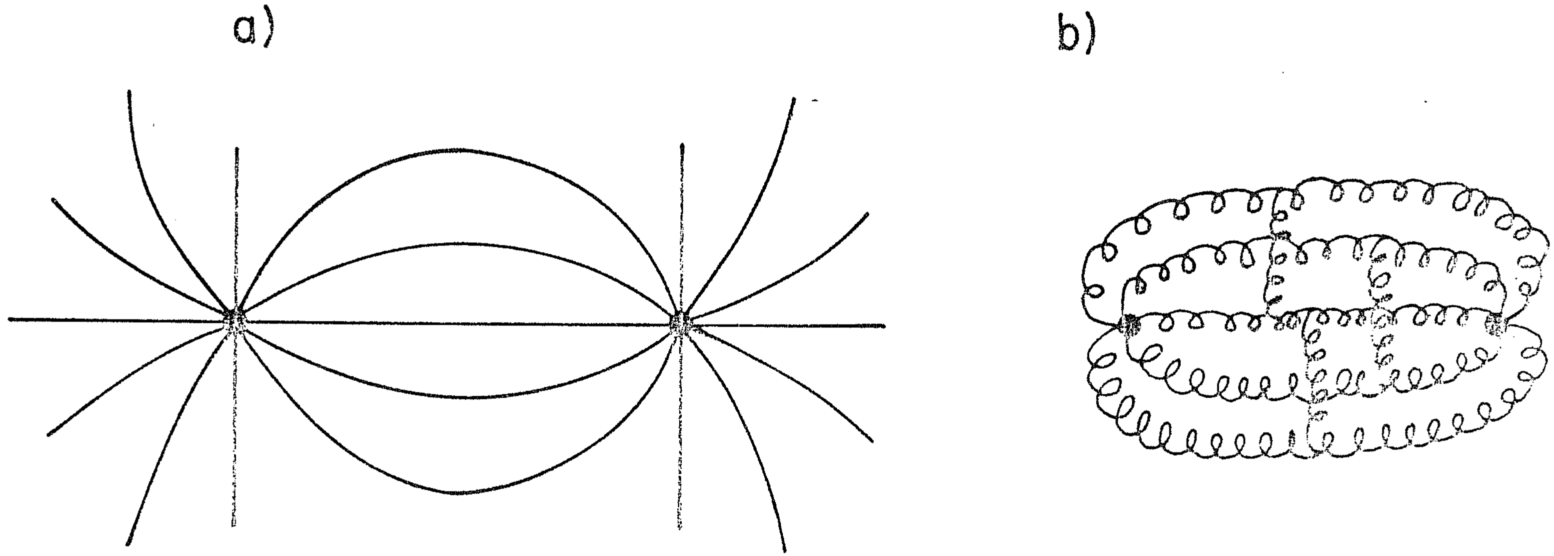

a) LINES OF FORCES IN QED

b) LINES OF FORCES IN QCD

Fig. 2·2

CHAPTER III

CONFINEMENT SCHEME FOR GLUONS

3.1. Introduction

This chapter describes a new confinement scheme for the gluons in line with the relativistic confinement model with scalar plus vector potential (RHM) for quarks. It contains a description of a colour confinement current which is motivated from the pure glue-field equations. This current in analogy with Ginzberg-Landau's theory of superconductivity [81] is introduced as a colour super current. Further the general expression for this current is reduced to that corresponding to the London equation [81] in super conductivity. The gluon-gluon pair interaction is considered as the cause for such an effective colour super current. In this formalism the gluons satisfy the quasi-Maxwellian fields with a source current satisfying the continuity equation. Section 3.2 describes the reduction of the colour gluon field to a pseudo-Maxwellian quasi-gluon field. With an appropriate choice, the above current leads to a confinement scheme for the quasi-gluons similar to that of RHM. This scheme will be referred to as the current confinement model (CCM). The confined quasi-gluon modes are obtained in a general frame of Lorentz gauge condition. The secondary gauge condition combined with the Lorentz gauge leads to a new gauge called the oscillator gauge [72]. In this gauge, transverse modes are obtained. The gluon field is expanded in these bases and the field is second quantized using the usual canonical procedure. The details are given in section 3.3.

An attempt has been made to get an equivalent dielectric picture for the current confinement model. The dielectric function thus obtained in section 3.4 is inhomogeneous and momentum dependent (non-local). A dielectric function is dedued from the usual Maxwell´s equations written in spin notation [38] in similarity with the Dirac spinor equations for RHM. This dielectric function is found to be identical with that obtained for CCM neglecting the dynamical momentum dependent part. Thus a new dielectric confinement model with an inhomogeneous dielectric function can be constructed. Such a dielectric confinement model (DCM) is discussed in section 3.5. However, there are difficulties for the choice of a proper gauge. With some approximations similar to that of the boundary conditions in the bag dielectric model [52,78], the physical transverse gluon modes are obtained. The second quantization of these gluons is carried out in a similar fashion as that in CCM.

Thus in this chapter two different confinement models for the colour gluons are described. The energies of the physical transverse modes of these gluons in both the models are calculated and the essential features of these two models are compared.

3.2. Gluons as Quasi-Maxwellian Fields

In this section the pure colour Yang-Mill's field equations are linearized. The resultant fields then obey quasi-Maxwell's equations.

Recalling the Lagrangian density for the colour Yang-Mill's fields,

$$\mathcal{L} = -\frac{1}{4} F^{l}_{\mu\nu} F^{l}_{\mu\nu} \tag{3.2.1}$$

where the colour field tensor $F^{l}_{\mu\nu}$ can be written as

$$F^{l}_{\mu\nu} = f^{l}_{\mu\nu} + G^{l}_{\mu\nu} \tag{3.2.2}$$

where

$$f^{l}_{\mu\nu} = \partial_\mu A^{l}_{\nu} - \partial_\nu A^{l}_{\mu} \tag{3.2.3}$$

and

$$G^{l}_{\mu\nu} = -g f^{lmn} A^{m}_{\mu} A^{n}_{\nu} \tag{3.2.4}$$

Here l,m,n are the colour indices, g is the coupling constant and f^{lmn} is the colour SU(3) structure constant. (Note: Here and in the following, repeated indices are summed over). From the variational principle the equation satisfying the field variable can be obtained

$$(\mathcal{D}_\mu F_{\mu\nu})^l = 0 \tag{3.2.5}$$

By expanding $\mathcal{D}_\mu$ the equation becomes

$$\partial_\mu F^l_{\mu\nu} + g f^{lmn} A^m_\mu F^n_{\mu\nu} = 0 . \tag{3.2.6}$$

Separating the linear and nonlinear parts using equation (3.2.2):

$$\begin{aligned}\partial_\mu f^l_{\mu\nu} &= -g f^{lmn} A^m_\mu f^n_{\mu\nu} - \partial_\mu G^l_{\mu\nu} \\ &\quad - g f^{lmn} A^m_\mu G^n_{\mu\nu}\end{aligned} \tag{3.2.7}$$

$$\begin{aligned}= + g f^{lmn}\Big[&(\partial_\mu A^m_\mu) A^n_\nu + A^m_\mu \partial_\nu A^n_\mu \\ &+ g f^{npq} A^m_\mu A^p_\mu A^q_\nu \Big]\end{aligned} \tag{3.2.8}$$

The r.h.s. of this equation now can be formally represented by a current. Such that

$$\partial_\mu f^l_{\mu\nu} = - J^l_\nu \tag{3.2.9}$$

where J_μ^ℓ is a nonlinear field current. In the Ginzberg-Landau's theory of superconductivity [81], the super current of the electron pair condensates is written as:

$$\underset{\sim}{J} = -\frac{e^*}{2m^* i}\left(\psi^* \nabla \psi - \psi \nabla \psi^*\right) - \frac{e^{*2}}{m^*}|\psi|^2 \underset{\sim}{A} \tag{3.2.10}$$

where ψ is a complex order parameter corresponding to the electron pair condensate, e^* and m^* are the effective charge and mass of such a pair, and $\underset{\sim}{A}$ is an external field potential. Generalising this super current to a four vector notation and taking the analogy with the current expression from equations (3.2.8) and (3.2.9), one can consider the current J_μ^ℓ as a colour gluon super current. Such an analogy has been taken by other [82] in the description of gluon condensate in QCD vacuum. Further the super current expression in (3.2.10) is reduced to that of the London equation as [81]

$$\underset{\sim}{J}(x) = -\frac{e^{*2}}{m^*}|\psi|^2 \underset{\sim}{A}(x) \tag{3.2.11}$$

with assuming an uniform order parameter ψ. Similar approximation can be done in the case of the colour gluon super current. Assuming an uniform gluon potential field within the confinement regime, the colour gluon super current expression can be reduced to that similar to the London equation given in (3.2.11). Thus the colour gluon super current is reduced to

$$J_\nu^{\,l} = -g^2 f^{lmn} f^{npq} A_\mu^m A_\mu^p A_\nu^q \,. \tag{3.2.12}$$

In this expression a summation over all the repeated indices has to be carried out. One can contract the colour indices in this expression. Here p and q cannot be contracted, while the possible contractions are those fields with indices (m,p) and (m,q). Thus the r.h.s. of the equation (3.2.12) can be written in a contracted form,

$$\begin{aligned} J_\nu^{\,l} &= -g^2 \sum_{m,n,q} f^{lmn} f^{nmq} (:A_\mu^m A_\mu^m:) A_\nu^q \\ &\quad - g^2 \sum_{m,n,p} f^{lmn} f^{npm} (:A_\mu^m A_\nu^m:) A_\mu^p \\ &= -g^2 \Big\{ \sum_q \Big[\sum_{m,n} f^{lmn} f^{nmq} \theta_{\mu\mu}^m \Big] A_\nu^q + \\ &\qquad \sum_p \Big[\sum_{m,n} f^{lmn} f^{npm} \theta_{\mu\nu}^m \Big] A_\mu^p \Big\} \end{aligned} \tag{3.2.13}$$

where

$$\theta_{\mu\mu}^m = (:A_\mu^m A_\mu^m:)$$

and

$$\theta_{\mu\nu}^m = (:A_\mu^m A_\nu^m:) \tag{3.2.14}$$

Using the properties of the structure function f^{lmn},

$$f^{nmq} = - f^{qmn} . \qquad (3.2.15)$$

Taking the summation over all possible m,n with non-zero value of the structure constants for the SU(3) colour group [43], one gets

$$\sum_{m,n} f^{lmn} f^{qmn} = 3 \delta_{lq} \qquad (3.2.16)$$

{see Appendix A}.

Thus

$$J_\nu^{\ l} = 3g^2 \left[\theta_{\mu\mu} A_\nu^l - \theta_{\mu\nu} A_\mu^l \right] \qquad (3.2.17)$$

Absorbing $3g^2$ in $\theta_{\mu\nu}$ and allowing μ , ν indices free, the current can be written in a more general form as

$$J_\nu^{\ l} = \theta_{\mu\nu} A_\mu^l \qquad (3.2.18)$$

The $\theta_{\mu\nu}$ here appears in a similar way as $|\Psi|^2$ appearing in the London equation of the super conducting theory. Thus $\theta_{\mu\nu}$ can be considered as the probability density of the gluon pair condensates. This expression in another way is similar to the Hartree-Fock approximation in which the gluon moves in an average background field provided by all other gluons in the medium. There are studies for the colour confinement by considering the QCD vacuum as filled with gluon condensates [82]. In this respect, the $\theta_{\mu\nu}$ can also be considered as representing the structue of the QCD vacuum.

3.3. A Current Confinement Model for Gluons (CCM)

A new confinement model for the gluons is described in this section. Confinement is assumed due to a colour super current described in the previous section. In this mean-field approach the gluons are described by quasi-Maxwell's equation. The nonlinear interaction effects are partially taken into account in the super current J_μ;

$$J_\mu = \theta_{\mu\nu} A_\nu \quad . \tag{3.3.1}$$

The colour index is suppressed since J_μ and A_μ carry the same colour index. The $\theta_{\mu\nu}$ is chosen as an inhomogeneous function of space. This indicates a varying field strength due to the 'cracking' of the medium. In this respect it is not different from the spirit of bag model but is closer to potential or dielectric approach. In analogy with the harmonic potential model for quarks (RHM), here $\theta_{\mu\nu}$ is chosen as

$$\theta_{\mu\nu} = \delta_{\mu,\nu}\, \theta_\mu \tag{3.3.2}$$

and

$$\theta_\mu = \alpha^2 r^2 - 2\alpha\, \delta_{\mu,0} \tag{3.3.3}$$

where α is a constant parameter in this model and r is the distance from the confinement centre. This particular choice has the following advantages. (1) The Lorentz gauge condition can be used for solving the quasi-Maxwell's equation, (2) the four vector current is conserved, and (3) The equation for the quasi-gluon field is similar to the equation satisfied by the quark field in RHM.

3.3.1. Equations of Motion of the Quasi-Gluon Field:

The phenomenological Lagrangian density for the current confinement model can be written as

$$\mathcal{L} = -\frac{1}{4} F_{\mu\nu} F^{\mu\nu} - \frac{1}{2} \theta_{\mu\nu} A_\nu A^\mu \tag{3.3.4}$$

where

$$F_{\mu\nu} = \partial_\mu A_\nu - \partial_\nu A_\mu \, . \tag{3.3.5}$$

The metric chosen here is

$$g_{\mu\nu} = (1, -1, -1, -1)$$

the vector

$$x^\mu = (t, \underset{\sim}{x}); \quad x_\mu = (t, -\underset{\sim}{x})$$

$$\partial_\mu = \left(\frac{\partial}{\partial t}, \underset{\sim}{\nabla}\right); \quad \partial^\mu = \left(\frac{\partial}{\partial t}, -\underset{\sim}{\nabla}\right)$$

The scalar product

$$x_\mu x^\mu = t^2 - \underset{\sim}{x} \cdot \underset{\sim}{x}$$

$$\partial_\mu \partial^\mu = \frac{\partial^2}{\partial t^2} - \nabla^2 \, . \tag{3.3.6}$$

$$A^{\mu} = (\phi, \underset{\sim}{A}) ; J^{\mu} = (\rho, \underset{\sim}{J}) . \tag{3.3.7}$$

By variational principle,

$$\delta \int dx^{\mu} \mathcal{L} = 0 . \tag{3.3.8}$$

From the lagrangian given in equation (3.3.4),

$$\delta \mathcal{L} = -\frac{1}{2} F_{\mu\nu} \delta F^{\mu\nu} - \theta_{\mu\nu} A_{\mu} \delta A^{\nu} . \tag{3.3.9}$$

Since $F_{\mu\nu} = - F_{\nu\mu}$

$$\delta \mathcal{L} = - F_{\mu\nu} \partial^{\mu} \delta A^{\nu} - \theta_{\mu\nu} A_{\mu} \delta A^{\nu} . \tag{3.3.10}$$

Substituting in eqn. (3.3.8) and the partial integration leads to

$$\partial^{\mu} F_{\mu\nu} + \theta_{\mu\nu} A_{\mu} = 0 . \tag{3.3.10}$$

Thus the equation of motion satisfied by the components of A_{μ} are

$$\left(\frac{\partial^2}{\partial t^2} - \nabla^2 + \alpha^2 r^2 \right) \underset{\sim}{A} = 0 \tag{3.3.11}$$

and

$$\left(\frac{\partial^2}{\partial t^2} - \nabla^2 + \alpha^2 r^2 - 2\alpha\right)\phi = 0 \tag{3.3.12}$$

where ϕ is the scalar component of A_μ. Here the Lorentz gauge condition

$$\partial_\mu A^\mu = \frac{\partial \phi}{\partial t} + \underset{\sim}{\nabla} \cdot \underset{\sim}{A} = 0 \tag{3.3.13}$$

is assumed. The time variation of the field is taken as $e^{-i\omega t}$, then the equations for $\underset{\sim}{A}$ and ϕ become

$$(-\nabla^2 + \alpha^2 r^2)\, \underset{\sim}{A} = \omega^2 \underset{\sim}{A} \tag{3.3.14}$$

and

$$(-\nabla^2 + \alpha^2 r^2)\ \phi = (\omega^2 + 2\alpha)\phi\ . \tag{3.3.15}$$

The above equations can be identified as that of an oscillator equation with the oscillator eigen value as ω^2 and $(\omega^2 + 2\alpha)$ respectively.

3.3.2. The Hamiltonian Formalism:

The Lagrangian density given in equation (3.3.4) can be rewritten, incorporating the Lorentz condition, as:

$$\mathcal{L} = -\frac{1}{4} F_{\mu\nu} F^{\mu\nu} - \theta_{\mu\nu} A_\mu A^\nu + \frac{1}{2}(\partial_\mu A^\mu)^2. \tag{3.3.16}$$

The canonical momentum conjugate to A_μ is given by

$$\pi_\mu = \frac{\partial \mathcal{L}}{\partial \partial_0 A^\mu} = -F_{0\mu} . \qquad (3.3.17)$$

Thus

$$\pi_i = -F_{0i} = \frac{\partial A_i}{\partial t} + \partial_i \phi \qquad (3.3.18)$$

and

$$\pi_0 = \partial_\mu A^\mu = 0 \qquad (3.3.19)$$

where A_μ and π_μ satisfy the fundamental Poisson bracket relations at equal times i.e.

$$\{A_\mu(\underset{\sim}{x}), \pi_\nu(\underset{\sim}{y})\} = -g_{\mu\nu}\,\delta^3(\underset{\sim}{x}-\underset{\sim}{y})$$

and

$$\{A_\mu(\underset{\sim}{x}), A_\nu(\underset{\sim}{y})\} = \{\pi_\mu(\underset{\sim}{x}), \pi_\nu(\underset{\sim}{y})\} = 0 . \qquad (3.3.20)$$

The Hamiltonian density is given by

$$\begin{aligned}\mathcal{H} &= \pi^\mu \dot{A}_\mu - \mathcal{L} \\ &= \pi^i(\pi_i - \partial_i \phi) - \tfrac{1}{2}\pi_i \pi^i + \tfrac{1}{4}F_{ij}F^{ij} \\ &\quad + \tfrac{1}{2}\theta_i A_i A^i - \tfrac{1}{2}\theta_0 \phi^2 \\ &= \tfrac{1}{2}\left[\pi^i \pi_i + \theta_i A^i A_i - \theta_0 \phi^2\right] + \tfrac{1}{4}F_{ij}F^{ij} \\ &\quad - \pi_i \partial_i \phi . \end{aligned} \qquad (3.3.21)$$

Thus the total Hamiltonian H

$$H = \int d^3x\, \mathcal{H} . \qquad (3.3.22)$$

After integrating by parts,

$$H = \int d^3x \left[\frac{1}{2} \pi^i \pi_i + \frac{1}{2} \theta_i A^i A_i - \frac{1}{2} \theta_0 \phi^2 + \frac{1}{4} F_{ij} F^{ij} + \phi \partial_i \pi^i \right] . \tag{3.3.23}$$

Thus the Hamiltonian is purely dependent on the canonical variables. But the Hamiltonian is not unique since the variable canonically conjugate to ϕ, i.e., π_0 is zero. Thus as discussed in the chapter one, an additional term proportional to π_0 is added to H. Thus

$$H = \int d^3x \left[\frac{1}{4} F_{ij}^2 + \frac{1}{2} (\pi_i^2 + \theta_i A_i^2 - \theta_0 \phi^2) + \phi \partial_i \pi^i + F \pi_0 \right] . \tag{3.3.24}$$

In order to find F, the Poisson's bracket

$$\{ \phi , H \} = \frac{\partial \phi}{\partial t} \tag{3.3.25}$$

i.e. $$\frac{\partial \phi}{\partial \phi} \frac{\partial H}{\partial \pi_0} - \frac{\partial \phi}{\partial \pi_0} \frac{\partial H}{\partial \phi} = \frac{\partial \phi}{\partial t}$$

i.e $$F = \frac{\partial \phi}{\partial t} . \tag{3.326}$$

Thus the time evolution of ϕ is determined by an arbitrary function F; i.e., ϕ is a non-physical degree of freedom. Considering now the Hamilton's equation for π_0,

$$\dot{\pi}_0 = \{ \pi_0 , H \} \tag{3.3.27}$$

$$= -\partial_i \pi^i + \theta_0 \phi \quad . \tag{3.3.28}$$

But π_0 is zero for all times by the canonical procedure. Hence $\dot{\pi}_0$ also must be equal to zero,

$$\partial_i \pi^i - \theta_0 \phi = 0 \quad . \tag{3.3.29}$$

This is a secondary constraint equation. This gives ϕ as a dependent variable in terms of π^i.

$$\phi(\pi^i) = \frac{\partial_i \pi^i}{\theta_0} \quad . \tag{3.3.30}$$

Eliminating ϕ from the Hamiltonian,

$$H = \int d^3x \, \frac{1}{2} \left[\pi^i \pi_i + \theta_i A^i A_i + B^i B_i + \frac{(\partial_i \pi^i)^2}{\theta_0} \right] \tag{3.3.31}$$

where $B^i = \epsilon_{ijk} F^{jk}$ is the magnetic component of $F^{\mu\nu}$.

This Hamiltonian has got yet another arbitrariness due to the secondary condition given by equation (3.3.29). But a true physical quantity should not have any arbitrariness. To make sure of this, the physical space is restricted such that any physical quantity in this theory must not depend on the variable that is conjugate to the secondary condition obtained in equation (3.3.29). Mathematically it is expressed as [39]

$$\{ f_{phy} , (\partial_i \pi^i - \theta_0 \phi) \} = 0 \quad . \tag{3.3.32}$$

This gives the freedom to choose yet another gauge condition restricting the space spanned by A_i's and π_i's. As discussed in the first chapter for the QED case, there are gauge conditions like Coulomb gauge, axial gauge, etc., called the secondary gauge conditions. Here in this phenomenological study, a different gauge condition is required which will be discussed in the next section. Before that, equations satisfied by the fields $\underset{\sim}{A}$ and $\underset{\sim}{\pi}$ can be obtained from the above Hamiltonian, expressed in terms of the vector fields,

$$H = \int d^3x \, \frac{1}{2} \left[\underset{\sim}{\pi}^2 + \frac{(\underset{\sim}{\nabla} \cdot \underset{\sim}{\pi})^2}{\theta_0} + \theta \underset{\sim}{A}^2 + (\underset{\sim}{\nabla} \times \underset{\sim}{A})^2 \right] \tag{3.3.33}$$

and after some partial integration

$$H = \int d^3x \, \frac{1}{2} \Big[\underset{\sim}{\pi}^2 - 2 \underset{\sim}{\pi} \cdot \underset{\sim}{\nabla} \left(\frac{\underset{\sim}{\nabla} \cdot \underset{\sim}{\pi}}{\theta_0} \right) + \theta \underset{\sim}{A}^2 + 2 \underset{\sim}{A} \cdot \underset{\sim}{\nabla} (\underset{\sim}{\nabla} \cdot \underset{\sim}{A}) - 2 \underset{\sim}{A} \cdot \nabla^2 \underset{\sim}{A} \Big] . \tag{3.3.34}$$

The Hamilton's equations of motion give

$$\frac{\partial \underset{\sim}{A}}{\partial t} = \frac{\partial H}{\partial \underset{\sim}{\pi}} = \underset{\sim}{\pi} - \underset{\sim}{\nabla} \left(\frac{\underset{\sim}{\nabla} \cdot \underset{\sim}{\pi}}{\theta_0} \right) \tag{3.3.35}$$

and

$$\frac{\partial \underset{\sim}{\pi}}{\partial t} = - \frac{\partial H}{\partial \underset{\sim}{A}} = \nabla^2 \underset{\sim}{A} - \theta \underset{\sim}{A} - \underset{\sim}{\nabla} (\underset{\sim}{\nabla} \cdot \underset{\sim}{A}) \quad . \tag{3.3.36}$$

Taking the time derivative of the equation (3.3.35),

$$\frac{\partial^2 \underset{\sim}{A}}{\partial t^2} = \frac{\partial \underset{\sim}{\Pi}}{\partial t} - \underset{\sim}{\nabla}\left(\frac{\underset{\sim}{\nabla}\cdot \frac{\partial \underset{\sim}{\Pi}}{\partial t}}{\theta_0}\right) \tag{3.3.37}$$

Substituting $\frac{\partial \Pi}{\partial t}$ from the second Hamilton´s equation,

$$\begin{aligned}\frac{\partial^2 \underset{\sim}{A}}{\partial t^2} &= \nabla^2 \underset{\sim}{A} - \theta \underset{\sim}{A} - \nabla(\nabla\cdot\underset{\sim}{A}) - \\ &\quad \underset{\sim}{\nabla}\left[\frac{\underset{\sim}{\nabla}\cdot(\nabla^2 \underset{\sim}{A} - \theta\underset{\sim}{A} - \underset{\sim}{\nabla}(\underset{\sim}{\nabla}\cdot\underset{\sim}{A}))}{\theta_0}\right] \\ &= \underset{\sim}{\nabla}^2 \underset{\sim}{A} - \theta\underset{\sim}{A} - \underset{\sim}{\nabla}(\underset{\sim}{\nabla}\cdot\underset{\sim}{A}) \\ &\quad - \underset{\sim}{\nabla}\left[\frac{\nabla^2\underset{\sim}{\nabla}\cdot\underset{\sim}{A} - \underset{\sim}{\nabla}\cdot\theta\underset{\sim}{A} - \nabla^2(\underset{\sim}{\nabla}\cdot\underset{\sim}{A})}{\theta_0}\right] \\ &= \nabla^2\underset{\sim}{A} - \theta\underset{\sim}{A} - \underset{\sim}{\nabla}(\underset{\sim}{\nabla}\cdot\underset{\sim}{A}) + \underset{\sim}{\nabla}\left(\frac{\underset{\sim}{\nabla}\cdot\theta\underset{\sim}{A}}{\theta_0}\right) \\ &= \nabla^2\underset{\sim}{A} - \theta\underset{\sim}{A} - \underset{\sim}{\nabla}\frac{1}{\theta_0}\left[-\underset{\sim}{\nabla}\cdot\theta\underset{\sim}{A} + \theta_0\underset{\sim}{\nabla}\cdot\underset{\sim}{A}\right] .\end{aligned} \tag{3.3.38}$$

But from the equation 3.3.11 the vector potential $\underset{\sim}{A}$ satisfies

$$\frac{\partial^2 \underset{\sim}{A}}{\partial t^2} = \nabla^2 \underset{\sim}{A} - \theta\underset{\sim}{A} . \tag{3.3.39}$$

This together with equation (3.3.38) gives:

$$\underset{\sim}{\nabla}\cdot\theta\underset{\sim}{A} - \theta_0\underset{\sim}{\nabla}\cdot\underset{\sim}{A} = 0 . \tag{3.3.40}$$

3.3.3. The Oscillator Gauge:

In the phenomenological current confinement model for gluons described in the above section, the consistency demands a condition given by equation (3.3.40). This condition on the gluon potential $\underset{\sim}{A}$ is quite different from the usual Coulomb gauge condition. Making use of the secondary gauge condition given by equation (3.3.29) it can be shown that the Lorentz gauge reduces to that given by equation (3.3.40).

The Lorentz gauge condition is written as

$$\underset{\sim}{\nabla} \cdot \underset{\sim}{A} + \frac{\partial \phi}{\partial t} = 0 \quad . \tag{3.3.41}$$

But from the secondary condition

$$\phi = \frac{\underset{\sim}{\nabla} \cdot \underset{\sim}{\Pi}}{\theta_0} \quad . \tag{3.3.42}$$

Thus eliminating ϕ , equation (3.3.41) reduces to

$$\underset{\sim}{\nabla} \cdot \underset{\sim}{A} + \frac{\underset{\sim}{\nabla} \cdot \frac{\partial \underset{\sim}{\Pi}}{\partial t}}{\theta_0} = 0 \quad . \tag{3.3.43}$$

Now using the Hamilton's equation for $\underset{\sim}{\Pi}$ given by equation (3.3.36), the Lorentz condition can be further reduced to

$$\underset{\sim}{\nabla} \cdot \underset{\sim}{A} + \frac{1}{\theta_0}\left[\nabla^2(\underset{\sim}{\nabla} \cdot \underset{\sim}{A}) - \underset{\sim}{\nabla} \cdot \theta \underset{\sim}{A} - \nabla^2(\underset{\sim}{\nabla} \cdot \underset{\sim}{A})\right] = 0 \tag{3.3.44}$$

Multiplying throughout by θ_0, it becomes

$$\underset{\sim}{\nabla} \cdot \theta \underset{\sim}{A} - \theta_0 \underset{\sim}{\nabla} \cdot \underset{\sim}{A} = 0 \quad . \tag{3.3.45}$$

Thus in this phenomenological confinement scheme with a general choice of θ and θ_0, instead of the Coulomb gauge one comes across to a non-trivial condition given by equation (3.3.45). With the particular choice of θ and θ_0 in this model given by equation (3.3.3), the above condition becomes

$$\underset{\sim}{\nabla} \cdot \alpha^2 r^2 \underset{\sim}{A} - (\alpha^2 r^2 - 2\alpha) \underset{\sim}{\nabla} \cdot \underset{\sim}{A} = 0 \tag{3.3.46}$$

i.e.

$$2\alpha \left[\underset{\sim}{\nabla} \cdot \underset{\sim}{A} + \alpha \underset{\sim}{r} \cdot \underset{\sim}{A} \right] = 0 \quad . \tag{3.3.47}$$

In terms of the oscillator annihilation operator notation it becomes

$$\underset{\sim}{a} \cdot \underset{\sim}{A} = 0 \tag{3.3.48}$$

where $\underset{\sim}{a}$ is the oscillator annihilation operator given as

$$\underset{\sim}{a} = \frac{1}{\sqrt{2\alpha}} \left(\underset{\sim}{\nabla} + \alpha \underset{\sim}{r} \right) \quad . \tag{3.3.49}$$

This is called the oscillator gauge [72,80]. In the oscillator representation $\underset{\sim}{a} . \underset{\sim}{A} = 0$ can be treated in a similar fashion as $\underset{\sim}{\nabla} . \underset{\sim}{A} = 0$ in the usual coordinate/momentum representation.

It can be seen that the conditon given by equation (3.3.45) provides the conservation of the four vector model current J^{μ} consistent with the fact that the nonlinear field current in the exact Yang-Mills´ theory is a conserved quantity. The components of the current J^{μ} here in this model is given by

$$\underset{\sim}{J} = \theta \underset{\sim}{A} \tag{3.3.50}$$

and

$$\rho = \theta_0 \phi \quad . \tag{3.3.51}$$

But from the Lorentz gauge condition

$$\underset{\sim}{\nabla} \cdot \underset{\sim}{A} = -\frac{\partial \phi}{\partial t} \tag{3.3.52}$$

Then

$$\underset{\sim}{\nabla} \cdot \underset{\sim}{J} + \frac{\partial \rho}{\partial t} = \underset{\sim}{\nabla} \cdot \theta \underset{\sim}{A} - \theta_0 \underset{\sim}{\nabla} \cdot \underset{\sim}{A} \quad . \tag{3.3.53}$$

By equation (3.3.45), the r.h.s. of equation (3.3.53) is zero,

$$\underset{\sim}{\nabla} \cdot \underset{\sim}{J} + \frac{\partial \rho}{\partial t} = 0 \tag{3.3.54}$$

i.e. the four vector current defined in equations (3.3.1) to (3.3.3) is also conserved.

3.3.4. Oscillator Transverse Gluon Modes:

The oscillator gauge obtained in equation (3.3.48) helps one to define the two physical transverse modes of the quasi-gluon field in this confinement model. The transverse polarisation vectors here can be written in terms of the oscillator basis vectors (the annihilation and creation operators) :

$$\underset{\sim}{a} = \frac{1}{\sqrt{2\alpha}}\left(\underset{\sim}{\nabla} + \alpha \underset{\sim}{r}\right)$$

and

$$\underset{\sim}{a}^{+} = \frac{1}{\sqrt{2\alpha}}\left(-\underset{\sim}{\nabla} + \alpha \underset{\sim}{r}\right) . \tag{3.3.55}$$

The equation satisfied by the vector potential $\underset{\sim}{A}$ (equation (3.3.4) now becomes

$$\left(\underset{\sim}{a}\cdot\underset{\sim}{a}^{+} + \underset{\sim}{a}^{+}\cdot\underset{\sim}{a}\right)\underset{\sim}{A} = \omega^{2}\underset{\sim}{A} . \tag{3.3.56}$$

The solution for $\underset{\sim}{A}$ then in general can be written as

$$\underset{\sim}{A} = \hat{e}\,\Psi \tag{3.3.57}$$

where $\hat{e}$ is the unit polarization vector and Ψ is the usual oscillator wave function given as [83]

$$\Psi_{nlm} = N_{nl}\left[\underset{\sim}{a}^{+}\cdot\underset{\sim}{a}^{+}\right]^{n} \mathcal{Y}_{lm}(\underset{\sim}{a}^{+})\,\Psi_{0} \tag{3.3.58}$$

where

$$\Psi_0 = \left[\alpha^{1/2} \pi^{-1/2}\right]^{3/2} exp\left[-\frac{\alpha r^2}{2}\right] \tag{3.3.59}$$

and

$$N_{nl} = \left[\frac{4\pi}{2n!!\,(2n+2l+1)!!}\right]^{1/2}. \tag{3.3.60}$$

The energy eigenvalue of the oscillator

$$E_N = \omega_N^2 = (2N+3)\alpha \tag{3.3.61}$$

where

$$N = 2n+l , \tag{3.3.62}$$

$\mathcal{Y}_{lm}(\underset{\sim}{a}^+)$ is the solid spherical harmonics and is related to the usual spherical harmonics as [83]

$$\mathcal{Y}_{lm}(\hat{a}^+) = |\underset{\sim}{a}^+|^l\, \mathcal{Y}_{lm}(\theta,\varphi) . \tag{3.3.63}$$

The unit vectors in the polarization direction can be chosen in the form

$$\hat{e}_1 \propto i\, \underset{\sim}{a} \times \underset{\sim}{a}^+ \tag{3.3.64}$$

$$\hat{e}_2 \propto \underset{\sim}{a} \times (\underset{\sim}{a}^+ \times \underset{\sim}{a}) \tag{3.3.65}$$

$$\hat{e}_3 \quad \propto \quad \underset{\sim}{a}^{+} \quad . \tag{3.3.66}$$

Now the gauge condition $\underset{\sim}{a}.\underset{\sim}{A} = 0$ implies

$$\underset{\sim}{A}_3 = 0 \tag{3.3.67}$$

and the two transverse modes of the confined gluons satisfy

$$\underset{\sim}{a} \cdot \underset{\sim}{A}^{T} = 0 \quad . \tag{3.3.68}$$

As in the case of cavity eigen modes for the transverse gluons [78] the 'magnetic' and 'electric' modes can be defined as

$$\underset{\sim}{a}^{+} \cdot \underset{\sim}{A}^{m} = 0 \tag{3.3.69}$$

and

$$(\underset{\sim}{a}^{+} \times \underset{\sim}{a}) \cdot \underset{\sim}{A}^{E} = 0 \tag{3.3.70}$$

respectively. The solution for $\underset{\sim}{A}^{m}$ can then be expressed as

$$\underset{\sim}{A}^{m}_{NJm} = \mathcal{N}^{m}_{NJ}\, i\,(\underset{\sim}{a} \times \underset{\sim}{a}^{+})\, \Psi_{NJm}\, \bar{e}^{i\omega_N t} \tag{3.3.71}$$

where

$$\mathcal{N}^{m}_{NJ} = \left[J(J+1)\, 2\alpha^{1/2} (2N+3)^{1/2} \right]^{-1/2} . \tag{3.3.72}$$

The electric mode solution is provided by the polarization vector in which the overlap of the $\hat{e}_3$ vector defined above in equation (3.3.36) has to be subtracted. Then the solution for $\underset{\sim}{A}^{E}$ can be written as

$$\underset{\sim}{A}^{E}_{NJm} = -W^{E}_{NJ}\left[\underset{\sim}{a} - \underset{\sim}{a}^{+}\frac{1}{\underset{\sim}{a}\cdot\underset{\sim}{a}^{+}}\underset{\sim}{a}\cdot\underset{\sim}{a}\right]\Psi_{N+1Jm}\, e^{-i\omega^{E}t} \tag{3.3.73}$$

where

$$W^{E}_{NJ} = \left[\frac{J(J+1)}{N+1}\left\{1 - \frac{J(J+1)}{(N+3)(N+1)}\right\} 2\alpha^{1/2}(2N+3)^{1/2}\right]^{-1/2}. \tag{3.3.74}$$

The above solutions for the 'magnetic' and 'electric' modes of the confined gluons can be expressed in terms of the usual vector spherical harmonics. The detailed derivation is given in the Appendix B. The final expressions for these modes are obtained as:

$$\underset{\sim}{A}^{m}_{NJm} = \left[J(J+1)\,2\alpha^{1/2}(2N+3)^{1/2}\right]^{-1/2} R^{(a^{+})}_{NJ}\, \vec{\mathcal{Y}}^{(\hat{a}^{+})}_{JJm}\, e^{-i\omega^{m}t} \tag{3.3.75}$$

and

$$\underset{\sim}{A}^{E}_{NJm} = -\left\{\left[\frac{(N+3)(N+4) - J(J+1)}{N+4}\right] 2\alpha^{1/2}(2N+3)^{1/2}\right\}^{-1/2}$$

$$\times \left\{\left[\frac{(N-J+2)J}{2J+1}\right]^{1/2} R^{(a^{+})}_{NJ+1}\, \vec{\mathcal{Y}}_{JJ+1m} + \right.$$

$$+\left[\frac{(N+J+3)(J+1)}{2J+1}\right]^{1/2} R_{NJ-1}(a t) \vec{\mathcal{Y}}_{JJ-1m}(\hat{a} t)\Big\} e^{-i\omega^E t} .$$

(3.3.76)

The canonical conjugate momenta $\underset{\sim}{\Pi}$ given by equation (3.3.18) and (3.3.30)

$$\underset{\sim}{\Pi} = \frac{\partial \underset{\sim}{A}}{\partial t} + \underset{\sim}{\nabla}\frac{(\underset{\sim}{\nabla}\cdot\underset{\sim}{\Pi})}{\theta_0} \tag{3.3.77}$$

$$\underset{\sim}{\Pi} = \underset{\sim}{\Pi}^T + \underset{\sim}{\Pi}^L \tag{3.3.78}$$

Using the oscillator gauge condition

$$\underset{\sim}{a}\cdot\underset{\sim}{A}^T = \underset{\sim}{a}\cdot\underset{\sim}{\Pi}^T = 0 . \tag{3.3.79}$$

Thus the longitudinal component depends upon the transverse component

$$\underset{\sim}{\Pi}^L(\underset{\sim}{\Pi}^T) = \underset{\sim}{\nabla}\left[\frac{1}{-\nabla^2+\theta_0}\underset{\sim}{\nabla}\cdot\underset{\sim}{\Pi}^T\right] \tag{3.3.80}$$

where

$$\underset{\sim}{\Pi}^T = \frac{\partial \underset{\sim}{A}^T}{\partial t} \tag{3.3.81}$$

By the construction of $\underset{\sim}{A}^T$, $\underset{\sim}{\Pi}^L$ depends on the canonical momenta corresponding to the 'electric' mode only. Thus,

$$\underset{\sim}{\Pi}^L = \underset{\sim}{\nabla}\left[\frac{1}{-\nabla^2+\theta_0}\underset{\sim}{\nabla}\cdot\underset{\sim}{\Pi}^E\right] . \tag{3.3.82}$$

The explicit solutions of $\underset{\sim}{\Pi}^{T}$ can now be written as

$$\underset{\sim}{\Pi}^{M}_{NJm} = \mathcal{N}^{M}_{NJ}\, i\,(\underset{\sim}{a} \times \underset{\sim}{a}^{+})\,\Psi_{NJm}\, e^{i\omega^{M} t} \tag{3.3.83}$$

and

$$\underset{\sim}{\Pi}^{E}_{NJm} = \mathcal{N}^{E}_{NJ}\left[\underset{\sim}{a} - \underset{\sim}{a}^{+}\frac{1}{\underset{\sim}{a}\cdot\underset{\sim}{a}^{+}}\,\underset{\sim}{a}\cdot\underset{\sim}{a}\right]\Psi_{N+1Jm}\, e^{i\omega^{E} t} \tag{3.3.84}$$

where the normalisation constants are

$$\mathcal{N}^{M}_{NJ} = \left[\frac{\alpha^{1/2}(2N+3)^{1/2}}{2J(J+1)}\right]^{1/2} \tag{3.3.85}$$

$$\mathcal{N}^{E}_{NJ} = \left[\frac{\alpha^{1/2}(2N+3)^{1/2}(N+1)}{2J(J+1)}\left(1 - \frac{J(J+1)}{(N+3)(N+1)}\right)\right]^{1/2}. \tag{3.3.86}$$

3.3.5. Quantization:

The confined gluon fields can be quantized using the canonical procedure. For quantization all the field variables are treated as operators and the Poisson bracket satisfy by the canonical conjugate variables $\underset{\sim}{A}$ and $\underset{\sim}{\Pi}$ are replaced by the commutation relations. The commutation relations between $\underset{\sim}{A}$ and $\underset{\sim}{\Pi}$ here in the oscillator gauge can be written as

$$[\Pi_i(\underset{\sim}{x}), A_j(\underset{\sim}{x}')] = -i\left(\delta_{ij} - \frac{a_i^+ a_j}{\underset{\sim}{a}\cdot\underset{\sim}{a}^+}\right)\delta^3(\underset{\sim}{x}-\underset{\sim}{x}')$$

(3.3.87)

Here the factor $(\delta_{ij} - a_i^+ a_j/\underset{\sim}{a}\cdot\underset{\sim}{a}^+)$ is just to ensure the oscillator gauge condition

$$\underset{\sim}{a}\cdot\underset{\sim}{A}\,|PHYS\rangle = 0$$

(3.3.88)

Accordingly the solutions given by equation (3.3.67) for $\underset{\sim}{A}^3$ is

$$\underset{\sim}{A}^3\,|PHYS\rangle = 0$$

(3.3.89)

Thus

$$\underset{\sim}{a}\cdot\underset{\sim}{A}^T|PHYS\rangle = \underset{\sim}{a}\cdot\underset{\sim}{\Pi}^T|PHYS\rangle = 0$$

(3.3.90)

and

$$\left\{\underset{\sim}{\Pi}^3 - \underset{\sim}{\nabla}\left(\frac{1}{-\nabla^2+\theta_0}\underset{\sim}{\nabla}\cdot\underset{\sim}{\Pi}^E\right)\right\}|PHYS\rangle = 0$$

(3.3.91)

Now the gluon field strength $\underset{\sim}{A}$ can be expanded in the oscillator eigen basis.

$$\underset{\sim}{A}(x) = \sum_{NJm\lambda}\left(C_{NJm\lambda}\underset{\sim}{A}^{\lambda}_{NJm}(x) + C^+_{NJm\lambda}\underset{\sim}{A}^{\lambda *}_{NJm}(x)\right)$$

(3.3.92)

where λ refers to the type of modes (E or M). And the summation is over all the oscillator eigenvalues. Here $C_{NJm\lambda}$ and $C^+_{NJm\lambda}$ are the annihilation and creation operators for the gluon quanta respectively. From the commutation relations between $\hat{A}$'s and Π's, it can be shown that $C_{NJm\lambda}$ and $C^{+}_{NJm\lambda}$ satisfy the following commutation relationships.

$$[C_{NJm\lambda}, C^{+}_{N'J'm'\lambda'}] = \delta_{NN'}\delta_{JJ'}\delta_{mm'}\delta_{\lambda\lambda'}$$

$$[C_{NJm\lambda}, C_{N'J'm'\lambda'}] = [C^{+}_{NJm\lambda}, C^{+}_{N'J'm'\lambda'}] = 0 \quad (3.3.93)$$

The Hamiltonian operator can be obtained from equation (3.3.33) using the expansion of (3.3.92)

$$H = \sum_{NJm\lambda} \omega_N \left(C^{+}_{NJm\lambda} C_{NJm\lambda} + \frac{3}{2} \right) \quad (3.3.94)$$

Here $C^{+}_{NJm\lambda} C_{NJm\lambda}$ is the number operator. The zero point fluctuation of the gluon field is to be removed, since this leads to an unobservable infinity. It is taken care by writing the Hamiltonian as the normal product:

$$H = :\sum_{NJm} \omega_N C^{+}_{NJm\lambda} C_{NJm\lambda}: \quad (3.3.95)$$

where

$$\omega_N = (2N+3)^{1/2} \alpha^{1/2} . \quad (3.3.96)$$

The spectroscopic implications of these gluon energy spectra will be discussed in the next chapter.

3.4. An Equivalent Dielectric Function Corresponding to the Current in CCM

Based on the colour dielectric picture proposed by T.D. Lee [52] an equivalent description can be obtained from the current confinement model. The colour super current J_μ assumed in CCM can be considered as a self induced polarization colour current in the gluon field described by $\underset{\sim}{A}$. In this case the usual Maxwell's displacement current $\underset{\sim}{D}$ can be written as

$$\underset{\sim}{D} = \underset{\sim}{E} + \underset{\sim}{P} \tag{3.4.1}$$

$\underset{\sim}{E}$ is the colour electric field causing the polarization and $\underset{\sim}{P}$ is the field due to polarization. In the absence of any external source $\underset{\sim}{D}$ satisfies

$$\underset{\sim}{\nabla} \cdot \underset{\sim}{D} = \rho_{ind} \tag{3.4.2}$$

and

$$\frac{\partial \underset{\sim}{D}}{\partial t} = \underset{\sim}{\nabla} \times \underset{\sim}{B} \tag{3.4.3}$$

where $\underset{\sim}{B}$ is the external magnetic field

$$\underset{\sim}{B} = \underset{\sim}{\nabla} \times \underset{\sim}{A} \tag{3.4.4}$$

and

$$\underset{\sim}{E} = -\frac{\partial \underset{\sim}{A}}{\partial t} - \underset{\sim}{\nabla}\phi \; . \tag{3.4.5}$$

From equations (3.4.1) and (3.4.2), the induced charge can be written as

$$\rho_{ind} = \nabla \cdot P \tag{3.4.6}$$

As $\underset{\sim}{\nabla} . \underset{\sim}{E}=0$ in absence of a source. And the induced polarization current density

$$\underset{\sim}{J} = -\frac{\partial \underset{\sim}{P}}{\partial t} \quad . \tag{3.4.7}$$

Thus the four vector current

$$J_{\mu} = \left(\frac{-\partial P}{\partial t} \, , \underset{\sim}{\nabla} \cdot \underset{\sim}{P}\right) \quad . \tag{3.4.8}$$

From the current expressions in CCM the polarization vector is given by

$$\underset{\sim}{P} = -\frac{i \theta \underset{\sim}{A}}{\omega} \tag{3.4.9}$$

and from the expression for $\underset{\sim}{E}$ from equation (3.4.5),

$$\underset{\sim}{\nabla} \cdot \underset{\sim}{E} = i\omega \underset{\sim}{\nabla} \cdot \underset{\sim}{A} - \nabla^2 \phi \tag{3.4.10}$$

and

$$\underset{\sim}{A} = \frac{\underset{\sim}{E} + \underset{\sim}{\nabla} \phi}{i\omega} \quad . \tag{3.4.11}$$

Using the Lorentz condition $\underset{\sim}{A}$ can be eliminated from the above equation :

$$\underset{\sim}{\nabla} \cdot \underset{\sim}{E} = -\omega^2 \phi - \nabla^2 \phi \tag{3.4.12}$$

Hence

$$\phi = \frac{-1}{\omega^2+\nabla^2} \underset{\sim}{\nabla} \cdot \underset{\sim}{E} . \tag{3.4.13}$$

Thus

$$\underset{\sim}{P} = \frac{-\theta}{\omega^2} \left[\underset{\sim}{E} + \underset{\sim}{\nabla} \phi \right] . \tag{3.4.14}$$

And finally, substituting for $\underset{\sim}{\nabla}\phi$ using 3.4.13,

$$\underset{\sim}{P} = \frac{-\theta}{\omega^2} \left[1 - \underset{\sim}{\nabla} \frac{1}{\omega^2+\nabla^2} \underset{\sim}{\nabla} \cdot \right] \underset{\sim}{E} . \tag{3.4.15}$$

The equation (3.4.1) gives

$$\underset{\sim}{D} = \left[1 - \frac{\theta}{\omega^2} \left(1 - \underset{\sim}{\nabla} \frac{1}{\omega^2+\nabla^2} \underset{\sim}{\nabla} \cdot \right) \right] \underset{\sim}{E} \tag{3.4.16}$$

$$= \epsilon(\theta, \underset{\sim}{\nabla}) \underset{\sim}{E} \tag{3.4.17}$$

where the dielectric function is given by the non local operator expression

$$\epsilon(\theta, \underset{\sim}{\nabla}) = 1 - \frac{\theta}{\omega^2} \left(1 - \underset{\sim}{\nabla} \frac{1}{\omega^2+\nabla^2} \underset{\sim}{\nabla} \cdot \right) . \tag{3.4.18}$$

With the particular choice of θ, it becomes an inhomogeneous non local function with both the asymptotic freedom and the confinement built in it:

$$\epsilon(\underset{\sim}{r}, \underset{\sim}{\nabla}) = 1 - \frac{\alpha^2 r^2}{\omega^2} \left(1 - \underset{\sim}{\nabla} \frac{1}{\omega^2+\nabla^2} \underset{\sim}{\nabla} \cdot \right) . \tag{3.4.19}$$

Thus, to get an equivalent dielectric confinement scheme to the CCM for gluons a dielectric function obtained in equation (3.4.19) is required.

3.5. Maxwell's Equation in a Dielectric Medium versus Dirac Equation in RHM

In this section, a comparative study of the Dirac equation for quarks in RHM with the Maxwell's equation in a dielectric medium is made. This helps us to obtain the form of the dielectric function similar to the potential used in RHM. The Dirac equations are written in the spinor two component form and the Maxwell's equations are written in the spin matrix form. Here the spin matrix for a vector field is used to represent the curl operator into $\underset{\sim}{S}.\underset{\sim}{P}$ form. Where $\underset{\sim}{S}$ is the spin matrix for the vector field given by [38],

$$S_x = \begin{pmatrix} 0 & 0 & 0 \\ 0 & 0 & -i \\ 0 & i & 0 \end{pmatrix} ; \quad S_y = \begin{pmatrix} 0 & 0 & i \\ 0 & 0 & 0 \\ -i & 0 & 0 \end{pmatrix} ; \quad S_z = \begin{pmatrix} 0 & -i & 0 \\ i & 0 & 0 \\ 0 & 0 & 0 \end{pmatrix} \tag{3.5.1}$$

and

$$\underset{\sim}{P} = -i \underset{\sim}{\nabla} , \tag{3.5.2}$$

Thus the curl operator becomes $\underset{\sim}{S}.\underset{\sim}{P}$.

The Maxwell's equations in a dielectric medium

$$\nabla \times \mathbf{E} = -\frac{\partial \mathbf{B}}{\partial t} \quad ; \quad \nabla \times \mathbf{B} = \epsilon(r)\frac{\partial \mathbf{E}}{\partial t} \tag{3.5.3}$$

can be rewritten in the form

$$(\mathbf{S}\cdot\mathbf{P})\,\mathbf{E} = i\omega\mathbf{B}$$

and

$$(\mathbf{S}\cdot\mathbf{P})\,\mathbf{B} = -\omega\epsilon(r)\,i\,\mathbf{E} \tag{3.5.4}$$

where the time variation of the fields are taken as exp(-iωt). Similarly the two component Dirac spinor equation for quarks in RHM is given by [23]

$$(\boldsymbol{\sigma}\cdot\mathbf{P})\,\chi = (E+m)\,\varphi$$
$$(\boldsymbol{\sigma}\cdot\mathbf{P})\,\varphi = (E-\alpha^2 r^2 - m)\,\chi \ . \tag{3.5.5}$$

By comparing these two set of equations (3.5.4) and (3.5.5), it would be possible to associate formally,

$$\varphi \rightarrow i\mathbf{B}$$
$$\chi \rightarrow \mathbf{E}$$
$$\omega \rightarrow E+m \ . \tag{3.5.6}$$

Then

$$\omega\epsilon(r) \rightarrow E-m-\alpha^2 r^2 \tag{3.5.7}$$

or

$$\epsilon(r) \rightarrow \frac{E-m}{E+m} - \frac{\alpha^2 r^2}{E+m} . \tag{3.5.8}$$

This analogy gives the form of a dielectric function

$$\epsilon(r) = b - a^2 r^2 \tag{3.5.9}$$

where b and a can be associated to

$$b \simeq \frac{E-m}{E+m} \quad ; \quad a^2 \simeq \frac{\alpha^2}{E+m} . \tag{3.5.10}$$

For a massless gluon case b is unity. Thus the dielectric function for the confinement of gluons could be in the form

$$\epsilon(r) = 1 - a^2 r^2 \tag{3.5.11}$$

Such that the dynamical equations satisfied by the gluons and the quarks in RHM become similar. Here, as $r \rightarrow 0$, $\epsilon(r) \rightarrow 1$ corresponds to the asymptotic free region; and as $r \rightarrow \pm \frac{1}{a}$, $\epsilon(r) \rightarrow 0$ corresponds to the confinement region. From the dielectric function obtained in section 3.4, equation (3.4.22), it can be seen that the similar expression for $\epsilon(r)$ can be deduced i.e.,

$$\epsilon(\underset{\sim}{r}, \underset{\sim}{\nabla}) \rightarrow \epsilon(r) = 1 - \frac{\alpha^2}{\omega^2} r^2 \tag{3.5.12}$$

after neglecting the momentum dependent part.

3.6. A Colour Dielectric Confinement Model for Gluons (DCM)

Here the gluons are considered as moving in a medium whose colour-dielectric property is defined by a simple inhomogeneous dielectric function given by equation (3.5.11) :

$$\epsilon(r) = 1 - a^2 r^2 \tag{3.6.1}$$

where a is the parameter in this model, and r is the spatial coordinate. For any value of $r \neq 0$,

$$\epsilon(r) < 1 . \tag{3.6.2}$$

This corresponds to the asymptotic freedom. As r goes to the confinement regime, say $r \rightarrow 1/a$,

i.e.

$$a = \frac{1}{R_{hadron}} \tag{3.6.3}$$

where

$$\epsilon(r) = 0 . \tag{3.6.4}$$

This makes the medium a perfect dielectric. In this case, the colour electric field is pushed inside the region, leading to colour confinement [43,52]. Thus this model is very close to the bag model, described earlier. In that case the dielectric function $\epsilon(r)$ is a step function with $\epsilon(r) = 1$ inside the bag and $\epsilon(r) = 0$ outside the bag. Here with a smoothly varying form of $\epsilon(r)$ avoids the difficulty arising out of the sharpness of the boundary.

As in the case of CCM, the gluons are considered here to obey the quasi-Maxwell's equations. With the colour-dielectric constant $\epsilon(r)$:

$$\begin{aligned} \underset{\sim}{\nabla} \times \underset{\sim}{E} &= i\omega \underset{\sim}{B} \\ \underset{\sim}{\nabla} \cdot \underset{\sim}{B} &= 0 \\ \underset{\sim}{\nabla} \times \underset{\sim}{B} &= -i\omega D \\ \underset{\sim}{\nabla} \cdot \underset{\sim}{D} &= \rho \end{aligned} \tag{3.6.5}$$

where

$$\underset{\sim}{D} = \epsilon(r) \underset{\sim}{E} \tag{3.6.6}$$

$$\underset{\sim}{E} = i\omega \underset{\sim}{A} - \underset{\sim}{\nabla} \phi \tag{3.6.7}$$

and

$$\underset{\sim}{B} = \underset{\sim}{\nabla} \times \underset{\sim}{A} \quad . \tag{3.6.8}$$

Thus the equation for the gluon vector potential $\underset{\sim}{A}$ can be obtained as

$$-\nabla^2 \underset{\sim}{A} - \omega^2 \epsilon(r) \underset{\sim}{A} = -\underset{\sim}{\nabla}(\underset{\sim}{\nabla} \cdot \underset{\sim}{A}) + i\omega\, \epsilon(r) \underset{\sim}{\nabla} \phi \, . \tag{3.6.9}$$

As the dielectric constant is a radially varying inhomogeneous function, a homogeneous equation for $\underset{\sim}{A}$ is possible only if the r.h.s. of the equation (3.6.9) is chosen to be zero.

$$\underset{\sim}{\nabla}(\underset{\sim}{\nabla}\cdot\underset{\sim}{A}) - i\omega\epsilon(r)\underset{\sim}{\nabla}\phi = 0 . \qquad (3.6.10)$$

This is quite different from the usual Lorentz gauge condition

$$\underset{\sim}{\nabla}\cdot\underset{\sim}{A} - i\omega\phi = 0 . \qquad (3.6.11)$$

But in the regions where $\epsilon(r) \rightarrow 1$, the equation (3.6.10) reduces to that of equation (3.6.11) and as $\epsilon(r) \rightarrow 0$, the equation reduces to the choice of

$$\underset{\sim}{\nabla}\cdot\underset{\sim}{A} = 0 \qquad (3.6.12)$$

By imposing the Lorentz condition on $\underset{\sim}{A}$ and ϕ it is possible to find the eigen modes of $\underset{\sim}{A}$ within the choice of Coulomb gauge condition. Here

$$\phi = \frac{\underset{\sim}{\nabla}\cdot\underset{\sim}{A}}{i\omega} \qquad (3.6.13)$$

Substituting ϕ in equation (3.6.9), we get

$$-\nabla^2\underset{\sim}{A} - \omega^2\epsilon(r)\underset{\sim}{A} = -\underset{\sim}{\nabla}(\underset{\sim}{\nabla}\cdot\underset{\sim}{A}) + i\omega\epsilon(r)\frac{\underset{\sim}{\nabla}(\underset{\sim}{\nabla}\cdot\underset{\sim}{A})}{i\omega} \qquad (3.6.14)$$

$$= \left[\epsilon(r) - 1\right]\underset{\sim}{\nabla}(\underset{\sim}{\nabla}\cdot\underset{\sim}{A}) . \qquad (3.6.15)$$

Further the choice of Coulomb gauge gives

$$-\nabla^2\underset{\sim}{A} - \omega^2\epsilon(r)\underset{\sim}{A} = 0 \qquad (3.6.16)$$

Using the expression for $\epsilon(r)$

$$-\nabla^2 \underset{\sim}{A} + a^2 \omega^2 r^2 \underset{\sim}{A} = \omega^2 \underset{\sim}{A} \quad . \tag{3.6.17}$$

The solution for $\underset{\sim}{A}$ now can be written as

$$\underset{\sim}{A}(r,\theta,\varphi) = R(r)\,\vec{y}(\theta,\varphi) \tag{3.6.18}$$

where $\vec{y}(\theta,\varphi)$ is the vector spherical harmonics [123] and R(r) satisfies the radial equation

$$\frac{d^2R}{dr^2} + \frac{2}{r}\frac{dR}{dr} + \left[\omega^2\epsilon(r) - \frac{l(l+1)}{r^2}\right]R = 0 \tag{3.6.19}$$

the radial solution is the usual 3-dimensional oscillator wave function (see Appendix C);

$$R_{Nl} = \mathcal{N}_{Nl}(\Omega_N r)^l \exp\left(-\frac{\Omega_n^2 r^2}{2}\right) L_{\frac{N-l}{2}}^{l+\frac{1}{2}}(\Omega_N^2 r^2) \tag{3.6.20}$$

where Ω_N the size parameter is

$$\Omega_N = (a\omega_N)^{1/2} \tag{3.6.21}$$

and the frequency

$$\omega_N = (2N+3)a \quad . \tag{3.6.22}$$

Here the quanta

$$N = 2n + l \tag{3.6.23}$$

and

$$W_{Nl} = \left[\frac{\Omega_N^3 \left(\frac{N-l}{2}\right)!}{4\pi\, \Gamma\left(\frac{N+l+3}{2}\right)} \right]^{1/2} . \qquad (3.6.24)$$

The two transverse gluon modes are defined by

$$\underset{\sim}{r} \cdot \underset{\sim}{A} = 0 \text{ for TE or M mode} \qquad (3.6.25)$$

and

$$\underset{\sim}{L} \cdot \underset{\sim}{A} = 0 \text{ for TM or E mode} \qquad (3.6.26)$$

Then the transverse electric or magnetic and the transverse magnetic or electric solutions are obtained as

$$\underset{\sim}{A}^{M}_{Nlm} = \underset{\sim}{L}\, R_{Nl}\, Y_{lm}(\theta,\varphi) \qquad (3.6.27)$$

and

$$\underset{\sim}{A}^{E}_{Nlm} = \underset{\sim}{\nabla} \times \underset{\sim}{L}\, R_{Nl}\, Y_{lm}(\theta,\varphi) \qquad (3.6.28)$$

respectively. In terms of the vector spherical harmonics [123], these solutions can be written as

$$\underset{\sim}{A}^{M}_{NJm} = \frac{[J(J+1)]^{-1/2}}{\sqrt{2\omega_N \epsilon(r)}} R_{NJ}(r)\, \vec{\mathcal{Y}}_{JJm}(\hat{n})\, e^{i\omega_N t} \qquad (3.6.29)$$

with parity

$$P = (-1)^J \qquad (3.6.30)$$

and

$$A^{E}_{NJm} = \frac{1}{\sqrt{2\omega_N \epsilon(r)}} \left\{ \sqrt{\frac{J}{2J+1}}\, R_{NJ+1}(r)\, \vec{\mathcal{Y}}_{JJ+1m}(\hat{n}) + \right.$$

$$+\sqrt{\frac{J+1}{2J+1}}\; R_{N\,J-1}(r)\; \vec{\mathcal{Y}}_{J\,J-1\,m}(\hat{n})\Big\}\, e^{-i\omega_N t}$$

(3.6.31)

with parity

$$P = (-1)^{J+1} \quad .$$

(3.6.32)

where the vector spherical harmonics satisfy

$$\int \vec{\mathcal{Y}}^{*}_{\ell J m}\, \vec{\mathcal{Y}}_{\ell' J' m'}\, d\Omega = \delta_{\ell\ell'}\, \delta_{JJ'}\, \delta_{mm'}$$

(3.6.33)

and

$$J^2\, \vec{\mathcal{Y}}_{\ell J m}(\hat{n}) = J(J+1)\, \vec{\mathcal{Y}}_{\ell J m}(\hat{n})$$

(3.6.34)

$$J_z\, \vec{\mathcal{Y}}_{\ell J m}(\hat{n}) = m\, \vec{\mathcal{Y}}_{\ell J m}(\hat{n}) \quad .$$

(3.6.35)

3.6.1. Quantization

The Lagrangian density for the DCM can be written as

$$\mathcal{L} = \frac{1}{2}\left[\epsilon(r)|\dot{\underset{\sim}{A}}|^2 - |\underset{\sim}{\nabla}\times\underset{\sim}{A}|^2\right] \quad .$$

(3.6.36)

The canonically conjugate momentum is given by:

$$\underset{\sim}{\Pi} = \frac{\partial \mathcal{L}}{\partial \dot{\underset{\sim}{A}}} = \epsilon(r)\,\dot{\underset{\sim}{A}}^{*} \quad .$$

(3.6.37)

Then the Hamiltonian density is given by:

$$\mathcal{H} = \underset{\sim}{\Pi}\cdot\dot{\underset{\sim}{A}} - \mathcal{L}$$

(3.6.38)

$$= \frac{1}{2}\left[\epsilon(r)|\dot{\underset{\sim}{A}}|^2 + |\underset{\sim}{\nabla} \times \underset{\sim}{A}|^2\right] . \tag{3.6.39}$$

Using the vector identity

$$\nabla \cdot (\underset{\sim}{u} \times \underset{\sim}{V}) = \underset{\sim}{V} \cdot \underset{\sim}{\nabla} \times \underset{\sim}{u} - \underset{\sim}{u} \cdot \underset{\sim}{\nabla} \times \underset{\sim}{V} \tag{3.6.40}$$

and after doing the partial integration, the Hamiltonian becomes

$$H = \frac{1}{2}\int d^3r\left[\epsilon(r)|\dot{A}|^2 + \underset{\sim}{A} \cdot (\underset{\sim}{\nabla} \times (\underset{\sim}{\nabla} \times \underset{\sim}{A}^*))\right] \tag{3.6.40}$$

$$= \frac{1}{2}\int d^3r\left[\epsilon(r)|\dot{\underset{\sim}{A}}|^2 - \underset{\sim}{A} \cdot \nabla^2 \underset{\sim}{A}^* + \underset{\sim}{A} \cdot \underset{\sim}{\nabla}(\underset{\sim}{\nabla} \cdot \underset{\sim}{A}^*)\right]. \tag{3.6.41}$$

Using the Coulomb gauge and the dynamical equation for $\underset{\sim}{A}$ given by equation (3.6.16), we obtain,

$$H = \int d^3r\, \epsilon(r)\omega^2 |\underset{\sim}{A}|^2 \tag{3.6.42}$$

For second quantization $\underset{\sim}{A}$ and $\underset{\sim}{\Pi}$ are treated as independent coordinates and they are expanded in the basis of two transverse eigen modes. Thus as in the case of CCM,

$$A_s = \sum_{\omega J m \lambda} c_{\omega J m \lambda} A^{\lambda}_{\omega J m s} + c^{\dagger}_{\omega J m \lambda} A^{\lambda *}_{\omega J m s} \tag{3.6.43}$$

and

$$\Pi_s = \sum_{\omega' J' m' \lambda'} \left[i\omega\, \epsilon(r)\, C^{+}_{\omega' J' m' \lambda'} A^{\lambda' *}_{\omega' J' m' s} + h.c. \right] \tag{3.6.44}$$

A_s and Π_s are the components of the canonical conjugate field variables satisfying the commutation relationships

$$\left[A_s(r), \Pi_{s'}(r') \right] = i\,\delta_{ss'}\,\delta(r - r')$$

and

$$\left[A_s(r), A_{s'}(r') \right] = \left[\Pi_s(r), \Pi_{s'}(r') \right] = 0 . \tag{3.6.45}$$

It can now be found that the q-numbers (the annihilation and creation operators) C and C^{+} satisfy

$$\left[C_{\omega J m \lambda}, C^{+}_{\omega' J' m' \lambda'} \right] = \delta_{\omega\omega'}\,\delta_{JJ'}\,\delta_{mm'}\,\delta_{\lambda\lambda'}$$

$$\left[C_{\omega J m \lambda}, C_{\omega' J' m' \lambda'} \right] = \left[C^{+}_{\omega J m \lambda}, C^{+}_{\omega' J' m' \lambda'} \right] = 0 . \tag{3.6.46}$$

The Hamiltonian operator becomes

$$:H: = : \sum_{\omega J m \lambda} \frac{1}{2}\omega \left[C_{\omega J m \lambda} C^{+}_{\omega J m \lambda} + C^{+}_{\omega J m \lambda} C_{\omega J m \lambda} \right] : . \tag{3.6.47}$$

Using the commutation relations given by equation (3.6.46), it becomes

$$:H: = \sum_{\omega J m \lambda} \omega \left[C^{+}_{\omega J m \lambda} C_{\omega J m \lambda} \right] \tag{3.6.48}$$

where ω is given by the eigenvalue $\omega_N = (2N+3)a$ from equation (3.6.28). It is to be noted that even though the DCM is very much analogous to RHM, the energy expression in DCM differs from that of RHM and that of CCM, while the CCM and RHM have similar energy spectra.

3.7. Summary

In this chapter two different confinement models for gluons (1) the current confinement model (CCM) and (2) the dielectric confinement model (DCM) are described. A probable connection between these models and the Yang-Mill's dynamics are shown. The CCM is itself characterised by a nonlocal dielectric function. Finally, the essential features of CCM and DCM are compared in the following.

Features	CCM	DCM
Confinement through	Colour super current	Inhomogeneous colour dielectric medium
Explicit form	$\underset{\sim}{J} = \alpha^2 r^2 \underset{\sim}{A}$ $\rho = (\alpha^2 r^2 - 2\alpha)\phi$	$\epsilon(r) = 1 - \alpha^2 r^2$
Lagrangian	$-\frac{1}{2}\left[E^2 - B^2 + J\cdot A - \rho\phi\right]$	$-\frac{1}{2}\left[E\cdot D - B^2\right]$
Primary gauge choice	$\nabla\cdot A - i\omega\phi = 0$	$\nabla\cdot A - i\omega\phi = 0$
Dynamical equation	$-\nabla^2 A + \alpha^2 r^2 A = \omega^2 A$	$-\nabla^2 A - \omega^2\epsilon(r) A = 0$
Secondary gauge	$(\nabla + \alpha r)\cdot \underset{\sim}{A} = 0$	$\nabla\cdot A = 0$

choice	(Oscillator gauge)	(Coulomb gauge)
The energy of the gluon quanta	$(2N+3)^{1/2}\alpha^{1/2}$	$(2N+3)a$
The transverse mode defined by	$a^{+}\cdot A^{m} = 0$ $(a^{+}\times a)\cdot A^{E} = 0$	$\gamma\cdot A^{m} = 0$ $L\cdot A^{E} = 0$
The lowest transverse gluon modes		
1) Magnetic	$R_{11}\,\vec{\mathcal{Y}}_{11m}\,e^{-i\sqrt{5\alpha}t}$	$R_{11}\,\vec{\mathcal{Y}}_{11m}\,e^{-i5ta}$
2) Electric	$R_{00}\,\vec{\mathcal{Y}}_{10m}\,e^{-i\sqrt{3\alpha}t}$	$R_{00}\,\vec{\mathcal{Y}}_{10m}\,e^{-i3at}$
The size parameter	α	$\Omega = (a\omega)^{1/2}$.

Appendix A

Let

$$\sum_{m,n} f^{lmn} f^{qmn} = S_{lq} :$$

Here f^{lmn}'s are the SU(3) colour structure constant. It is antisymmetric in its colour permutations. Using the non zero values of f^{lmn}'s given [43]

lmn	f
123	1
147	1/2
156	-1/2
246	1/2
257	1/2
345	1/2
367	-1/2
458	1/2 3
678	1/2 3

(A.2)

Since f^{lmn}'s are antisymmetric,

$$\sum_{m,n} f^{lmn} f^{qmn} = 2 \sum_{m<n} f^{lmn} f^{qmn} . \tag{A.3}$$

Thus for particular choice of l=1, q=1

$$S_{11} = 2\left[f^{123} f^{123} + f^{147} f^{147} + f^{156} f^{156} \right] \tag{A.4}$$

From (A.2),

$$S_{11} = 3 . \tag{A.5}$$

For l=1, q=2,

$$S_{12} = 2\left[f^{123} f^{223} + f^{147} f^{247} + f^{156} f^{256}\right] . \tag{A.6}$$

Using (A.2),

$$S_{12} = 0 . \tag{A.7}$$

Similarly it can be seen that

$$S_{22} = S_{33} = S_{44} = \ldots S_{88} = 3 \tag{A.8}$$

and all other lq combinations vanish. Thus

$$\sum_{m,n} f^{lmn} f^{qmn} = 3\,\delta_{lq} . \tag{A.9}$$

Appendix B

Normalized CCM Solutions in terms of the Vector Spherical Harmonics

The oscillator state in three dimension can be written as [83]

$$|nJm\rangle = N_{nJ}\,(\underset{\sim}{a}^{+}\cdot\underset{\sim}{a}^{+})^{n}\,\mathcal{Y}_{Jm}(\underset{\sim}{a}^{+})\,|0\rangle \tag{B.1}$$

where $\underset{\sim}{a}^{+}$ is the oscillator creation operator, $|0\rangle$ is the ground state given as

$$|0\rangle = \frac{b^{3/2}}{\pi^{3/4}}\exp\left[-\frac{b^{2}r^{2}}{2}\right] \tag{B.2}$$

the normalization coefficient N_{nJ} is given by [83]

$$N_{nJ} = (-1)^{J}\left[\frac{4\pi}{2n!!\,(2n+2J+1)!!}\right]^{1/2} \tag{B.3}$$

and the $\mathcal{Y}_{Jm}(a^{+})$ is the solid spherical harmonic given by

$$\mathcal{Y}_{Jm}(a^{+}) = (a^{+})^{l}\,Y_{Jm}(\theta,\varphi) \quad . \tag{B.4}$$

Here n is the radial quantum number, which is related to the oscillator quanta N by

$$N = 2n+l \quad . \tag{B.5}$$

Here the normalization N_{nJ} is obtained by computing the scalar product of $|nJm\rangle$ with itself i.e.

$$\langle nJm|nJm\rangle = 1 = N_{nJ}^2 \langle 0| \mathcal{Y}^{+}_{Jm}(a^{+}) (a \cdot a)^n (a^{+} \cdot a^{+})^n \mathcal{Y}_{Jm}(a^{+}) |0\rangle . \tag{B.6}$$

Here it can be seen that $(\underset{\sim}{a}.\underset{\sim}{a})$ operate on $(a^{+} \cdot a^{+})^n \mathcal{Y}_{Jm}(a^{+})$ is the same way as the Laplacian ∇^2 operating on $(\underset{\sim}{r}.\underset{\sim}{r})^n \mathcal{Y}_{Jm}(r)$ [83].

Using this correspondence $a_j \rightarrow \frac{\partial}{\partial a_j^{+}}$ the polarization of the gluons in CCM can be expressed in terms of the vector spherical harmonics. The three possible polarization in CCM are taken as

$$\underset{\sim}{A}^1 = \mathcal{N}_1 \, (\underset{\sim}{a}^{+} \times \underset{\sim}{a}) \, |nJm\rangle \tag{B.7}$$

$$\underset{\sim}{A}^2 = \mathcal{N}_2 \left[\underset{\sim}{a} - \underset{\sim}{a}^{+} \frac{1}{\underset{\sim}{a} \cdot \underset{\sim}{a}^{+}} \underset{\sim}{a} \cdot \underset{\sim}{a} \right] |n'Jm\rangle \tag{B.8}$$

and

$$\underset{\sim}{A}^3 = \mathcal{N}_3 \, \underset{\sim}{a}^{+} \, |nJm\rangle \tag{B.9}$$

It can be shown that [83]

$$\underset{\sim}{a}^{+} \times \underset{\sim}{a} = i \underset{\sim}{L} \tag{B.10}$$

where $\underset{\sim}{L}$ is the angular momentum operator. Thus

$$\underset{\sim}{A}^1 = \mathcal{N}_1 \, \underset{\sim}{L} \, |nJm\rangle \tag{B.11}$$

where i is absorbed in $\mathcal{N}_1$. Since $\underset{\sim}{L}$ operates only on the angular part of the state $|nJm\rangle$, one has [123],

$$\underset{\sim}{L} Y_{Jm} = \sum_{\mu} (-1)^{\mu} \xi_{-\mu} L_{\mu} Y_{Jm} \tag{B.12}$$

$$L_{\mu} Y_{Jm} = (-1)^{\mu} \sqrt{J(J+1)}\, C(J1J; -\mu, m+\mu)\, Y_{J\,m+\mu} \tag{B.13}$$

where ξ_{μ}'s are the spin component of the wave function and $C(J1J; -\mu, m+\mu)$ is the CG coefficient for the spin and angular momentum coupling. Thus

$$\underset{\sim}{L} Y_{Jm} = \sqrt{J(J+1)} \sum_{\mu} (-1)^{\mu} C(J1J; -\mu, m+\mu)\, \xi_{-\mu} Y_{J\,m+\mu} \tag{B.14}$$

$$= \sqrt{J(J+1)}\, \vec{\mathcal{Y}}_{JJm}(\hat{n}) \tag{B.15}$$

where $\vec{\mathcal{Y}}_{JJm}$ is the vector spherical harmonics defined by [123]

$$\vec{\mathcal{Y}}_{JJm} = \sum_{\mu} (-1)^{\mu} C(J1J; -\mu, m+\mu)\, \xi_{-\mu} Y_{J,m+\mu} \tag{B.16}$$

Thus the normalized '$\underset{\sim}{A}$' solution is given as

$$A'_{nJm} = \frac{1}{\sqrt{J(J+1)}} |nJJm\rangle \tag{B.17}$$

where

$$|nJJm\rangle = N_{nJ} (a^{+} \cdot a^{+})^{n} \vec{\mathcal{Y}}_{JJm}(a^{+}) |0\rangle \tag{B.18}$$

where the solid vector spherical harmonic

$$\vec{\mathcal{Y}}_{JJm}(a^{+}) = (a^{+})^{J} \vec{\mathcal{Y}}_{JJm}(\hat{n}) \tag{B.19}$$

and the vector spherical harmonic $\vec{\mathcal{Y}}_{Jlm}(\hat{n})$ satisfy the following equations

$$\int \vec{\mathcal{Y}}^{*}_{Jlm} \vec{\mathcal{Y}}_{J'l'm'} \, d\Omega = \delta_{JJ'} \delta_{ll'} \delta_{mm'} \tag{B.20}$$

$$J^{2} \vec{\mathcal{Y}}_{lJm}(\hat{n}) = J(J+1) \vec{\mathcal{Y}}_{lJm}(\hat{n}) \tag{B.21}$$

$$J_{z} \mathcal{Y}_{lJm}(\hat{n}) = m \vec{\mathcal{Y}}_{lJm}(\hat{n}) \, . \tag{B.22}$$

Extending the gradient formula the second gluon mode can also be expressed in terms of the vector spherical harmonics:

:

$$\nabla \left[\phi(r) Y_{Jm}(\hat{r}) \right] = -\sqrt{\frac{J+1}{2J+1}} \left[\frac{d\phi}{dr} - \frac{J}{r}\phi \right] \vec{\mathcal{Y}}_{JJ+1m}(\hat{r})$$

$+$

$$+\sqrt{\frac{J}{2J+1}}\left[\frac{d\phi}{dr}+\frac{J+1}{r}\phi\right]\vec{\mathcal{Y}}_{JJ-1m}(\hat{r}) \tag{B.23}$$

~~Since~~ The oscillator operators $\underset{\sim}{a}$ and $\underset{\sim}{a}^+$ satisfy

$$[a_i, a_j^+] = \delta_{ij} \; ; \; [a_i, a_j] = [a_i^+, a_j^+] = 0 \tag{B.24}$$

From this one concludes that a_j, when acting on a polynomial in the creation operators a_j^+ can be interpreted as the operator $\frac{\partial}{\partial a_j^+}$, for the same reason that $P_j = -i\frac{\partial}{\partial x_j}$. [83]. Thus $\underset{\sim}{a}$ operating on any polynomial of $\underset{\sim}{a}^+$'s is the same way as $\underset{\sim}{\nabla}$ operating on the polynomial in $\underset{\sim}{r}$. Thus the gradient formula can be used directly in evaluating the $\underset{\sim}{a}$ operation on the oscillator state. Thus from (B.23), (B.25) and (B.19),

$$\underset{\sim}{a}\left[(\underset{\sim}{a}^+\cdot\underset{\sim}{a}^+)^n \mathcal{Y}_{Jm}(\underset{\sim}{a}^+)\right]$$

$$= -\sqrt{\frac{J+1}{2J+1}}\left[2n+J-J\right]|a^+|^{2n+J-1}\vec{\mathcal{Y}}_{JJ+1m}(\hat{n})$$

$$+\sqrt{\frac{J}{2J+1}}\left[2n+2J+1\right]|a^+|^{2n+J-1}\vec{\mathcal{Y}}_{JJ-1m}(\hat{n}) \tag{B.25}$$

$$= -\sqrt{\frac{J+1}{2J+1}}\; 2n\,(a^+\cdot a^+)^{n-1}\vec{\mathcal{Y}}_{JJ+1m}(\underset{\sim}{a}^+)$$

$$+\sqrt{\frac{J}{2J+1}}\;(2n+2J+1)(a^+\cdot a^+)^n\,\mathcal{Y}_{JJ-1m}(\underset{\sim}{a}^+) \tag{B.26}$$

where

$$\vec{\mathcal{Y}}_{J\,J+1\,m}(\underset{\sim}{a}^{+}) = (a^{+})^{J+1}\,\vec{\mathcal{Y}}_{J\,J+1\,m}(\hat{n}) \tag{B.27}$$

and

$$\vec{\mathcal{Y}}_{J\,J-1\,m}(\underset{\sim}{a}^{+}) = (a^{+})^{J-1}\,\vec{\mathcal{Y}}_{J\,J-1\,m}(\hat{n}) \tag{B.28}$$

Thus

$$\underset{\sim}{a}\,|n\,J\,m\rangle = -\sqrt{\frac{J+1}{2J+1}}\;\frac{N_{nJ}}{N_{n-1\,J+1}}\;2n\,|n-1\;J\;J+1\,m\rangle + \sqrt{\frac{J}{2J+1}}\;\frac{N_{nJ}}{N_{n\,J-1}}(2n+2J+1)\,|n\;J\;J-1\,m\rangle \tag{B.29}$$

where

$$N_{nJ} = (-1)^{J}\left[\frac{4\pi}{2n!!\,(2n+2J+1)!!}\right]^{1/2} \tag{B.30}$$

$$N_{n-1\,J+1} = (-1)^{J+1}\left[\frac{4\pi}{(2n-2)!!\,(2n+2J+3-2)!!}\right]^{1/2} \tag{B.31}$$

and

$$N_{n\,J-1} = (-1)^{J-1}\left[\frac{4\pi}{2n!!\,(2n+2J+1-2)!!}\right]^{1/2} \tag{B.32}$$

Finally

$$\underset{\sim}{a}\,|nJm\rangle = \sqrt{\frac{2n(J+1)}{2J+1}}\,|n-1\,J\,J+1\,m\rangle - \sqrt{\frac{(2n+2J+1)J}{2J+1}}\,|n\,J\,J-1\,m\rangle\,. \tag{B.33}$$

Another useful result is [123]

$$\hat{r}\,y_{Jm}(\hat{n}) = -\sqrt{\frac{J+1}{2J+1}}\,\vec{\mathcal{Y}}_{JJ+1m}(\hat{n}) + \sqrt{\frac{J}{2J+1}}\,\vec{\mathcal{Y}}_{JJ-1m}(\hat{n})\,. \tag{B.34}$$

Making use of this formula,

$$\underset{\sim}{a}^{+}(\underset{\sim}{a}^{+}\cdot\underset{\sim}{a}^{+})^{n}\,y_{Jm}(\underset{\sim}{a}^{+}) = (a^{+})^{2n+J+1}\,\hat{a}^{+}\,y_{Jm}(\hat{n}) \tag{B.35}$$

$$= (a^{+})^{2n+J+1}\left[-\sqrt{\frac{J+1}{2J+1}}\,\vec{\mathcal{Y}}_{JJ+1m}(\hat{n}) + \sqrt{\frac{J}{2J+1}}\,\vec{\mathcal{Y}}_{JJ-1m}(\hat{n})\right] \tag{B.36}$$

$$= -\sqrt{\frac{J+1}{2J+1}}\,(a^{+}\cdot a^{+})^{n}\,\vec{\mathcal{Y}}_{JJ+1m}(\underset{\sim}{a}^{+}) + \sqrt{\frac{J}{2J+1}}\,(a^{+}\cdot a^{+})^{n+1}\,\vec{\mathcal{Y}}_{JJ-1m}(\underset{\sim}{a}^{+})\,. \tag{B.37}$$

Then

$$\underset{\sim}{a}^{+}\,|nJm\rangle = -\sqrt{\frac{J+1}{2J+1}}\,\frac{N_{nJ}}{N_{nJ+1}}\,|n\,J\,J+1\,m\rangle +$$

$$+\sqrt{\frac{J}{2J+1}}\;\frac{N_{nJ}}{N_{n+1\,J-1}}\;|n+1\,J\;J-1\;m\rangle \tag{B.38}$$

$$\underset{\sim}{a}^{+}|nJm\rangle = \sqrt{\frac{(J+1)(2n+2J+3)}{2J+1}}\;|n\,J\;J+1\;m\rangle - \sqrt{\frac{J(2n+2)}{2J+1}}\;|n+1\,J\;J-1\;m\rangle\,. \tag{B.39}$$

Also one can have the $\underset{\sim}{a}.\underset{\sim}{a}$ operation which leads to [83]

$$\underset{\sim}{a}\cdot\underset{\sim}{a}\,(\underset{\sim}{a}^{+}\cdot\underset{\sim}{a}^{+})^{n}\,y_{Jm}(\underset{\sim}{a}^{+}) = 2n\,(2n+2J+1)(a^{+}\cdot a^{+})^{n-1}\,y_{Jm}(\underset{\sim}{a}^{+}) \tag{B.40}$$

$$\frac{1}{a\cdot a^{+}}\,\underset{\sim}{a}\cdot\underset{\sim}{a}\,(a^{+}\cdot\underset{\sim}{a}^{+})^{n}\,y_{Jm}(\underset{\sim}{a}^{+}) = \frac{2n\,(2n+2J+1)}{2n-2+J+3}\,(a^{+}\cdot a^{+})^{n-1}\,y_{Jm}(\underset{\sim}{a}^{+})\,. \tag{B.41}$$

Then by using equation (B.39),

$$\left[\underset{\sim}{a}^{+}\frac{1}{\underset{\sim}{a}\cdot\underset{\sim}{a}^{+}}\underset{\sim}{a}\cdot\underset{\sim}{a}\right]|nJm\rangle = \sqrt{\frac{2n\,(2n+2J+1)}{(2n+J+1)^{2}}}\left\{\sqrt{\frac{(2n+2J+1)(J+1)}{2J+1}}\;|n-1\,J\,J+1\,m\rangle - \sqrt{\frac{2nJ}{2J+1}}\;|n\,J\,J-1\,m\rangle\right\} \tag{B.42}$$

Using (B.33) and (B.42),

$$\left[\underset{\sim}{a} - \underset{\sim}{a}^{+}\frac{1}{\underset{\sim}{a}\cdot\underset{\sim}{a}^{+}}\underset{\sim}{a}\cdot\underset{\sim}{a}\right]|nJm\rangle$$

$$= \left[1 - \frac{2n+2J+1}{2n+J+1}\right]\sqrt{\frac{2n\,(J+1)}{2J+1}}\;|n-1\,J\,J+1\,m\rangle +$$

$$+\left[\frac{2n}{2n+J+1}-1\right]\sqrt{\frac{2n+2J+1}{2J+1}}\,|n\,J\,J{-}1\,m\rangle$$

(B.43)

$$= -\sqrt{\frac{J(J+1)}{(2n+J+1)^2}}\left\{\sqrt{\frac{2nJ}{2J+1}}\,|n{-}1\,J\,J{+}1\,m\rangle + \sqrt{\frac{(2n+2J+1)(J+1)}{2J+1}}\,|n\,J\,J{-}1\,m\rangle\right\}.$$

(B.44)

From (B.8) for the second polarization of the gluon mode

$$\underset{\sim}{A}^2_{nJm} = -\mathcal{N}^2_{nJ}\left[\underset{\sim}{a} - \underset{\sim}{a}^{+}\frac{1}{\underset{\sim}{a}\cdot\underset{\sim}{a}^{+}}\underset{\sim}{a}\cdot\underset{\sim}{a}\right]|nJm\rangle .$$

(B.45)

The normalization factor $\mathcal{N}_{nJ}$ is such that

$$\langle \underset{\sim}{A}^2_{nJm} | \underset{\sim}{A}^2_{n'J'm'}\rangle = \delta_{nn'}\delta_{JJ'}\delta_{mm'} .$$

(B.46)

Using (B.44) and (B.45) i.e.

$$1 = |\mathcal{N}^2_{nJ}|^2 \frac{J(J+1)}{(2n+J+1)^2}\left\{\frac{2nJ}{2J+1} + \frac{(2n+2J+1)(J+1)}{2J+1}\right\}$$

(B.47)

$$= |\mathcal{N}^2_{nJ}|^2 \frac{J(J+1)}{2n+J+1} .$$

(B.48)

Thus

$$\mathcal{N}^2_{nJ} = \sqrt{\frac{2n+J+1}{J(J+1)}} .$$

(B.49)

Thus the normalized second gluon mode is

$$\underset{\sim}{A}^2_{nJm} = -\frac{1}{\sqrt{2n+J+1}}\left\{\sqrt{\frac{2nJ}{2J+1}}\,|n{-}1\,J\,J{+}1\,m\rangle\right.$$

$$+\sqrt{\frac{(2n+2J+1)(J+1)}{2J+1}}\,|n\,J\,J-1\,m\rangle\Big\}. \tag{B.50}$$

Similarly from (B.39), the normalized solution for the 3rd component of the gluon field is given by

$$A^3_{nJm} = \frac{1}{\sqrt{2n+J+3}}\Big\{\sqrt{\frac{(2n+2J+3)(J+1)}{2J+1}}\,|n\,J\,J+1\,m\rangle - \sqrt{\frac{(2n+2)J}{2J+1}}\,|n+1\,J\,J-1\,m\rangle\Big\}. \tag{B.51}$$

To have the same quanta for $\underset{\sim}{A}^2$ and $\underset{\sim}{A}^3$ one has chosen for A^2 as

$$\underset{\sim}{A}^2 = W^2_{nJ}\left[\underset{\sim}{a} - \underset{\sim}{a}^+\frac{1}{\underset{\sim}{a}\cdot\underset{\sim}{a}^+}\,\underset{\sim}{a}\cdot\underset{\sim}{a}\right]|n+1\,J\,m\rangle. \tag{B.52}$$

Thus the equation (B.50) becomes,

$$A^2_{nJm} = -\frac{1}{\sqrt{2n+J+3}}\Big\{\sqrt{\frac{(2n+2)J}{2J+1}}\,|n\,J\,J+1\,m\rangle + \sqrt{\frac{(2n+2J+3)(J+1)}{2J+1}}\,|n+1\,J\,J-1\,m\rangle\Big\}. \tag{B.53}$$

Appendix C

The Radial Solution of the Oscillator Equation in CCM and DCM

The radial part of the field in CCM satisfies the differential equation;

$$\frac{d^2R}{dr^2} + \frac{2}{r}\frac{dR}{dr} - \frac{l(l+1)}{r^2}R - \alpha^2 r^2 R + \omega^2 R = 0 \qquad (C.1)$$

Let

$$\rho = \alpha^{1/2} r \qquad (C.2)$$

Thus

$$\frac{d}{dr} = \frac{\partial\rho}{\partial r}\frac{d}{d\rho} = \alpha^{1/2}\frac{d}{d\rho} \qquad (C.3)$$

$$\frac{d^2}{dr^2} = \alpha\frac{d^2}{d\rho^2} \qquad (C.4)$$

Thus (C.1) becomes

$$\alpha\frac{d^2R}{d\rho^2} + \frac{2\alpha}{\rho}\frac{dR}{d\rho} - \frac{\alpha l(l+1)}{\rho^2}R - \alpha\rho^2 R + \omega^2 R = 0 \qquad (C.5)$$

$$\frac{d^2R}{d\rho^2} + \frac{2}{\rho}\frac{dR}{d\rho} - \frac{l(l+1)}{\rho^2}R - \rho^2 R + \frac{\omega^2}{\alpha}R = 0 \qquad (C.6)$$

Let

$$\frac{\omega^2}{\alpha} = \lambda . \tag{C.7}$$

Then

$$\frac{d^2R}{d\rho^2} + \frac{2}{\rho}\frac{dR}{d\rho} - \left[\frac{l(l+1)}{\rho^2} + \rho^2 - \lambda\right]R = 0 \tag{C.8}$$

Let

$$R = \rho^l e^{-\rho^2/2} f(\rho) \tag{C.9}$$

Then $f(\rho)$ satisfies the equation

$$f'' + 2\left[(l+1)\rho^{-1} - \rho\right]f' + (\lambda - 3 - 2l)f = 0 \tag{C.10}$$

Let

$$\xi = \rho^2$$

$$\frac{d\xi}{d\rho} = 2\rho = 2\xi^{1/2} \tag{C.11}$$

$$\frac{d}{d\rho} = 2\xi^{1/2}\frac{d}{d\xi} \tag{C.12}$$

$$\frac{d^2}{d\rho^2} = 4\xi\frac{d^2}{d\xi^2} + 2\frac{d}{d\xi} \tag{C.13}$$

(C.14)

Then equation (C.10) becomes

$$\xi\frac{d^2f}{d\xi^2} + \left[(l+\tfrac{1}{2})+1-\xi\right]\frac{df}{d\xi} + \frac{1}{4}(\lambda-3-2l)f = 0. \tag{C.15}$$

Comparing this differential equation with the standard confluent hypergeometric differential equation,

$$\rho \frac{d^2 w}{d\rho^2} + (c-\rho)\frac{dw}{d\rho} - a w = 0 \tag{C.16}$$

whose solution is given by [116]

$$w = {}_1F_1(a, c, \rho) \quad . \tag{C.17}$$

The solution is convergent only when a is negative integer. Thus the solution of (C.15) can be obtained as

$$f(\xi) = {}_1F_1(-n, l+\tfrac{3}{2}, \xi) \tag{C.18}$$

where n = 1/4 (λ-3-2l) and n = 0,1,2..... Thus the radial solution is obtained as

$$R_{nl}(r) = (\alpha^{1/2} r)^l \, e^{-\alpha r^2/2} \, {}_1F_1(-n, l+\tfrac{3}{2}, \alpha r^2) \, . \tag{C.19}$$

Let

$$\alpha^{1/2} = b \, . \tag{C.20}$$

Then

$$R_{nl}(r) = (br)^l \, e^{-\frac{b^2 r^2}{2}} \, {}_1F_1(-n, l+\tfrac{3}{2}, b^2 r^2) \, . \tag{C.21}$$

It is related with the associated Lagurre polynomial [119]

$$L_n^{\mu}(z) = \frac{\Gamma(n+\mu+1)}{n! \, \Gamma(\mu+1)} \, {}_1F_1(-n, 1+\mu, z) \tag{C.22}$$

Thus

$$R_{nl}(r) = (br)^{l}\, e^{-\frac{b^2r^2}{2}}\, \frac{n!\,\Gamma(l+3/2)}{\Gamma(n+l+\frac{3}{2})}\, L_n^{l+\frac{1}{2}}(b^2r^2) \tag{C.23}$$

$$= \frac{n!\,\Gamma(l+3/2)}{\Gamma(n+l+3/2)}\,(br)^{l}\, e^{-\frac{b^2r^2}{2}}\, L_n^{l+1/2}(b^2r^2) . \tag{C.24}$$

Normalizing the radial solution using the orthogonality of the Lagurre polynomials:

$$\int_0^\infty dx\; x^{l+\frac{1}{2}}\, e^{-x}\left[L_n^{l+1/2}(x)\right]^2 = \frac{\Gamma(n+l+3/2)}{n!} . \tag{C.25}$$

Thus defining

$$R_{nl}(r) = N_{nl}\,\frac{n!\,\Gamma(l+3/2)}{\Gamma(n+l+3/2)}\,(br)^{l}\, e^{-\frac{b^2r^2}{2}}\, L_n^{l+\frac{1}{2}}(b^2r^2) \tag{C.26}$$

and

$$\int_0^\infty |R_{nl}(r)|^2\, d^3r = 1 . \tag{C.27}$$

Then

$$1 = 4\pi\int_0^\infty (N_{nl})^2\left[\frac{n!\,\Gamma(l+3/2)}{\Gamma(n+l+3/2)}\right]^2 (br)^{2l}\, e^{-b^2r^2}\left[L_n^{l+\frac{1}{2}}(b^2r^2)\right]^2 r^2 dr \tag{C.28}$$

$$1 = 4\pi |N_{nl}|^2 \left[\frac{n!\,\Gamma(l+3/2)}{\Gamma(n+l+3/2)}\right]^2 \frac{1}{b^3} \int_0^\infty (br)^{2l} e^{-b^2r^2} \left[L_n^{l+\frac{1}{2}}\right]^2 b^2r^2\, d(br) \tag{C.29}$$

Let

$$b^2 r^2 = x \tag{C.30}$$

$$2br\, d(br) = dx$$

$$1 = 4\pi |N_{nl}|^2 \left[\frac{n!\,\Gamma(l+3/2)}{\Gamma(n+l+3/2)}\right]^2 \frac{1}{2b^3} \int_0^\infty x^{l+\frac{1}{2}} e^{-x} \times \left[L_n^{l+\frac{1}{2}}(x)\right]^2 dx \tag{C.31}$$

(C.32)

Using (C.25),

$$4\pi |N_{nl}|^2 \left[\frac{n!\,\Gamma(l+3/2)}{\Gamma(n+l+3/2)}\right]^2 \frac{1}{2b^3} \cdot \frac{\Gamma(n+l+3/2)}{n!} = 1 \tag{C.33}$$

$$4\pi |N_{nl}|^2 \frac{n!\,(\Gamma(l+3/2))^2}{\Gamma(n+l+3/2)} \frac{1}{2b^3} = 1 \tag{C.34}$$

$$|N_{nl}|^2 = \frac{2b^3}{4\pi} \frac{\Gamma(n+l+3/2)}{n!\,(\Gamma(l+3/2))^2} \tag{C.35}$$

$$N_{nl} = \left[\frac{b^3}{2\pi} \frac{\Gamma(n+l+3/2)}{n!(\Gamma_{l+3/2})^2} \right]^{1/2} . \tag{C.36}$$

Thus

$$R_{nl}(r) = \left[\frac{b^3}{2\pi} \frac{\Gamma(n+l+3/2)}{n!(\Gamma_{l+3/2})^2} \right]^{1/2} \frac{n!\,\Gamma_{l+3/2}}{\Gamma_{n+l+3/2}} \times$$

$$(br)^l \, e^{-b^2r^2/2} \, L_n^{l+1/2}(b^2r^2) . \tag{C.37}$$

$$\therefore R_{nl}^{ccm}(r) = \left[\frac{b^3}{2\pi} \frac{n!}{\Gamma_{n+l+3/2}} \right]^{1/2} (br)^l \, e^{-\frac{b^2r^2}{2}} L_n^{l+1/2}(b^2r^2) . \tag{C.38}$$

From (C.18),

$$\lambda = 2n+2l+3 \tag{C.39}$$

$$\frac{\omega^2}{\alpha} = 4n+2l+3 \tag{C.40}$$

$$\omega^2 = [2(2n+l)+3]\alpha . \tag{C.41}$$

Let

$$2n+l = N , \tag{C.42}$$

then

$$\omega = (2N+3)^{1/2} b . \tag{C.43}$$

where N = 0,1,2,...... In the DCM case the radial function satisfies

$$\frac{d^2R}{dr^2} + \frac{2}{r}\frac{dR}{dr} + \left[\epsilon(r)\,\omega^2 - \frac{l(l+1)}{r^2}\right]R = 0 \tag{C.44}$$

where

$$\epsilon(r) = 1 - a^2 r^2 . \tag{C.45}$$

Then

$$\frac{d^2R}{dr^2} + \frac{2}{r}\frac{dR}{dr} + \left[\omega^2 - a^2\omega^2 r^2 - \frac{l(l+1)}{r^2}\right]R = 0 . \tag{C.46}$$

This differs from the CCM radial differential equation only in its constants i.e. α^2 in CCM is identified here as

$$\alpha^2 = a^2\omega^2 . \tag{C.47}$$

Then the rest of the calculation goes exactly identical. Where the parameter b in CCM here becomes

$$b \equiv (a\omega)^{1/2} . \tag{C.48}$$

and

$$\lambda \equiv \frac{\omega^2}{b^2} = \frac{\omega}{a} \tag{C.49}$$

where the eigen value

$$\omega = (4n + 2l + 3)\,a \tag{C.50}$$

or

$$\omega = (2N+3)\,a \tag{C.51}$$

and

$$R^{\mathrm{Dcm}}_{nl}(r) = \left[\frac{a^3\omega^3}{2\pi}\,\frac{n!}{\sqrt{n+l+3/2}}\right]^{1/2}\left[(a\omega)^{1/2} r\right]^{l} \times \tag{C.52}$$

$$e^{-\frac{a\omega r^2}{2}}\, L_n^{l+1/2}(a\omega r^2) \, .$$

CHAPTER IV

GLUEBALLS

4.1. Introduction

The QCD is a highly non-linear theory and the resulting gluon-gluon interactions are the fundamental characteristics of quantum chromodynamics [62]. The various properties of QCD such as antiscreening nature of QCD vacuum or asymptotic freedom, the infrared slavery or confinement, are due to this colour-colour interactions. This also leads to the prediction of exotic colour singlet bound states of gluons. Such a state is called glueball or gluonium. A theoretical description of purely gluonic matter from its free state to a highly interacting state producing massive glue state against temperature is shown in figure 4.1. The critical temperature T_c for this hadronization is shown. The smallest units of such exotic matter i.e. glueballs are then a necessary consequence of the theory of QCD. Their existence and experimental confirmation are very crucial for the validity of QCD and any other theory where the SU(3) colour gauge invariance is utilized.

All the phenomenological confinement models and lattice calculations predicted the existence of the pure gluonic colour singlet bound states in the energy range 1-3 GeV [84-87]. And a couple of very strong glueball candidates exists experimentally [88-90].

In this chapter the low lying digluon and trigluon glueball energies and their quantum numbers are calculated using the current confinement model and the dielectric confinement model for gluons described in Chapter 3. Before going to the calculations the construction of the colour singlet multigluon states are described and the various possible combinations of the spatial, angular momentum, spin and colour symmetries are discussed in section 4.2. The question one asks now is how to identify a glueball state or how to distinguish glue balls from qq mesons. With the help of Okubo-Zweig-Iisuka (OZI) rule for mesonic decays [91-93], the modus operandi of identification of a glueball state and the decay processes favouring the glueball intermediate states are described in section 4.3. The experiments, particularly in the J/ψ decays and $\pi^- p \rightarrow n\phi\phi$ processes - both the OZI forbidden processes - give very strong evidence for the detection of iota (1440 MeV) [88], θ(1700 MeV) [94,95] and g_T($\simeq$2300 MeV) [90] as glueball candidates. The experimental results of these decay processes are reviewed and discussed in section 4.4.

Considering the iota (1440 MeV $J^{PC} = 0^{-+}$) as a digluon glueball state the parameter in CCM as well as in DCM are calculated to predict all other low lying digluon and trigluon glueball states. The construction and the calculations are shown in section 4.5. As in the case of quark bound states the spurious motion of the centre of the multigluon bound system is also removed exactly in CCM and DCM models. The details are given in section 4.6. Finally in section 4.7 the corrected digluon and trigluon glueball energies are calculated by fitting the same iota (1440) as a digluon state. The results are then tabulated in comparison with similar results from bag model calculations and experimental candidates and discussed.

4.2. Construction of Colour Singlet Multigluon State

As mesons are colour singlet bound states of quark-antiquark systems, glueballs are the colour singlet bound states of multigluons [94] i.e.

$$|meson\rangle = \frac{1}{\sqrt{3}} \sum_{\alpha=1}^{3} |\bar{q}_\alpha q_\alpha\rangle \tag{4.2.1}$$

and

$$|glueball\rangle = \frac{1}{\sqrt{8}} \sum_{l,m,n\ldots n=1}^{8} |g_l g_m \cdots {}^m g_n\rangle C_{lm\ldots n} \tag{4.2.2}$$

where $|q_\alpha\rangle$ is the quark state and $|\bar{q}_\alpha\rangle$ is the corresponding antiquark state. Similarly, $|g_l\rangle$ represents the gluon state. Here α = 1,2,3 represent the colour index of the quarks, l = 1,2,...8 correspond to the colour charge of the gluons and m is the number of gluons constituting the glueball state. For example, m=2 is a digluon glueball state and m=3 is a trigluon glueball state. The wave function which corresponds to the multi-gluon state must be totally symmetric under the interchange of space, spin and colour quantum numbers.

The colour part of the multi-gluon wave function is governed by the combination of the Gell Mannn's λ-matrices [43]

$$[\lambda_l, \lambda_m] = 2i f_{lmn} \lambda_n \tag{4.2.3}$$

$$\{\lambda_l, \lambda_m\} = \frac{4}{3}\delta_{lm} + 2d_{lmn}\lambda_n . \tag{4.2.4}$$

Here l,m,n are the colour indices, f_{lmn} are the antisymmetric in the permutations of their indices while d_{lmn} are the symmetric in the permutations of their indices. For digluon systems the colour charge coupling is of the form δ_{lm} giving rise to the colour charge conjugation quantum number C = +1, whereas in the case of a tri-gluon state the colour symmetric coupling of the type d_{lmn} gives the colour charge conjugation quantum number C = -1 and that of the colour antisymmetric coupling of the type f_{lmn} gives C = +1. Thus the colour singlet glueball states with orbital spin and colour symmetries can have the following combinations.

Orbital	Spin	Colour
S	S	S
S	A	A

A	S	A
A	A	S
(MS/MA	MS/MA)$_S$	S
(MA/MS	MS/MA)$_A$	A

The abbreviations, S is for symmetric, A for antisymmetric, MS and MA are the mixed symmetric and mixed antisymmetric respectively. Accordingly, the various possible digluon and trigluon glueball states are calculated using phenomenological confinement models. Here Table 4.1 shows the ordering of the digluon states and Table 4.2 shows the various combinations of the orbital, spin and colour symmetries in the construction of trigluon glueball states. The underlined states in both the tables are those states which do not occur in models where gluons are considered as massless vector particles. This is explained using the theorem by Yang [96] that two on-shell massless vector particles (i.e. transverse gluons) do not couple to 1^{++} or (odd) -+ states. Phenomenological models like the potential models, by calculating the eigenvalues of massive gluons [79] the bag models, by calculating the eigen modes of the transverse colour electric and magnetic fields [76], the lattice gauge theories, by computing the Plaquette-Plaquette correlation length in the pure gluonic sector [84], the string models and from the effective Lagrangian models [97]; all have predicted the lowest lying glueball states in the energy range 1-3 GeV with specific J^{PC} values. The general characteristics of these exotic states are described in the next section.

4.3. Characteristics of Glueball States

The primary property that characterises the glueball states is that they are flavour singlets. They should have flavour symmetric decays. The annihilation of quark-antiquark produces an intermediate glueball state which then decays into quark-antiquark pairs of new flavours. The quark-antiquark annihilations are forbidden in mesonic decays by Okubo, Zweig, Iisuka (OZI) rule [91-93]. The other properties which can reliably be used to identify a glueball state are, firstly glueballs do not fit in the qq multiplets of the quark models, and secondly, glueballs are produced in hard gluon channels. But the difficulty is that these are not easy to apply, because to know a particle which does not belong to a qq meson, a complete understanding of the qq spectra is required. The hardness depends on the ratio of Q^2/Λ^2 and Λ is not well known. But quark-antiquark annihilation occurs at very small distances and so they must emit hard gluons. Thus so far OZI forbidden decays are the most fruitful channels to look for glueballs.

4.3.1. OZI Allowed and Forbidden Decays:

The OZI rule for meson decays states that the two quarks ($q,\bar{q}$) in a meson state do not annihilate, instead the decay is given by the connected quark diagrams. Figure 4.2 shows some of the OZI allowed decay processes and reactions by the connected quark diagrams. Each line here corresponds to a particular flavour quark. The forward and backward arrows represent quark and antiquark respectively. In OZI forbidden processes the quark lines are not connected and the diagram looks like a hairpin. Here the heavier quarks annihilate to produce new lighter quarks. These represent the flavour symmetric decays. Figures 4.3 show some of the decay processes which are OZI forbidden.

In the OZI allowed processes without violating the colour confinement one gluon exchange between the quarks is allowed. On the other hand disjoint or hairpin diagrams requires multigluon exchange. Two gluon exchange is required if the meson is a scalar or three gluon exchange is required if the meson is a vector. Thus in an OZI forbidden reaction the intermediate state which connects the two disconnected parts must be a multigluon state [64]. Figure 4.4 describes such processes where the multigluon exchanges are shown. Because of the colour confinement property each of these multigluon intermediate states forms a glueball resonance which further decays to either a pair of gluon resonances or into a pair of excited hadrons. Thus the OZI rule extended to glueball decay is shown in figure 4.5.

According to this generalization of OZI rule one expects a relatively narrow gluon resonance above 1 GeV, where the quark-gluon coupling may be very small [98]. Thus the gluon resonances above 1 GeV do not mix strongly with qq resonances. Likewise the production cross section of the glueballs is also expected to be small due to the smallness of the gluon-gluon coupling at the relevant energy. This may be attributed to the reason that the hadronic sector is not dominated by the glueballs as expected from the QCD theory. In the absence of heavier quarks then probably immediately above 1 GeV the gluonic sector may dominate. In conclusion, a flavourless particle qualifies as a gluonic meson if it does not fit into any available meson nonet with the appropriate quantum numbers in the energy range. For this reason it is very important to obtain as much information as possible particularly from the OZI forbidden processes where the hard gluons are produced. Together with the precise observation of masses, spins and decay widths one will be able to ascertain the gluonic nature of any new objects being found.

4.4. The Experimental Status of Glueballs

Since the theoretically predicted low-lying glueball energy is in the range of 1-3 GeV, the decay of J/ψ (3097 MeV, $J^{PC} = 1^{--}$) discovered by SPEAR and BNL-MIT group) [99,100] is the process to look for the glueball production. It is a $C\overline{C}$ bound system whose decays containing one charmed quark are energetically prohibited and the main decay mechanism proceeds via annihilation of the charmed quark-antiquark into gluons. All the J/ψ decays are then OZI suppressed. The study of J/ψ spectroscopy is the current field of interest in experimental particle physics. The radiative decays of the J/ψ provide few potential candidates for the glueball states. The present experimental status of the radiative decays of J/ψ is reported by K. Konigsmann in 1986 [101] and latest by Usha Mallik in 1987 [102]. The principal decay mechanisms of the J/ψ are shown in figure 4.6. The strong decay proceeds through atleast three gluon exchange. The two gluon exchange alone is forbidden by the charge conjugation for a colour singlet. The decay strength is given by [101-103]

$$\Gamma(J/\psi \to ggg) = \frac{16}{9\pi}(\pi^2 - 9)\frac{5}{18}\alpha_s^3 \frac{|\Psi(0)|^2}{M_{J/\psi}^2} \qquad (4.4.1)$$

$\Psi(0)$ is the value of the radial wave function of the J/ψ at the origin. $M_{J/\psi}$ is the mass of the J/ψ and α_s is the strong coupling constant. This is around 62% of the total J/ψ branching ratios. Thus the decay proceeds mainly by the emission of the three gluons which fragment into lighter hadrons. The electromagnetic decay through a virtual photon exchange is reported to be around 29% and the radiative decay into a photon and two gluons as shown by figure 4.6c is around 7% [102]. Its decay strength is determined by

$$\Gamma(J/\psi \rightarrow \gamma gg) = \frac{32}{9\pi}(\pi^2-9)\alpha_s^2\alpha Q_c^2 \frac{|\Psi(0)|^2}{M_{J/\psi}^2} \quad (4.4.2)$$

Here α is the electromagnetic coupling constant, Q_c is the charge of the charmed quark (2/3 e). Since the photon in the final state does not carry colour, the two gluons could form a colour singlet bound state. This is then an intermediate step that makes the radiative decay the hunting ground for the glueballs. The J/ψ can decay electromagnetically into η_c through a magnetic dipole transition before the $C\bar{C}$ annihlate. This is shown in figure 4.6e. This is around 1% of the total J/ψ branching ratio. The spin parity analysis of the two gluon system in the gg emissions have been carried out by others [104,105] and found a strong presence of $J^{PC} = 0^{++}, 0^{-+}$ and 2^{++} contributions in accordance with the theoretical predictions from the confinement models. Unfortunately, the QCD predictions on masses, widths and decay channels for glueballs are not very precise. This makes it difficult to distinguish these states from normal mesons. Two candidates for the glueballs are observed in the radiative decays of J/ψ. The details of the experimental results of these states are given in the following sub-sections.

4.4.1. $J/\psi \rightarrow \gamma$ + iota (1440):

As per the prediction, the first experimental candidate for a glueball state was found in J/ψ radiative decay mode [88]

$$J/\psi \rightarrow \gamma\iota \, ; \, \iota \rightarrow K_S^0 K^{\pm} \pi^{\mp} \tag{4.4.3}$$

with the energy 1440 $\pm$ 10 MeV in Mark II and width 50 $\pm$ 30 MeV from around 85 events recorded. In 1982 Crystal ball group recorded around 170 events of the iota decay

$$\iota \rightarrow K^+ K^- \pi^0 \, . \tag{4.4.4}$$

The energy estimation was 1440 $\pm$ 20 MeV and its width 55 $\pm$ 20 MeV [89]. The spin parity analysis in both cases assigned as $J^{PC} = 0^{-+}$ and the branching ratio

$$BR(J/\psi \rightarrow \gamma\iota, \iota \rightarrow K\bar{K}\pi) \times 10^3 = \underset{(\text{MARK II})}{4.3 \pm 1.7}$$

$$= \underset{(\text{CRYSTAL BALL})}{4 \pm 1.2} \tag{4.4.5}$$

give identical results. Speculation on a glueball hypothesis was nourished by the very large radiative branching ratio. The latest experimental results with higher statistics from MARK III and DM2 [106] fix the mass of the iota as 1459 $\pm$ 5 MeV and 1456 $\pm$ 6 MeV respectively. The width was 99 $\pm$ 11 and 98 $\pm$ 13 MeV respectively. A complete Dalitz plot analysis was performed [106] and the spin parity was determined to be 0^- in consistent with the earlier identification. The measured branching ratios were

$$BR(J/\psi \rightarrow \gamma\iota(1440)) \cdot (\iota(1440) \rightarrow K^{\pm} K_S^0 \pi^{\mp})$$

$$= 4.8 \pm 0.6 \times 10^{-3} \tag{4.4.6}$$

and

$$BR(J/\psi \rightarrow \gamma\iota(1440)) \cdot (\iota \rightarrow K^{+}K^{-}\pi^{0}) = 4.1 \pm 0.7 \times 10^{-3}. \tag{4.4.7}$$

With all the data put together the average mass, width and the branching ratio for the iota is assigned to be

$$M_{\iota} = 1455 \pm 4 \text{ meV} \tag{4.4.8}$$

$$\Gamma_{\iota} = 89 \pm 8 \text{ MeV} \tag{4.4.9}$$

and

$$BR(J/\psi \rightarrow \gamma\iota) \cdot BR(\iota \rightarrow K\bar{K}\pi) = 4.4 \pm 0.4 \times 10^{-3}. \tag{4.4.10}$$

The mass and spin parity are well suited for iota to be a glueball candidate. The additional information on the nature of the iota is provided by its electromagnetic decays. For pure gluonic mesons these decays which are expected to be suppressed as gluons do not couple to photons. The decay

$$\iota \rightarrow \gamma\rho^{0} \tag{4.4.11}$$

is then an additional test for its true nature. The experimental signal from the proceses [107] is also found to be compatible with the glueball interpretation for the iota. Still there are difficulties like more than one resonance contributing to the main peak and more and more statistics is required for the unambigous identification of this peak at 1460 MeV. Till then this state remains to be a strong candidate only for the glueball state.

4.4.2. $J/\psi \rightarrow \gamma + \theta$ (1700):

The other strong candidate for the glueball state is the theta resonance observed in the radiative decay of J/ψ [89], in the channel

$$J/\psi \rightarrow \gamma\eta\eta \quad . \tag{4.4.12}$$

The analysis shows its spin parity to be 2^+ and the measured branching ratio by summing over all known decay modes is

$$BR(J/\psi \rightarrow \gamma\theta) = (1.3 \pm 0.2) \times 10^{-3} \, . \tag{4.4.13}$$

The average mass and width from all other experimental results [101] yield

$$M_\theta = 1710 \pm 5 \;\; MeV \tag{4.4.14}$$

and

$$\Gamma_\theta = 153 \pm 10 \; MeV \, . \tag{4.4.15}$$

The mass and width predictions qualify it to be a glueball suppressing all other possibilities such as $q\bar{q}$ or hybrids. The various groups analysed the possible nature of the θ(1700) $J^{PC}=2^{++}$ [108,109] and it is almost certainly concluded, being a non-$q\bar{q}$ state, it as a glueball candidate. The various decay patterns of this state have to be studied more precisely before conclusively assigning it as a pure glueball state.

4.4.3. $\pi^- p \rightarrow n\phi\phi$

This is another beautiful channel for the production of glueballs. As shown in figure 4.7, it is an OZI forbidden process. The $\pi^- p$ reactions give OZI allowed reactions also such as $\pi^- p \rightarrow K^+ K^- K^+ K^- n$ and

$$\pi^- p \rightarrow \phi K^+ K^- n \tag{4.4.16}$$

as shown in figure 4.8. But the reaction channel

$$\pi^- p \rightarrow n\phi\phi \tag{4.4.17}$$

is a double hairpin diagram (figure 4.7) where two or three gluons are produced connecting the disconnected parts. The exchanged multigluons to form $\phi\phi$ system, in the absence of glueballs, would lead to only Zweig suppressed $\phi\phi$ production. But at the mass range of $\phi\phi$ production the multigluons form an intermediate glueball state with charge conjugation quantum number, C = +. The Zweig suppression will be broken down and the $\phi\phi$ system will contain the glueball resonance parameters and quantum numbers. Thus the $\phi\phi$ system in this reaction acts as a filter passing glueball states and rejecting the other $q\bar{q}$ states. In the experiment done by BNL/CCNY group [90], the $\phi\phi$ signal was found out to be around ten times greater than the background from the K^- induced ϕ production shown by figure 4.8b. In the analysis of around 4,000 events three prominent resonance peaks $g_T(2120)$, $g_{T'}(2220)$ and $g_{T''}(2360)$ having identical spin parity

$J^{PC} = 2^{++}$ were observed [90,98]. The energy range and the J^{PC} value matches it to be the glueball states from the various QCD motivated models [76,87,110]. T.D. Lee has analytically calculated J=2 glueballs in the strong coupling limit and obtained three glueball states [97] which are in agreement with the observed three g_T resonances. Thus if QCD is correct and if the OZI rule is universal for weakly coupled gluons in Zweig disconnected diagrams, the resonance state with an average energy of 2233 MeV represents a pure glueball state [98].

4.5. Model Calculation of the Glueball States

Using the bound states of gluons in the current confinement model as well as in the dielectric confinement model the low lying digluon and trigluon glueball states are calculated [80]. The energy eigenvalues of these confined gluons are (from equation 3.3.61 and 3.6.22)

$$\omega_N^{CCM} = (2N+3)^{1/2} b \tag{4.5.1}$$

and

$$\omega_N^{DCM} = (2N+3) a \tag{4.5.2}$$

The constant b and a are the model parameters in CCM and DCM respectively. The quantum number N takes values 0,1,2,... The lowest gluon modes in both the models are

$J^{PC} = 1^{--}$ (the 'E' gluon) and $J^{PC} = 1^{+-}$ (the 'M' gluon) as defined in Chapter 3.

The low lying digluon glueball states are obtained by coupling the two gluons. The spin composition of the two J=1 states is given by the Young diagram

$$\overset{1}{\square} \otimes \overset{1}{\square} = \overset{0,2}{\square\square} + \overset{1}{\begin{array}{c}\square\\ \square\end{array}} \tag{4.5.3}$$

Here the 1^{+} and 1^{-} are the spurious states and are not allowed as the two massless gluons do not couple to 1^{++} or $(\text{odd})^{-+}$ states by Yang's theorem [96]. The possible low-lying digluon states using the various combinations of the E-gluon and M-gluon are shown in Table 4.3. the wave functions corresponding to these states are written symbolically,

$$|g_1 g_2\rangle = \sum_{\ell,m} C_\ell C_m \delta_{\ell m} [\chi_1 \chi_2]_S^{J=0,2} [\varphi_1 \varphi_2]_S \tag{4.5.4}$$

Here χ , φ and C_ℓ are the spin, orbital and colour wave functions respectively. The subscripts (1,2) correspond to E or M-gluons. The colour coupling is the $\delta_{\ell m}$ type. For example, the MM-glueball wave function can be written as

$$|g_m g_m\rangle = \sum_{l,m} C_l C_m \delta_{lm} \left[\chi_m \chi_m\right]_S^{J=0,2} \left[\varphi_m \varphi_m\right]_S \tag{4.5.5}$$

Similarly the trigluon low-lying states are calculated by coupling three E-gluons or two E-gluons and one M-gluon or one E-gluon and two M-gluons or three M-gluons. The spin composition of the three J=1 states is

$$\overset{1}{\ydiagram{1}} \otimes \overset{1}{\ydiagram{1}} \otimes \overset{1}{\ydiagram{1}} = \overset{0,2}{\ydiagram{2}} \otimes \overset{1}{\ydiagram{1}} + \overset{1}{\ydiagram{1,1}} \otimes \overset{1}{\ydiagram{1}}$$

$$= \overset{3,1}{\ydiagram{3}} + \overset{2,1}{\ydiagram{2,1}} + \overset{1,2}{\ydiagram{2,1}} + \overset{0}{\ydiagram{1,1,1}} \tag{4.5.6}$$

Thus for three M-gluon coupling case,

$$\begin{aligned} 1^+ \otimes 1^+ \otimes 1^+ &= 3^+ \text{(symmetric)} \oplus 2\text{x}2^+ \text{(mixed symmetric)} \\ &\oplus 1^+ \text{(symmetric)} \oplus 2\text{x}1^+ \text{(mixed symmetric)} \\ &\oplus 0^+ \text{(antisymmetric)} \end{aligned} \tag{4.5.7}$$

Using the various combinations of the space and the colour symmetries so many trigluon colour singlet glueball states are possible as shown in Table 4.2. The wave functions corresponding to some of these states can be written symbolically,

$$|ggg\rangle_{J=0} = \sum_{l,m,n} C_l C_m C_n f_{lmn} (\chi_1 \chi_2 \chi_3)_A^{J=0} (\varphi_1 \varphi_2 \varphi_3)_S \tag{4.5.8}$$

$$|ggg\rangle_{J=1,3} = \sum_{l,m,n} c_l c_m c_n d_{lmn} \left[\chi_1 \chi_2 \chi_3\right]_S^{J=1,3} (\varphi_1 \varphi_2 \varphi_3)_S \qquad (4.5.9)$$

In the case of M^3 glueball state the parity is even since the lowest M-gluon is in the $J^{PC} = 1^{+-}$ state. In this state, the space part of the wave function is symmetric. The colour part of the wave function is either totally symmetric (d-coupling) or totally antisymmetric (f-coupling). Then the mixed symmetric state in the spin-space is forbidden by Bose statistics [111]. The antisymmetric state in the spin space combines with the f-type colour singlet state to lead to $J^{PC} = 0^{++}$ state, and the symmetric state combine with the d-type colour singlet state to lead to the $J^{PC} = 3^{+-}$ and 1^{+-} states. The other J^{PC} states are not allowed as the low-lying M^3-glueball states.

In the case of low-lying M^2E glueball state the parity is negative since the parity of E-gluon is odd. The space part of the colour singlet wave function can be symmetric or mixed symmetric. Then the symmetric spin state combines with the symmetric colour coupling which leads to the $J^{PC} = 3^{--}, 1^{--}$ and with the antisymmetric spin state combines with the antisymmetric colour coupling which leads to the $J^{PC} = 0^{-+}$. The wave functions of these states are then written symbolically

$$|g_m g_m g_E\rangle_{3^{--},1^{--}} = \sum_{l,m,n} c_l c_m c_n d_{lmn} \left[\chi_{M^2E}^{J=3,1}\right]_S (\varphi_{M^2E})_S \qquad (4.5.10)$$

and

$$|g_M g_M g_E\rangle_{0^{-+}} = \sum_{l,m,n} c_l c_m c_n f_{lmn} \left[\chi^{J=0}_{M^2E}\right]_A \left[\varphi_{M^2E}\right]_S \tag{4.5.11}$$

correspond to the symmetric space wave functions. Similarly, corresponding to the mixed space symmetric state combinations yield J^{PC} =1 1^{--}, 2^{--} with the colour coupling of the type d_{lmn} and J^{PC} = 1^{-+}, 2^{-+} with colour coupling of tye type f_{lmn} . Their wave functions can be written as

$$|g_M g_M g_E\rangle_{1^{--}2^{--}} = \sum_{l,m,n} c_l c_m c_n d_{lmn} \frac{1}{\sqrt{2}} \left[\chi^{J=1,2}_{M(ME)_S} \varphi_{M(ME)_S} + \chi^{J=1,2}_{M(ME)_A} \varphi_{M(ME)_A}\right] \tag{4.5.12}$$

and

$$|g_M g_M g_E\rangle_{1^{-+}2^{-+}} = \sum_{l,m,n} c_l c_m c_n f_{lmn} \frac{1}{\sqrt{2}} \left[\chi^{J=1,2}_{M(ME)_A} \varphi_{M(ME)S} - \chi^{J=1,2}_{M(ME)S} \varphi_{M(ME)A}\right] . \tag{4.5.13}$$

Thus there are seven low-lying M^2E glueball states possible. Same is the case for E glueball states whose parity is negative. But in the CCM and DCM models the lowest E-gluon mode is the one whose orbital angular momentum is zero and hence only the space symmetric combinations are possible. This yields the possible J^{PC} states as J^{PC} = 0^{-+}, 1^{--} and 3^{--}. In the case of E^2M-glueball, the parity is positive and the space part of the colour singlet wavefunction can be symmetric or mixed symmetric. Then the allowed states are $J^{PC} = 3^{+-}, 1^{+-}, 0^{++}, 1^{+-}, 2^{+-}, 1^{++}, 2^{++}$. The allowed trigluon low-lying glueball states in the CCM or DCM models are given in Table 4.4 with various symmetry combinations.

The lowest E-gluon energy in CCM and DCM is

$$\omega^{CCM}(g_E) = \sqrt{3}\, b \tag{4.5.14}$$

and

$$\omega^{DCM}(g_E) = 3a \tag{4.5.15}$$

respectively. And the lowest M-gluon energy is

$$\omega^{CCM}(g_m) = \sqrt{5}\, b \tag{4.5.16}$$

and

$$\omega^{DCM}(g_m) = 5a \tag{4.5.17}$$

where the CCM parameter α is related to b as

$$b = \alpha^{1/2} . \tag{4.5.18}$$

The constant unknown parameter a and b in DCM and CCM respectively are obtained by fitting the first glueball candidate iota (1440 MeV) 0^{-+} as a digluon state [80]. This state is accessible in the EM coupled modes. Thus

$$(\sqrt{3} + \sqrt{5})\, b \quad = \quad 1440 \tag{4.5.19}$$

and

$$(3 + 5)\, a \quad = \quad 1440 \tag{4.5.20}$$

yield the values of a and b as 180 MeV and $\sim$363 MeV respectively. using these values for the parameters the confined gluon energies are calculated for various N-values. The results are shown in Table 4.5. The lowest E-gluon and M-gluon energy lies $\sim$ 600 and $\sim$ 800 MeV respectively in CCM calculations and $\sim$550 and $\sim$900 MeV respectively in DCM calculations. The energy levels of the confined gluon are drawn in figure 4.9.

Using the energy of g_E and g_m-gluons the energies of the digluon and trigluon glueballs are calculated. The results are shown in Table 4.6. The calculations are updated by fitting the recent experimental value on the iota energy as iota (1460 MeV). The results are found to be insensitive. The energy levels are shown in fig. 4.10 in comparison with the bag model results and the experimental candidates.

4.6. The Spurious Motion of the Centre of Multi-Gluon State

In the construction of the multigluon bound states the centre is quite arbitrary. Thus as in the case of any shell model like calculations the spurious motion of the centre of the glueball state should also be taken into account. Such calculations in the shell model for nuclear structure was found to have appreciable contributions [112]. Such corrections in the quark model (RHM) was also found to be crucial for its successful predictions [23]. These calculations are extended here in the multigluon bound systems containing m-number of gluons. The difficulty in accounting the spurious motion of the centre is one of the major problems in bag like models. Whereas the CCM and DCM have got the advantage that the spurious motion of the centre can be treated exactly.

Let R be the centre of mass position of a multigluon system containing m-number of gluons. Then

$$\underset{\sim}{R} = \frac{1}{m} \sum_{i=1}^{m} \underset{\sim}{x}_i \tag{4.6.1}$$

and the relative position of the gluon

$$\underset{\sim}{r}_i = \underset{\sim}{x}_i - \underset{\sim}{R} \tag{4.6.2}$$

where $\underset{\sim}{x}_i$ is the position vector of the i-th gluon. The motion of the gluons in the bound state is described by the equation, for example, in the CCM case,

$$\left[\left(\sum_{i=1}^{m} -\nabla_i^2 + \sum_{i=1}^{m} \alpha^2 x_i^2 \right) - \left(-\nabla_R^2 + \alpha^2 R^2 \right)\right] \Psi = \omega^2 \Psi . \tag{4.6.3}$$

The internal motion of the gluons around the centre $\underset{\sim}{R}$ is given by the equation

$$\left(-\nabla_i^2 + \alpha^2 r_i^2\right)\Psi_i = \epsilon^2 \Psi_i \tag{4.6.4}$$

where ϵ is the intrinsic energy of the gluon, and Ψ_i's are the relative wave functions. The motion of the centre is given by

$$\left(-\nabla_R^2 + \alpha^2 R^2\right)\Psi(R) = E^c \Psi(R) \tag{4.6.5}$$

where

$$E_N^c = (2N+3)\alpha \tag{4.6.6}$$

Now as has been done in the case of RHM for quarks [23], the centre is fixed at the lowest possible eigen state, i.e., the centre is at an energy

$$E_0^c = 3\alpha \tag{4.6.7}$$

and an equal contribution from all the m-gluons to the centre is assumed. Equation (4.6.3) then reduces to

$$\left(-\nabla_i^2 + \alpha^2 x_i^2\right)\Psi_i(x_i) = \left(\epsilon^2 + \frac{E_0^c}{m}\right)\Psi_i(x_i) \tag{4.6.8}$$

where

$$\epsilon_N^2 + \frac{E_0^c}{m} = (2N+3)\alpha \tag{4.6.9}$$

i.e.

$$\epsilon_N^2 = \left(2N+3-\frac{3}{m}\right)\alpha \tag{4.6.10}$$

Thus the intrinsic energy of the gluon in m-gluon system is

$$\epsilon_N^{CCm} = \left(2N+3-\frac{3}{m}\right)^{1/2} b \tag{4.6.11}$$

and

$$\epsilon_N^{DCm} = \left(2N+3-\frac{3}{m}\right) a \tag{4.6.12}$$

in CCM and DCM respectively. In the case of a digluon system, m=2 and that of a trigluon system, m=3. The intrinsic energy expressions in the digluon systems and trigluon systems are shown in Table 4.7.

The corrected low-lying glueball energies are calculated using the intrinsic gluon energies of digluon systems and of trigluon systems. The possible linear combinations of the low-lying states are taken to ensure that the centre of the multigluon bound system remains at the ground state. It is shown in Table 4.8, how these combinations are done in the case of low-lying digluon and trigluon systems.

The parameters a and b are calculated by fitting iota $(1440)0^{-+}$ as a $|g_E g_m\rangle$ digluon colour singlet state and all other low-lying glueball energy states are predicted. The results obtained in CCM are in excellent agreement with the other experimental candidates. The calculated energies are tabulated in Table 4.9 with the naive bag model results [78] and for comparison the energy levels are shown in figure 4.12.

Using the recent experimental result on the energy of the iota (0^{-+}) as 1460 MeV the results are recalculated and are listed in Table 4.10. It is noted that there is not any appreciable change from the earlier predictions. Also considering the g resonances at the average energy of 2233 MeV (perhaps the strongest glueball candidate [90] as a trigluon glueball state, the parameters are calculated and the digluon glueball energies and the other trigluon energies are calculated. The results are shown in Table 4.11. The results do not change appreciably.

4.7. Discussions

The results obtained from the DCM calculations are, in general, poor agreement with the experimental candidates. The CCM results show an excellent agreement with the experimental candidates (see Table 4.9) when the spurious motion of the centre is taken into account The predicted results by fitting iota (1440 MeV) as a di-gluon glueball state gives excellent agreement with the θ(1700 MeV)2^{++} state. The predicted E^2M-glueball energy is also found in good agreement with the experimentally observed g_T resonances. The DCM result for this state is close to the $g_T(2360)2^{++}$ state and that of the CCM result is close to the

g_T (2220)2^{++} state. The predicted lowest trigluon glueball state is in the energy range 1.7 to 2 GeV and the lowest glueball energy in the case of DCM is very close to the value of 750 MeV as predicted by the Lattice calculations, whereas the CCM result in this case is close to the probable glueball candidate g_S (1240 MeV)0^{++}. But its glueball candidature is more ambiguous than the other candidates. Overall the lowest glueball energy is around 1 GeV . Also from Table 4.5 the lowest E-gluon to M-gluon energy ratio is 0.6 in DCM and 0.78 in CCM as compared to the ratio of 1.6 in the bag model. The reason is that in the case of bag model the lowest gluon energy state is the magnetic mode with orbital angular momentum $\ell = 1$, $J^P = 1^+$, while in the CCM or DCM case it is the electric mode with orbital angular momentum $\ell = 0$, $J^P = 1^-$. Most of the other potential models also neglect the $\ell = 0$ solution for massless spin one fields. But it will be incorrect to neglect such solutions in phenemenological models like CCM or DCM for gluons, where the inhomogeneous medium provides a dynamical gluon mass for transverse gluon modes through Schwinger mechanism [113]. This is unlike the usual Higg's mechanism whose action leads to massive vector bosons with physical longitudinal components. Overall the current confinement model (CCM) is found to be more successful and is in close similarity to the RHM for quarks theoretically.

Table 4.1. Ordering of digluon glueball states

L	J^{PC}
0	0^{++} 2^{++}
1	0^{-+} 1^{-+} 2^{-+}
2	2^{++} 0^{++}, 1^{++}, 2^{++}, 3^{++}, 4^{++}
3	2^{-+}, 3^{-+}, 4^{-+}

Table 4.2. Shell Model of trigluon glueball states

Configuration	Spatial symm.	Orbital ang. momentum	Spin symm.	Spin ang. momentum	Colour symm.	J^{PC}
$(1S)^3$	S	0	S	1,3	d	$1^{--}, 3^{--}$
$(1S)^2(1P)$	S	0	A	0	f	0^{-+}
$(1S)^2(1P)$	S	1	S	1,3	d	$0,1,2^{+-}, 2^{+-}, 3^{+-}, 4^{+-}$
	S	1	A	0	f	1^{++}
	M	1	M	1,2	d	$0,1,2^{+-}, 1,2,3^{+-}$
	M	1	M	1,2	f	$0,1,2^{++}$, $1,2,3^{++}$
$(1S)(1P)^2$	S	0,2	S	1,3	d	$1^{--}, 3^{--}$ $1,2,3^{--}$ $1, +3$ $1,2$
	S	0,2	A	0	f	$0^{-+}, 2^{+}$
	M	0,2	M	1,2	d	$1^{--}, 2^{--}$ $1,2,3^{-}$ $0, 4$
$(1S)(1P)^2$	M	0,2	M	1,2	f	$1^{-+}, 2^{-+}$ $1,2,3^{-+}$ $1,4$
	M	1	M	1,2	d	$0,1,2^{--}$ $1,2,3^{--}$
	M	1	M	1,2	f	$0,1,2^{-+}$ $1,2,3^{-+}$
	A	1	S	1,3	f	$0,1,2^{-+}$ $2,3,4^{-+}$
	A	1	A	0	d	1^{--}

Table 4.3. Allowed low-lying digluon glue ball states

Coupled Models	J^{PC}
EE	0^{++}, 2^{++}
EM	0^{-+}, 2^{-+}
MM	0^{++}, 2^{++}

Table 4.4. Allowed trigluon low-lying glueball states

Coupled modes	Space symmetry	Spin symmetry	Colour symmetry	J^{PC}
EEE	S	S A	S A	1^{--}, 3^{--} 0^{-+}
	M	M	S A	1^{--}, 2^{--} 1^{-+}, 2^{-+}
E^2M	S	S A	S A	1^{+-}, 3^{+-} 0^{++}
	M	M	S A	1^{+-}, 2^{+-} 1^{++}, 2^{++}
EM^2	S	S A	S A	3^{--}, 1^{--} 0^{-+}
	M	M	S A	1^{--}, 2^{--} 1^{-+}, 2^{-+}
M^3	S	S A	S A	1^{+-}, 3^{+-} 0^{++}

Table 4.5. Calculated gluon energies for various N-values

Quanta N	Gluon energy expressions		Calculated energy	
	DCM $W_N=(2N+3)a$	CCM $W_N=(2N+3)^{1/2}b$	DCM	CCM
0	3a	$\sqrt{3}b$	540	629
1	5a	$\sqrt{5}b$	900	811
2	7a	$\sqrt{7}b$	1260	960
3	9a	$\sqrt{9}b$	1620	1089
4	11a	$\sqrt{11}b$	1980	1204

Table 4.6. Low-lying digluon and trigluon glueball energy states calculated using iota as a $g_E g_M$> state.

Coupled Modes	J^{PC}	Calculated glueball energies: Using iota (1440 MeV) DCM	Using iota (1440 MeV) CCM	Using iota (1460 MeV) DCM	Using iota (1460 MeV) CCM
EE	$0^{++}, 2^{++}$	1080	1257	1095	1275
EM	$0^{-+}, 2-+$	1440	1440	1460	1460
MM	$0^{++}, 2^{++}$	1800	1623	1825	1645
EEE	$0^{-+}, 1^{--}, 3^{--}$	1620	1886	1643	1912
EEM	$3^{+-}, 1^{+-}, 0^{++}$ $1^{+-}, 2^{+-}, 1^{++}$ 2^{++}	1980	2069	2008	2097
EMM	$3^{--}, 1^{--}, 0^{-+}$ $1^{--}, 2^{--}, 1^{-+},$ 2^{-+}	2340	2251	2373	2283
MMM	$0^{++}, 1^{+-}, 3^{+-}$	2700	2434	2738	2468

Table 4.7. Intrinsic energy expressions of the confined gluons in digluon and trigluon systems

Quanta	Intrinsic Energy Expressions			
	$\epsilon_N^{DCM} = (2N+3-3/m)a$		$\epsilon_N^{CCM} = (2N+3-3/m)^{1/2}b$	
N	m = 2	m = 3	m = 2	m = 3
0	3a/2	2a	$(3/2)^{1/2}b$	$2^{1/2}b$
1	7a/2	4a	$(7/2)^{1/2}b$	2b
2	11a/2	6a	$(11/2)^{1/2}b$	$6^{1/2}b$
3	15a/2	8a	$(15/2)^{1/2}b$	$8^{1/2}b$
4	19a/2	10a	$(19/2)^{1/2}b$	$10^{1/2}b$

Table 4.8. Energy expressions of the low-lying digluon and trigluon glueballs ensuring its centre at the lowest eigen state.

Coupled Modes	Combinations of the gluon intrinsic energies	Final energy of the glueballs in terms of the parameter DCM	CCM
EE(00)	$2\epsilon_0$	3a	2.44949b
EM(01)	$\epsilon_0+\epsilon_1$	5a	3.095574b
MM(11,02)	$(2\epsilon_1+\epsilon_0+\epsilon_2)/2$	7a	3.655806b
EEE(000)	$3\epsilon_0$	6a	4.242641b
EEM(01)	$2\epsilon_0+\epsilon_1$	8a	4.828427b
EMM(11) (0) (02)	$\epsilon_0+(2\epsilon_1+\epsilon_0+\epsilon_2)/2$	10a	5.346066b
MMM(111) (012) (003)	$(3\epsilon_1+\epsilon_0+\epsilon_1+\epsilon_2+2\epsilon_0+\epsilon_3)/3$	12a	5.840186b

Table 4.9. Corrected glueball energies in DCM and CCM.

Coupled Modes	J^{PC}	Model Calculations DCM	CCM	J^{PC}	Experiment Energy
EE	$0^{++}, 2^{++}$	864	1139	0^{++}	1240 (g_s)
EM	$0^{-+}, 2^{-+}$	$\underline{1440}$	$\underline{1440}$	0^{-+}	1440 (ι)
MM	$0^{++}, 2^{++}$	2016	1701	2^{++}	1700 (θ)
EEE	$0^{-+}, 1^{--}, 3^{--}$	1728	1974	–	–
EEM	$0^{++}, 2^{++}$ $1^{+-}, 3^{+-}, 2^{+-}$ $1^{++}, 1^{+-}$	2304	2246	2^{++}	2120 (g_T) 2220 ($g_{T'}$) 2360 ($g_{T''}$)
EMM	$3^{--}, 1^{--}, 0^{-+}$ $1^{--}, 2^{--}, 1^{-+}$ 2^{-+}	2880	2487	–	–
MMM	$0^{++}, 1^{+-}, 3^{+-}$	3456	2717	–	–

Table 4.10. Low-lying glueball energies by fitting iota (1460, 0^{-+}) as a $|g_E g_m\rangle$ state.

Coupled	Calculated glueball energies DCM	CCM	Experimental details
EE	876	1155	1240
EM	1460	1460	1455 + 4
MM	2044	1724	1710 + 5
EEE	1752	2001	–
EEM	2336	2277	(2120,2220,2360)
EMM	2960	2521	–
MMM	3504	2754	–

Table 4.11. Low-lying glueball energies by fitting $\langle g_T \rangle$ 2233 MeV as the $|g_E g_E g_M\rangle$ state.

Coupled Modes	Calculated glueball energies DCM	CCM	Experimental details
EE	837	1133	1240 ± 10
EM	1396	1432	1455 ± 4
MM	1954	1691	1710 ± 5
EEE	1675	1962	–
EEM	2233	2233	(2120,2220,2360)
EMM	2791	2472	–
MMM	3350	2701	–

THEORETICAL DESCRIPTION OF PURELY GLUONIC MATTER

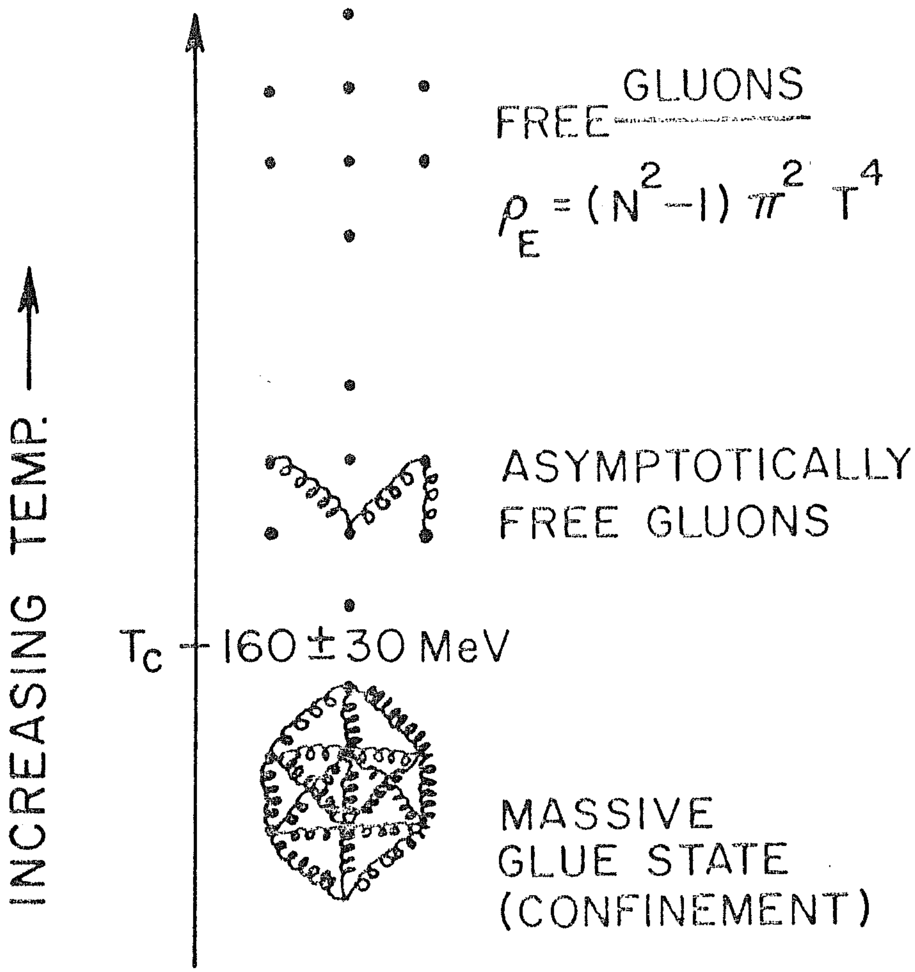

Fig. 4·1

OZI ALLOWED PROCESSES

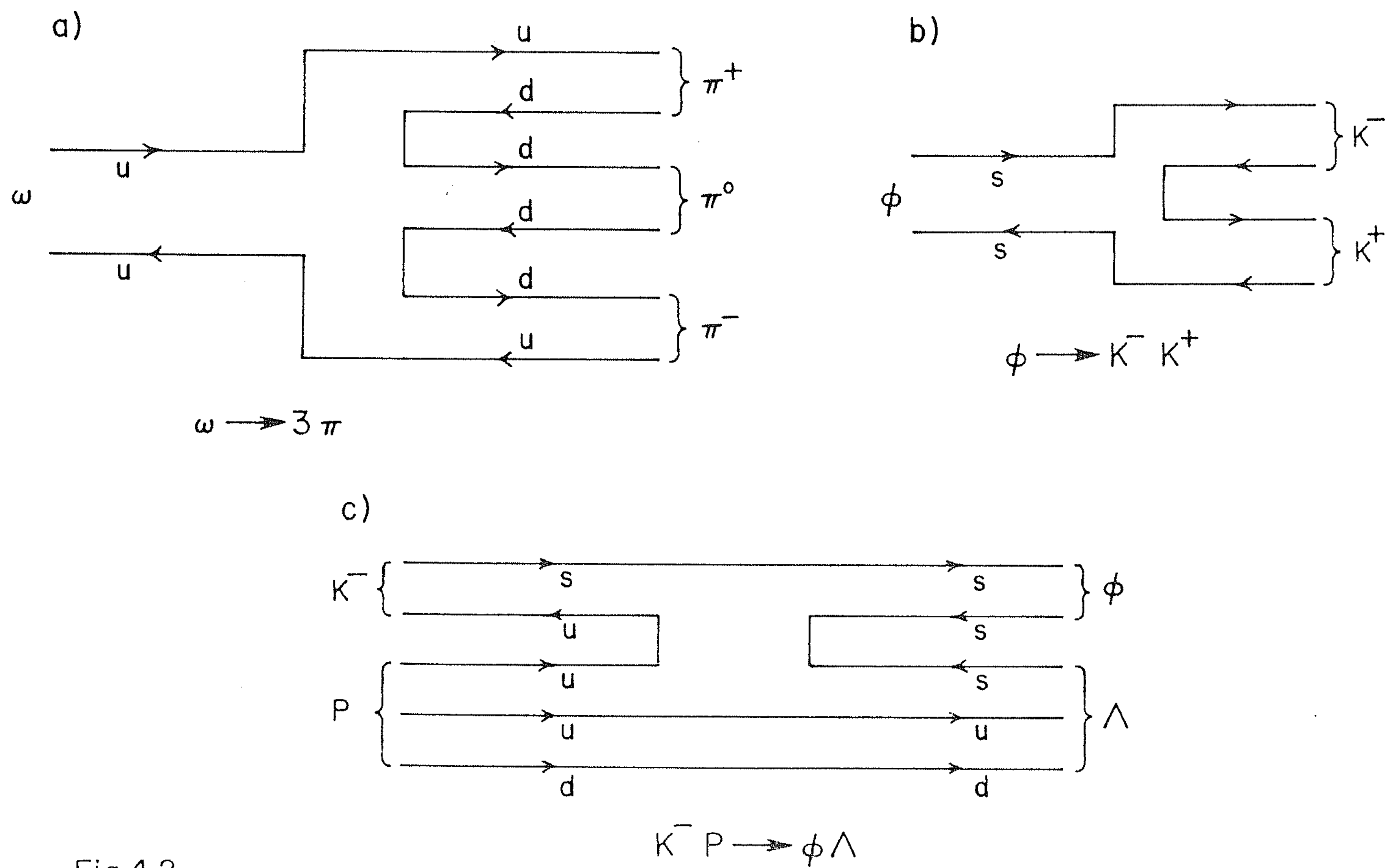

Fig.4·2

OZI FORBIDDEN PROCESSES

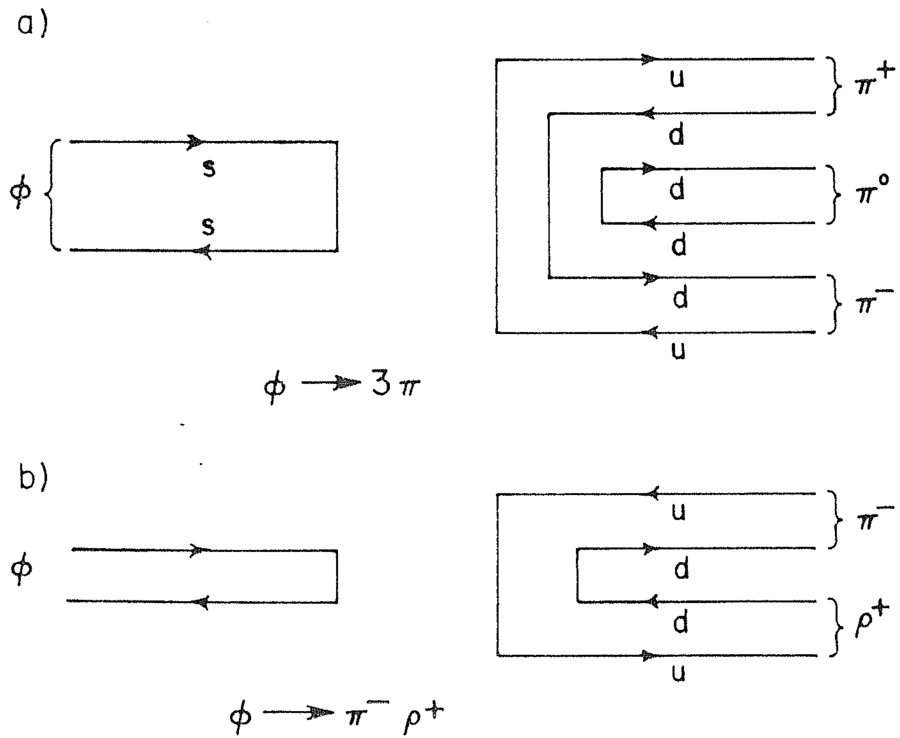

Fig. 4·3

a)

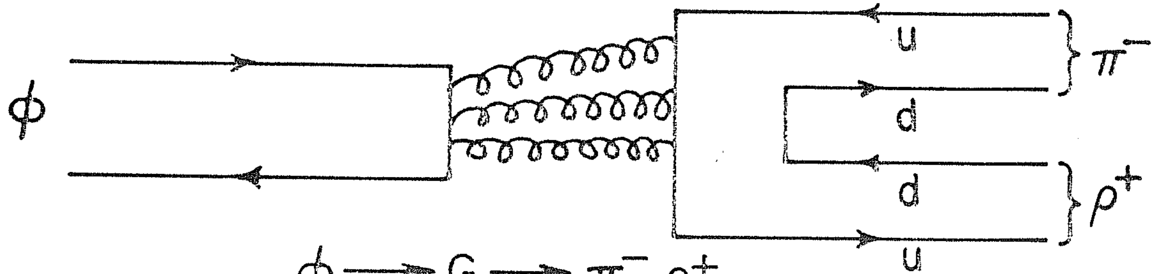

Fig. 4·4 $\phi \longrightarrow G \longrightarrow \pi^- \rho^+$

b)

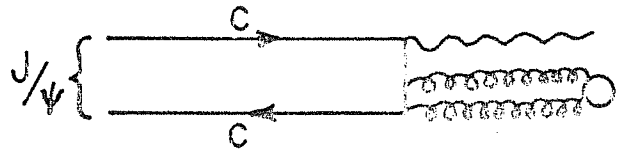

$J/\psi \longrightarrow r_{gg}$

OZI RULE EXTENDED TO GLUE-MESON DECAYS

a)

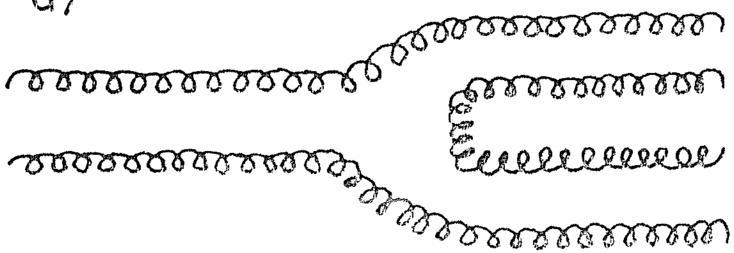

Glue-meson decay in to a pair of Glue resonances.

b)

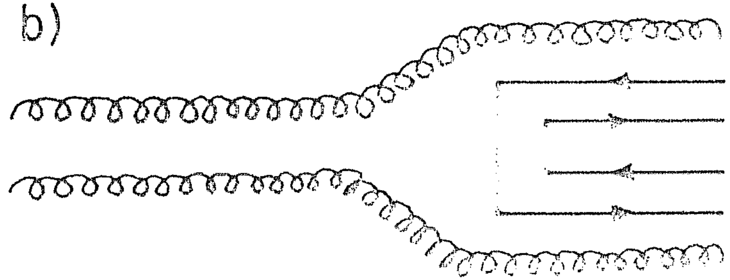

Glue-meson decay in to a pair of excited hadrons.

Fig. 4·5

FEYNMAN DIAGRAM J/ψ DECAY

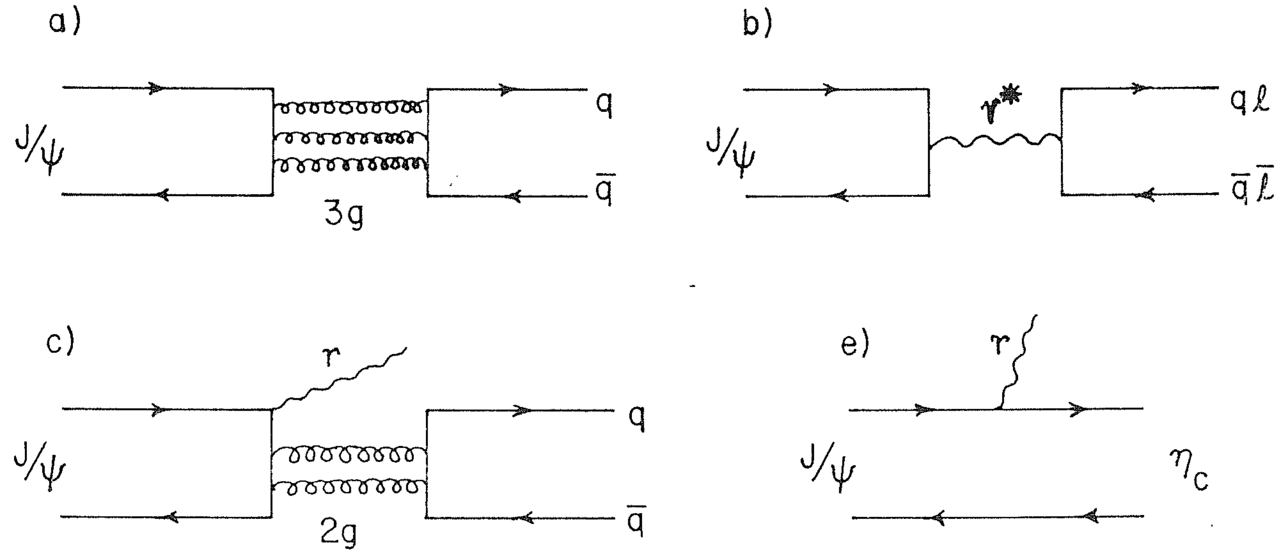

a) Three gluon decay

b) Electromagnetic decay to leptons and quarks

c) Radiative decay to two gluons

d) Radiative decay via glueball

e) Radiative decay to η_c

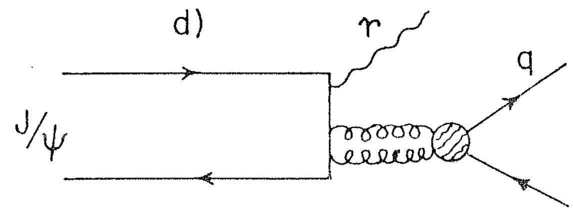

Fig. 4·6

MULTIGLUON RESONANCES IN OZI FORBIDDEN PROCESSES

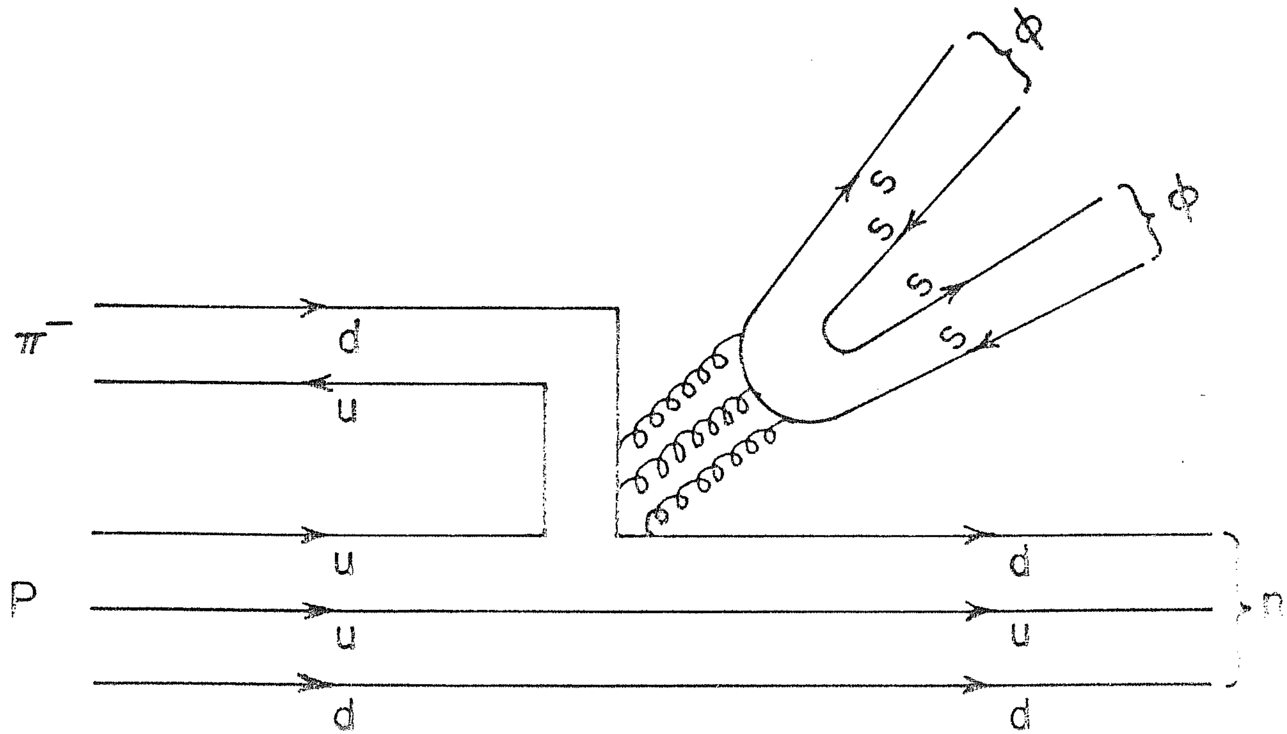

$P + \pi \longrightarrow G \longrightarrow \phi\phi$

Fig. 4·7

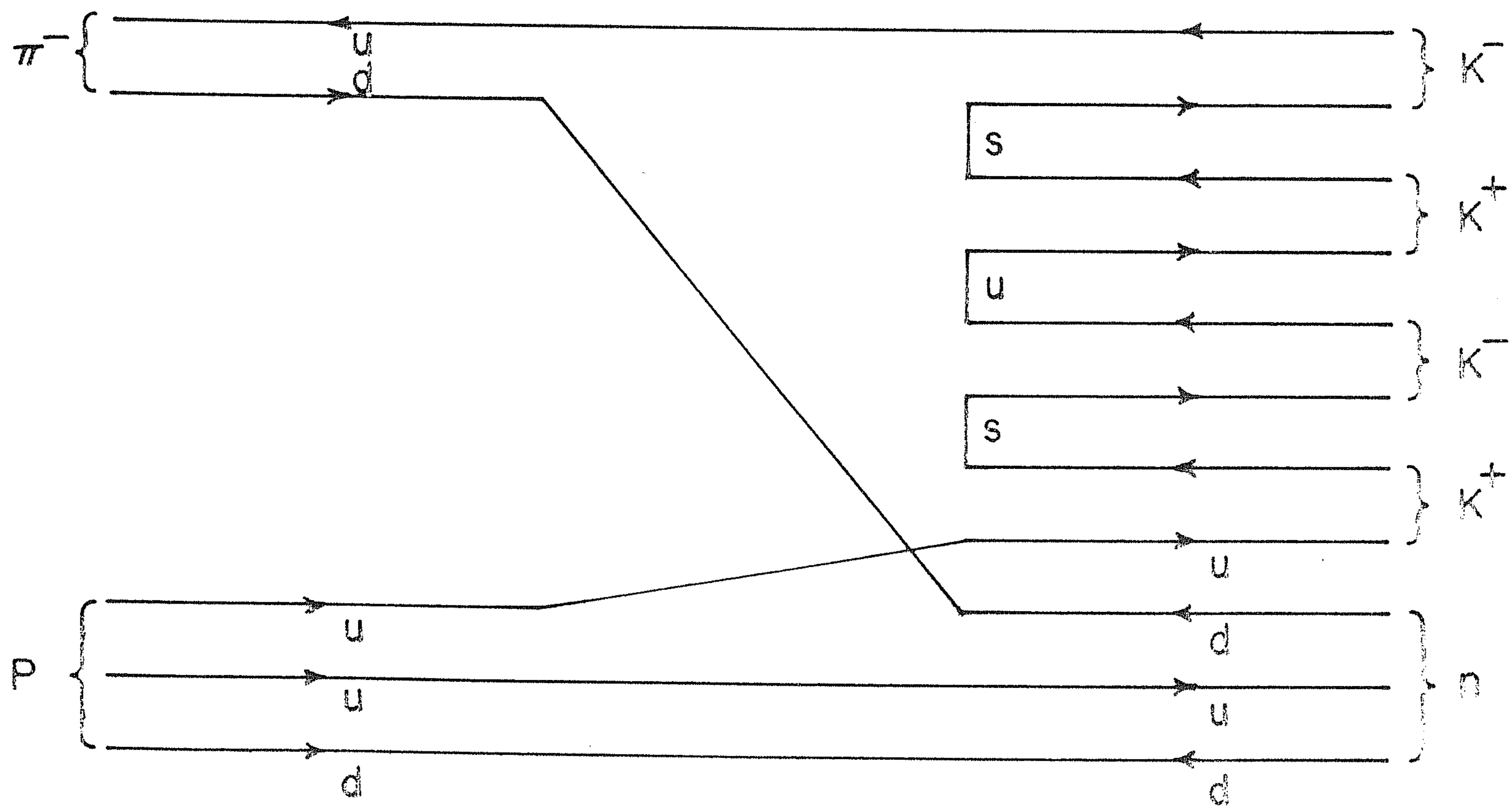

$\pi^- P \longrightarrow K^+ K^- K^+ K^- n$

Fig. 4·8 a

OZI ALLOWED PROCEES

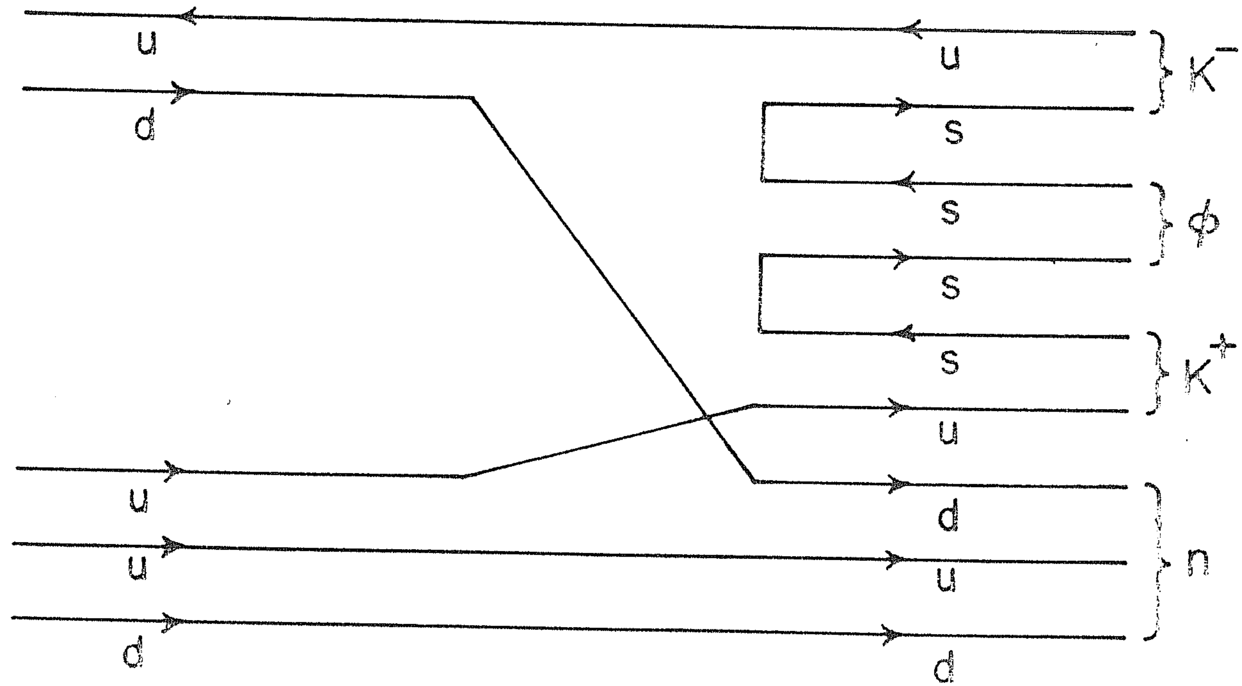

$\pi^- P \longrightarrow \phi K^+ K^- n$

Fig. 4-8b

THE CONFINED GLUON ENERGY LEVELS

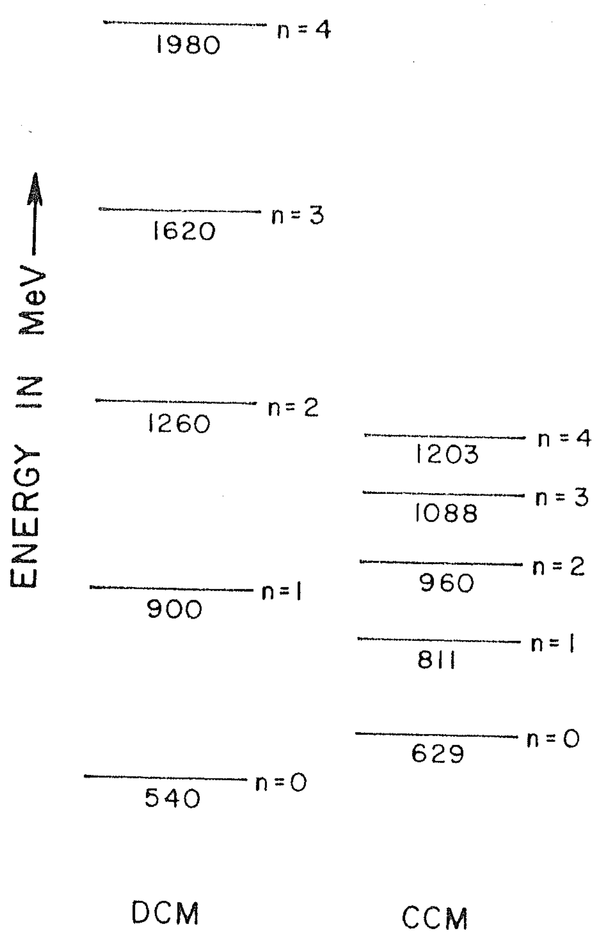

Fig. 4·9

DI-GLUON ENERGY LEVELS WITHOUT
THE CENTRE OF MASS CORRECTION

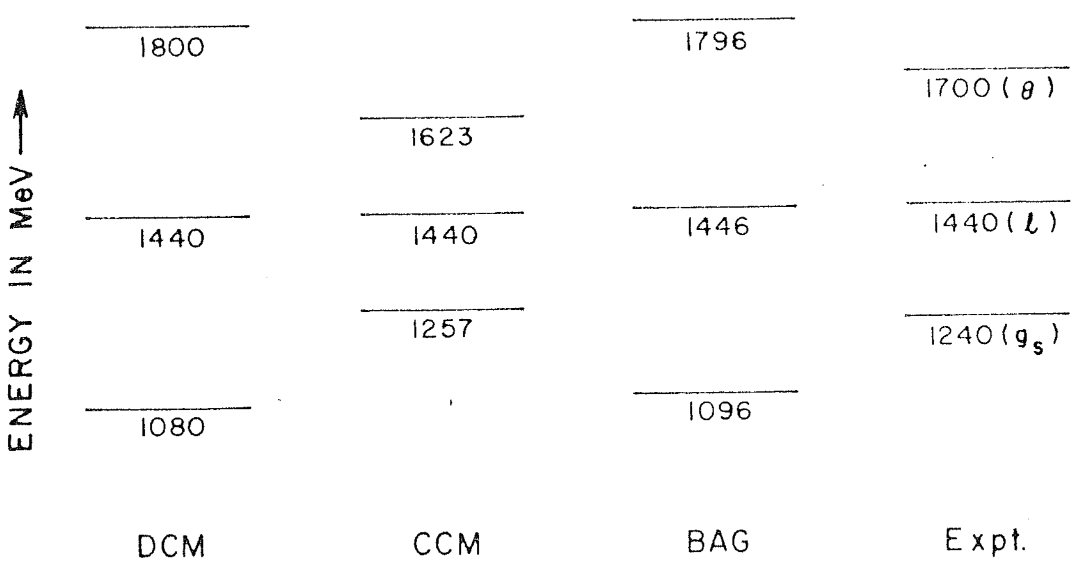

Fig. 4·10 a

TRI-GLUON ENERGY LEVELS WITHOUT THE CENTRE OF MASS CORRECTION

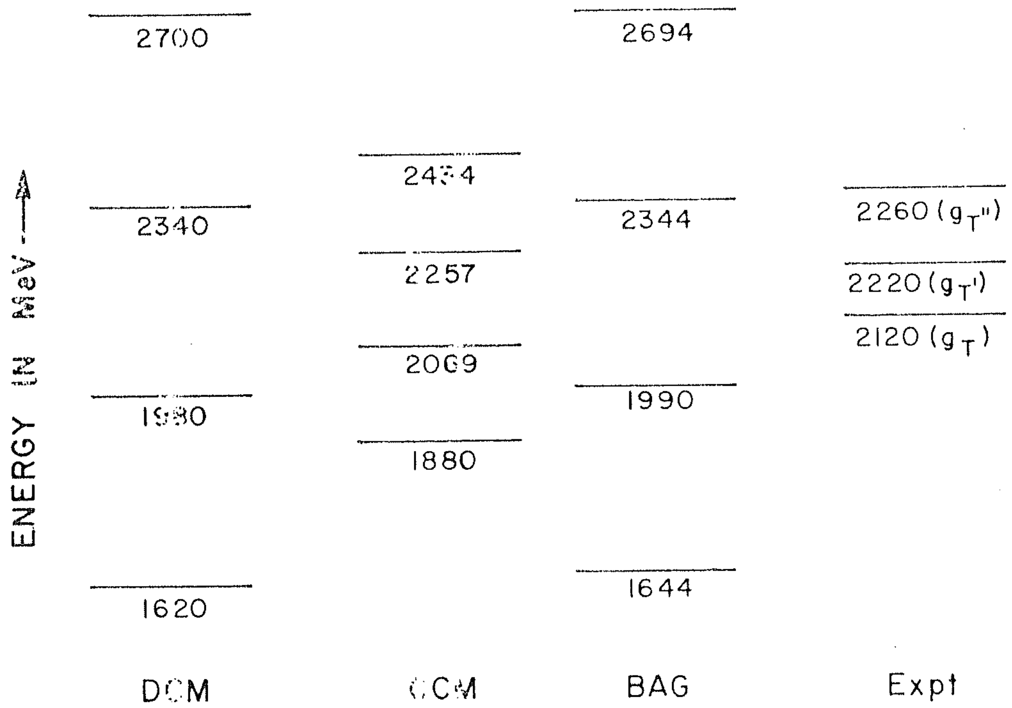

Fig. 4·10b

CO-ORDINATE SYSTEM FOR MULTIGLUON STATES

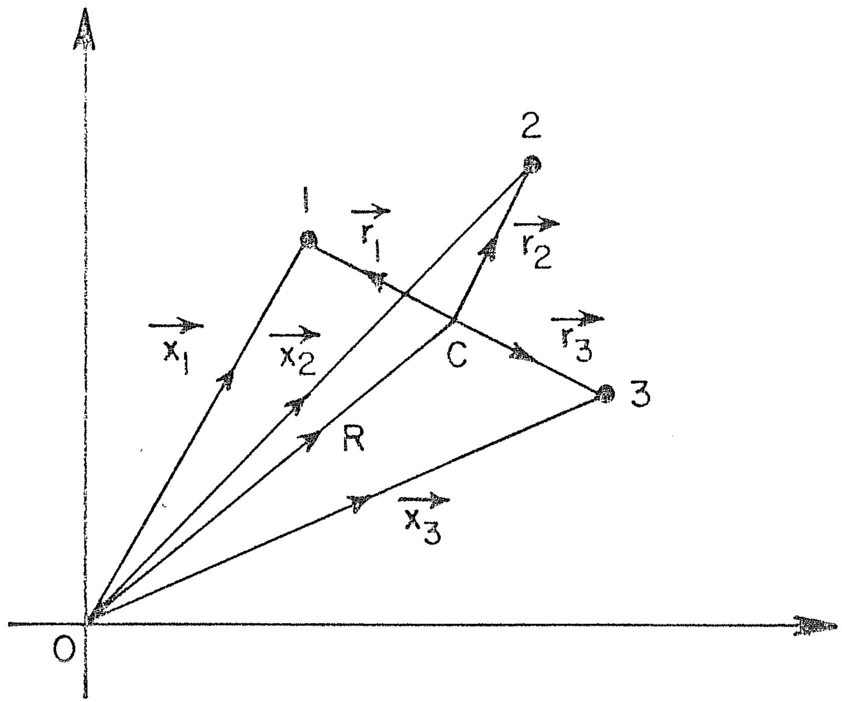

Fig. 4·11

LOW LYING DI-GLUON GLUEBALL ENERGY LEVELS

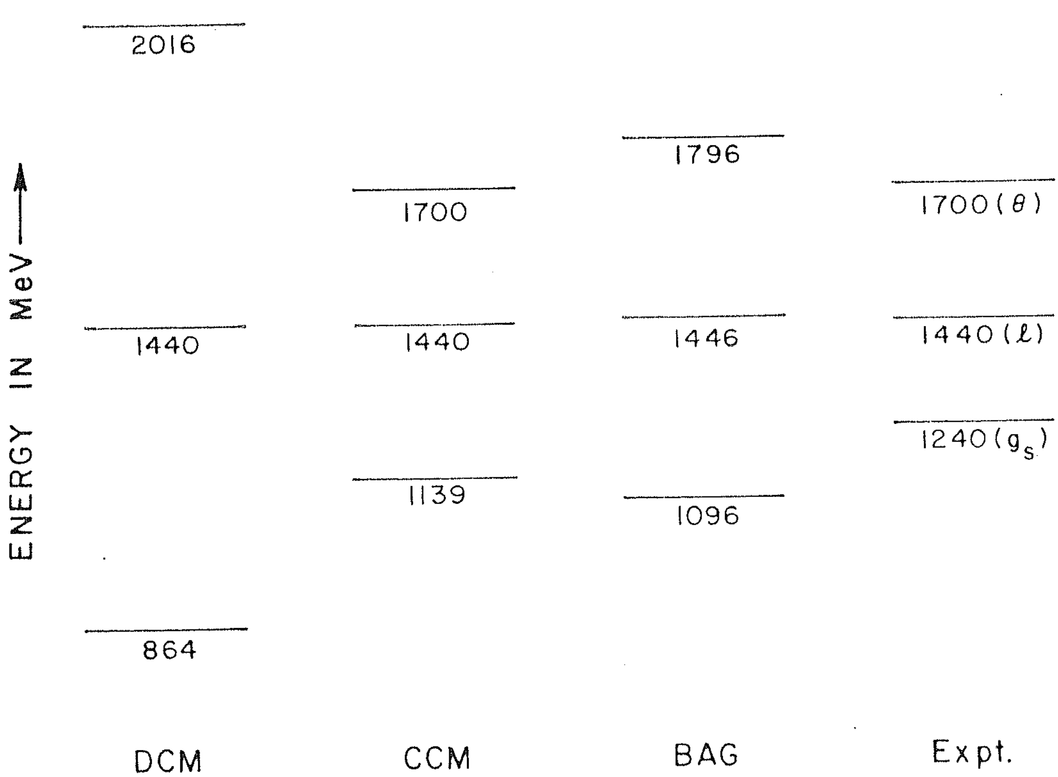

Fig. 4·12a

LOW LYING TRI-GLUON GLUEBALL ENERGY LEVELS

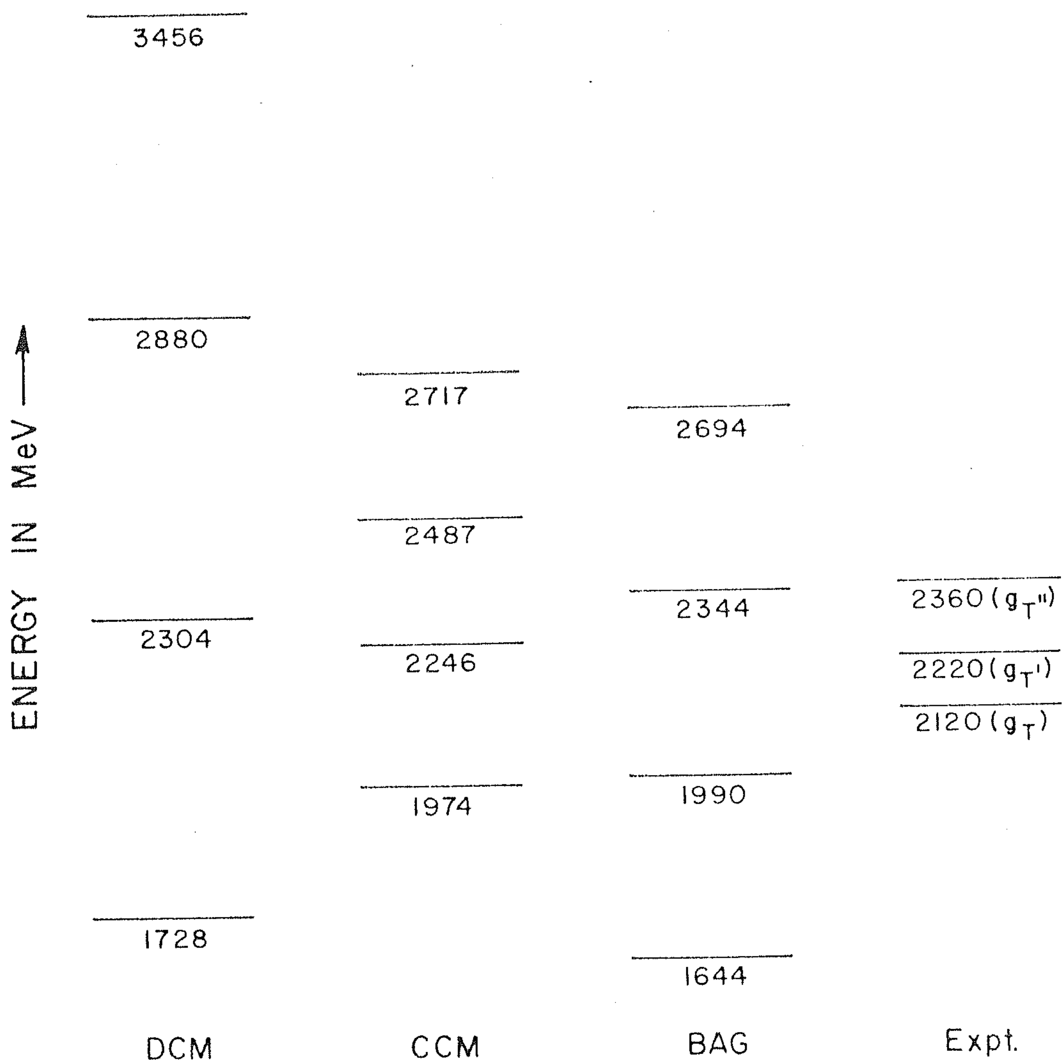

Fig. 4·12 b

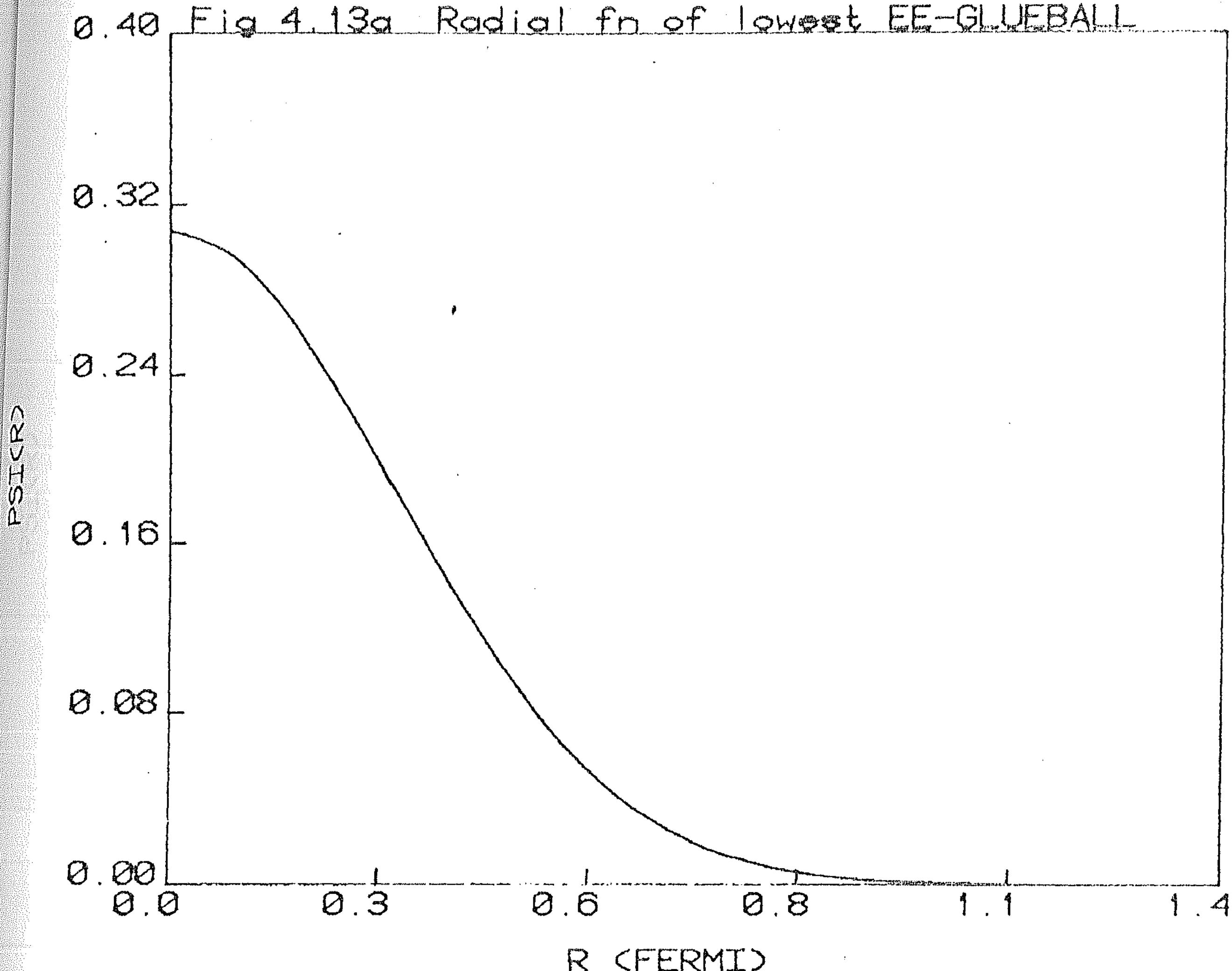

Fig 4.13a Radial fn of lowest EE-GLUEBALL
0.40
0.32
0.24
0.16
0.08
0.00
PSI(R)
0.0
0.3
0.6
0.8
1.1
1.4
R (FERMI)

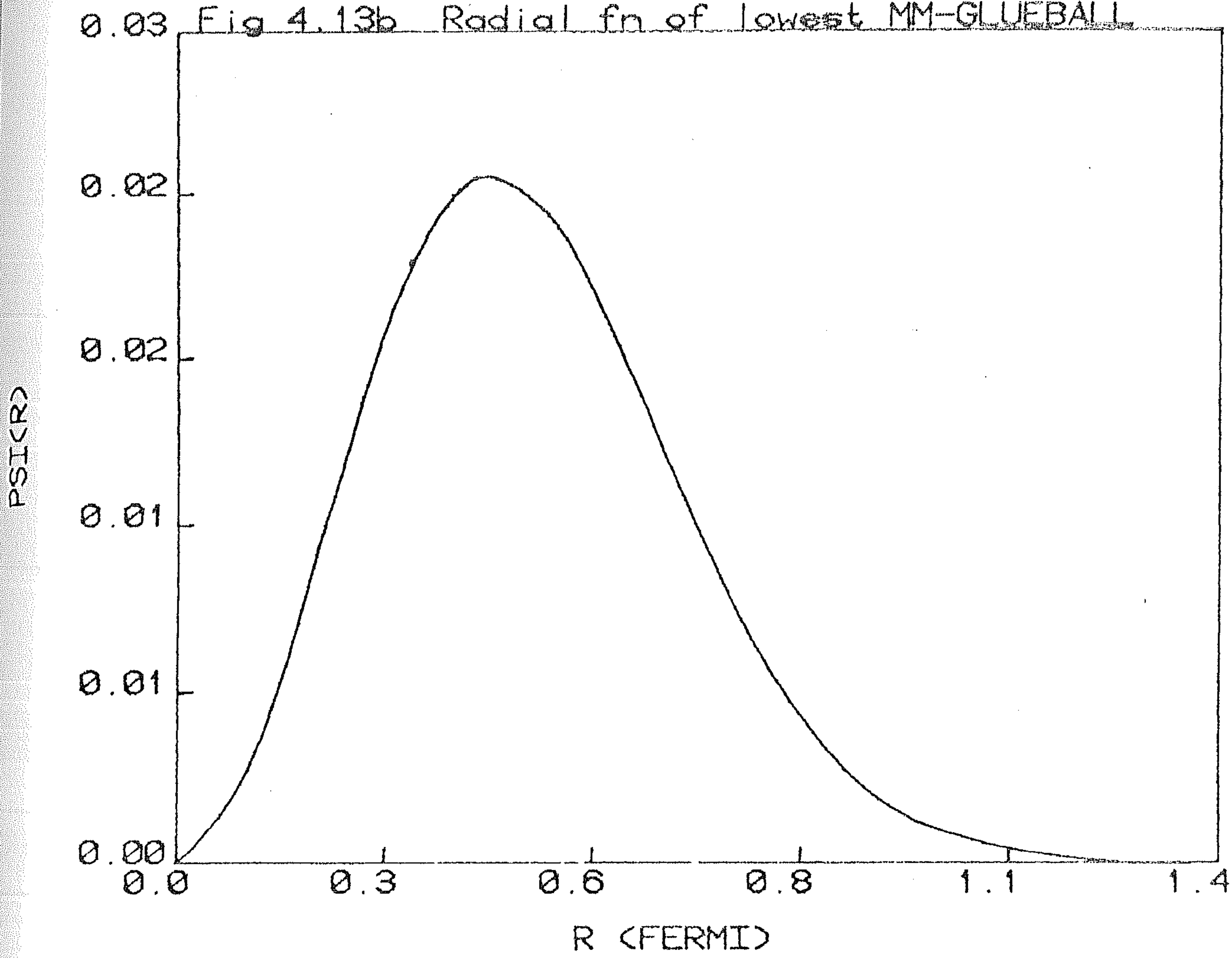
0.03
Fig 4.13b Radial fn of lowest MM-GLUEBALL
0.02
0.02
0.01
0.01
0.00
PSI(R)
0.0
0.3
0.6
0.8
1.1
1.4
R (FERMI)

CHAPTER V

THE CONFINED GLUON PROPAGATOR IN A TRANSLATIONALLY INVARIANT OSCILLATOR BASIS

5.1. Introduction

The success of the gluon confinement model particularly the CCM provides a consistent confinement basis for the gluons in an identical manner to that of the quarks in RHM [23]. The essential requirement in the construction of a unified scheme with quarks and gluons together including their interaction is to obtain the confined gluon propagator.

In this unified confinement theory the RHM-quarks interact via the exchange of the CCM-gluons. Thus as in the case of electron-electron interaction via the photon [121] the scattering amplitude of the quark-quark interaction can be written as

$$M_{fi} = g^2 (\bar{q}_i \gamma_\mu \tfrac{1}{2} \lambda_i^a q_i) D_{\mu\nu} (\bar{q}_j \gamma_\nu \tfrac{1}{2} \lambda_j^b q_j) \tag{5.1.1}$$

where g is the quark-gluon coupling constant, q_i's are the confined solutions of quarks, λ_i^a are the colour matrices (a=1,2,3) and $D_{\mu\nu}$ is the confined gluon propagator. In the case of CCM gluons, from equations (3.3.14) and (3.3.15), the relevant propagators are given by,

$$\mathcal{D}_{00}(r, r') = \frac{4\pi}{-\nabla^2 + \alpha^2 r^2 - (\omega^2 + 2\alpha)} \delta^3(r - r') \tag{5.1.2}$$

corresponding to the 'Coulombic' interaction, and

$$\mathcal{D}_{ij}(r, r') = \frac{4\pi}{-\nabla^2 + \alpha^2 r^2 - \omega^2} \left[\delta_{ij} - \frac{a_i^+ a_j}{\underset{\sim}{a} \cdot \underset{\sim}{a}^+} \right] \tag{5.1.3}$$

in the oscillator gauge for the transverse gluon exchange. Since they are in a confined bound system the propagator has to be chosen such that the spurious motion of the centre of confinement is taken into account. Thus as in the case of the glueball energy calculations in section 4.6 of Chapter 4, a translationally invariant ansatz for the confined gluon propagator has been made by choosing the centre of confinement at the origin (corresponding to R=0). In the case of CCM gluons the propagator is the harmonic oscillator propagator as given by equations (5.1.2) and (5.1.3). In this chapter, a closed analytical expression for the relevant propagator is derived. It is different from the usual oscillator Green's function obtained through path integral formalism [114] which is not translationally invariant. Section 5.2 justifies the translationally invariant ansatz by fixing the centre of confinement at the origin. In Section 5.3, the propagator in the three-dimensional spherical polar coordinate is formally derived. It can be generalized to the m-dimensional case (see Appendix D).

5.2. The Translationally Invariant Ansatz for the Propagator

The propagator in a bound state oscillator system satisfies

$$(-\nabla^2 + r^2 - \lambda)\, G(\underset{\sim}{r}, \underset{\sim}{r}') = \delta(\underset{\sim}{r} - \underset{\sim}{r}') \tag{5.2.1}$$

since G(r,r′) and δ(r−r′) are symmetric functions,

$$(-\nabla'^2 + r'^2 - \lambda)\, G(\underset{\sim}{r}, \underset{\sim}{r}') = \delta(\underset{\sim}{r} - \underset{\sim}{r}') \tag{5.2.2}$$

on adding these two equations,

$$\left\{\frac{1}{2}(-\nabla^2 - \nabla'^2) + \frac{r^2 + r'^2}{2} - \lambda\right\} G(r, r') = \delta(r - r'). \tag{5.2.3}$$

Defining now

$$\underset{\sim}{\rho} = \frac{\underset{\sim}{r} - \underset{\sim}{r}'}{2} \tag{5.2.4}$$

and

$$\underset{\sim}{R} = \frac{\underset{\sim}{r} + \underset{\sim}{r}'}{2}\ ; \tag{5.2.5}$$

Then the above equation (5.2.3) becomes,

$$\left[-\frac{\partial^2}{\partial R^2} + R^2 - \frac{\partial^2}{\partial \rho^2} + \rho^2 - \lambda\right] G(\underset{\sim}{R}, \underset{\sim}{\rho}) = \delta(2\underset{\sim}{\rho}). \tag{5.2.6}$$

Now decomposing the $\underset{\sim}{R}$, $\underset{\sim}{\rho}$ coordinates,

$$\left[-\frac{\partial^2}{\partial R^2} + R^2 - \lambda_R\right] G(\underset{\sim}{R}-0) = 0 \tag{5.2.7}$$

and

$$\left[-\frac{\partial^2}{\partial \rho^2} + \rho^2 - \lambda_\rho\right] G(\underset{\sim}{\rho},0) = \delta(2\underset{\sim}{\rho}) = \frac{1}{2}\,\delta(\rho). \tag{5.2.8}$$

(5.2.9)

Thus the translationally invariant part of the propagator is defined as

$$\mathcal{G}(\underset{\sim}{\rho},0) = 2G(\underset{\sim}{\rho}) \tag{5.2.10}$$

such that it satisfies the equation

$$\left[-\frac{\partial^2}{\partial \rho^2} + \rho^2 - \lambda_\rho\right] \mathcal{G}(\underset{\sim}{\rho},0) = \delta(\underset{\sim}{\rho}). \tag{5.2.11}$$

Here the centre of the bound system is fixed at $\underset{\sim}{R} = 0$ (the origin) with the spurious energy corresponding to the lowest oscillator mode. In the case of CCM gluon propagator the λ_ρ corresponds to the gluon intrinsic energy square as defined in section 4.6 of Chapter 4. The propagator which corresponds to the centre of the bound system is written as

$$G(0,0,\lambda) = \frac{\Psi_0(0)\,\Psi_0(0)}{\lambda_0-\lambda} \tag{5.2.12}$$

and the propagator in the relative coordinate system (which is translationally invariant) is written as

$$\mathcal{G}(\underset{\sim}{\rho}, 0, \lambda) = \sum_N \frac{\varphi_N(\rho)\,\varphi_N^*(0)}{\lambda_N - \lambda} \tag{5.2.13}$$

5.3. The 3-dimensional Harmonic Oscillator Propagator in Spherical Polar Co-ordinate

The propagator expression in 3-dimensional spherical polar coordinate is given by [115]

$$G_3(\underset{\sim}{r}, \underset{\sim}{r}', \lambda) = \frac{1}{2\pi r r'} \sum_{\ell=0}^{\infty} (\ell + \tfrac{1}{2})\, G_\ell(r, r', \lambda)\, P_\ell\{\cos\theta\cos\theta' - \sin\theta\sin\theta\cos(\varphi - \varphi')\} \tag{5.3.1}$$

where $G_\ell(r, r', \lambda)$ satisfies the equation

$$G_\ell'' + \left(\lambda - r^2 - \frac{\ell(\ell+1)}{r^2}\right) G_\ell = -\delta(r - r'). \tag{5.3.2}$$

It is the inhomogeneous radial equation for the 3-dimensional harmonic oscillator. The spectral expression for $G_\ell(r, r', \lambda)$ can be written as;

$$G_3(r, r', \lambda) = \frac{\pi^{-3/2}}{2\pi r r'} \sum_{\ell=0}^{\infty} 2^{\ell+1}(\ell + \tfrac{1}{2}) \times \sum_{N=2n+\ell=0}^{\infty} \frac{n!}{\Gamma(n+\ell+3/2)} \times \left[\frac{r^{\ell+1}\, r'^{\ell+1}}{\lambda_N - \lambda}\, e^{-\left(\frac{r^2 + r'^2}{2}\right)} L_n^{\ell+1/2}(r^2)\, L_n^{\ell+\frac{1}{2}}(r'^2)\right] \times P_\ell\{\cos\theta\cos\theta' - \sin\theta\sin\theta'\cos(\varphi - \varphi')\}. \tag{5.3.3}$$

Making use of the translationally invariant ansatz, the origin is chosen at the centre of mass of the bound system and the propagator in the relative coordinate system is obtained by shifting the coordinate $r \to r-r'$ and $r' \to 0$. By this translation of the coordinate, it can be seen that the only non-vanishing terms are those for which $\ell = 0$. Thus the expression for the translationally invariant propagator corresponds to those terms with $\ell=0$, and is written as

$$\mathcal{G}_3(\underset{\sim}{\rho}, \lambda) = \frac{\pi^{-3/2}}{2\pi} \sum_{N=2n=0}^{\infty} \frac{n!}{\Gamma(n+3/2)} e^{-\rho^2/2} \times \frac{L_n^{1/2}(\rho^2)\, L_n^{1/2}(0)}{4n+3-\lambda} \tag{5.3.4}$$

where

$$L_n^{1/2}(0) = \frac{\Gamma(n+3/2)}{n!\,\Gamma(3/2)} . \tag{5.3.5}$$

Thus,

$$\mathcal{G}_3(\underset{\sim}{\rho}, \lambda) = \pi^{-3} \exp\left(-\frac{\rho^2}{2}\right) \sum_{n=0}^{\infty} \frac{L_n^{1/2}(\rho^2)}{4n+3-\lambda} . \tag{5.3.6}$$

This expression can be generalized for m-dimensional case as done in Appendix D and in the m-dimensional hyper spherical case the propagator expression is obtained as

$$\mathcal{G}_m(\underset{\sim}{\rho}, 0, \lambda) = \pi^{-m} \exp -\frac{\rho^2}{2} \sum_{n=0}^{\infty} \frac{L_n^{\frac{m-2}{2}}(\rho^2)}{\lambda_{2n} - \lambda} . \tag{5.3.7}$$

The above expression is further simplified to a compact form by computing the infinite summation of the Lagaurre polynomial analytically. The simple poles are avoided by the choice of λ. The final expression is obtained in Appendix E. For the m-dimensional case it is obtained as

$$\mathcal{G}_m(\underset{\sim}{\rho}, \lambda) = \frac{\Gamma\left(\frac{m-\lambda}{4}\right)}{4\pi^m} \rho^{-\frac{m}{2}} W_{\frac{\lambda}{4}; -\left(\frac{m-2}{4}\right)}(\rho^2) \tag{5.3.8}$$

Here $W_{\frac{\lambda}{4}; -\left(\frac{m-2}{4}\right)}(\rho^2)$ is the Whittacker's function. Thus the compact expression in the three-dimensional case is obtained as

$$\mathcal{G}_3(\underset{\sim}{\rho}, \lambda) = \frac{\Gamma\left(\frac{3-\lambda}{4}\right)}{4\pi^3} \rho^{-3/2} W_{\frac{\lambda}{4}; -\frac{1}{4}}(\rho^2) \tag{5.3.9}$$

and

$$\mathcal{G}_3(\underset{\sim}{\rho} \to \infty, \lambda) = \frac{\Gamma\left(\frac{3-\lambda}{4}\right)}{4\pi^3} \rho^{\frac{\lambda-3}{2}} e^{-\rho^2/2} \tag{5.3.10}$$

and

$$\mathcal{G}_3(\rho \to 0, \lambda) = \frac{\Gamma\left(\frac{3-2}{4}\right)}{4\pi^3}\, \rho^{-1}. \qquad (5.3.11)$$

The propagator for $\rho \to 0$ is independent of the choice of λ. The expressions are plotted with the various choices of λ corresponding to the CCM gluon solutions (see figure 5.1).

5.6. Conclusion

Compact expressions for the propagator for 3-dimensional harmonic oscillator in a translationally invariant ansatz have been obtained. This propagator which corresponds to the confined gluons in the current confinement scheme will be used to calculate the colour Coulombic interactions and the modified Fermi-Breit like interactions among quarks due to the exchange of confined gluons. The derivation is generalized to the case of m-dimensional harmonic oscillator case. The higher dimensional forms can be used in various situations such as four-dimensional form in relativistic oscillator model of Feynmann-Kisslinger and Ravndal [120].

Appendix D
A General Construction for m-dimensional Oscillator Propagator

The Hamiltonian for the m-dimensional harmonic oscillator is given by

$$H_0 = \sum_{i=1}^{m} \left(-\frac{\partial^2}{\partial x_i^2} + x_i^2 \right) \tag{D.1}$$

in a suitable unit where the corresponding constants are absorbed. The eigen function φ_N which corresponds to H can be written in the form

$$\varphi_N(x_1 \cdots x_m) = \prod_{i=1}^{m} \varphi_{n_i}(x_i) \tag{D.2}$$

where $\varphi_{n_i}(x_i)$'s satisfy the one-dimensional oscillator equation

$$-\frac{\partial^2 \varphi_i}{\partial x_i^2} + (x_i^2 - \lambda_i)\varphi_i(x_i) = 0 \tag{D.3}$$

where λ_i is the corresponding oscillator eigenvalue

$$\lambda_i = 2n_i + 1 \quad . \tag{D.4}$$

The eigen function $\varphi_{n_i}(x_i)$ in cartesian coordinate is given by [115]

$$\varphi_{n_i}(x_i) = 2^{-n_i/2}(n_i!\,\pi)^{-1/2}\, e^{-x_i^2/2}\, H_{n_i}(x_i) \tag{D.5}$$

Here $H_{n_i}(x_i)$ is the Hermite polynomial of order n_i. Thus the m-dimensional eigen value equation is written as

$$(H_0 - \lambda_N)\,\varphi_N = 0 \tag{D.6}$$

where eigen value,

$$\lambda_N = \sum_{i=1}^{m}(2n_i + 1) \tag{D.7}$$

$$= (2N + m) \tag{D.8}$$

and

$$\varphi_N(x_1 \cdots x_m) = \prod_{i=1}^{m}\left\{2^{-n_i/2}(n_i\pi)^{-1/2}\, e^{-x_i^2/2} \times H_{n_i}(x_i)\right\}. \tag{D.9}$$

If $\underset{\sim}{r}$ is defined as the position vector in m-dimensional space, then

$$r^2 = \sum_{i=1}^{m} \underset{\sim}{x}_i^2 \tag{D.10}$$

and the general propagator expression can be written as [116]

$$G_m(\underset{\sim}{r}, \underset{\sim}{r}'; \lambda) = \sum_{N=0}^{\infty} \frac{\pi^{-m}}{\lambda_N - \lambda} \prod_{i=1}^{m} \sum_{n_i=0}^{\infty} \left[\frac{2^{-n_i}}{n_i!}\, e^{-\frac{(x_i^2 + x_i'^2)}{2}} \times\right.$$

$$\times H_{n_i}(x_i)\, H_{n_i}(x_i')\Big]\,\delta_{N,\sum_{i=1}^{m} n_i} \quad , \tag{D.11}$$

Expressing the delta function in terms of a contour integral:

$$\delta_{N,\sum_{i=1}^{m} n_i} = \frac{1}{2\pi i}\oint \frac{dz}{z^{N+1-\sum_{i=1}^{m} n_i}} \tag{D.12}$$

helps to carry out the summation over each n_i 's independently. Thus, equation (D.11) becomes

$$G_m(r, r', \lambda) = \frac{\pi^{-m}}{2\pi i}\, e^{-\frac{(r^2+r'^2)}{2}} \times \sum_{N=0}^{\infty} \frac{1}{\lambda_N - \lambda}\Big[\oint \frac{dz}{z^{N+1}} \prod_{i=1}^{m} \sum_{n_i=0}^{\infty} \Big(\frac{2^{-n_i}}{n_i!} \times H_{n_i}(x_i)\, H_{n_i}(x_i')\, z_i^{n_i}\Big)\Big] . \tag{D.13}$$

Using the generating function for the Hermite polynomials [117]:

$$\sum_{n=0}^{\infty} 2^{-n} \frac{H_n(x)\, H_n(y)}{n!} z^n = (1-z^2)^{-1/2} \exp\Big[y^2 - \frac{(y-zx)^2}{1-z^2}\Big] \tag{D.14}$$

the summation over n 's in equation (D.13) can be carried out, resulting,

$$G_m(x, x', \lambda) = \frac{\pi^{-m}}{2\pi i}\, e^{-\frac{(r^2+r'^2)}{2}} \sum_{N=0}^{\infty}\Big\{\frac{1}{\lambda_N - \lambda} \oint \frac{dz}{z^{N+1}} (1-z^2)^{-m/2}$$

$$\times \exp\left[r^2 - \frac{(\underline{r} - z\underline{r}')^2}{1 - z^2} \right] . \quad \text{(D. 15)}$$

$$= \frac{\pi^{-m}}{2\pi i} e^{-\frac{(r^2 + r'^2)}{2}} \sum_{N=0}^{\infty} \frac{1}{\lambda_N - \lambda} \times$$

$$\left[\oint \frac{dz}{z^{N+1}} (1 - z^2)^{-m/2} \exp\left[\frac{(r^2 + r'^2) z^2 - 2 \underline{r} \cdot \underline{r}' z}{z^2 - 1} \right] \right] .$$

(D. 16)

Making use of the generating function of the Lagaurre polynomial [117],

$$(1 - z)^{-\alpha - 1} \exp \frac{x z}{z - 1} = \sum_{n=0}^{\infty} L_n^{\alpha}(x) z^n$$

(D. 17)

and choosing the contour in such a way that $|z| < 1$, the m-dimensional full propagator reduces to

$$G_m(r, r', \lambda) = \frac{\pi^{-m}}{2\pi i} \exp - \left(\frac{r^2 + r'^2}{2} \right)$$

$$\sum_{N=0}^{\infty} \frac{1}{\lambda_N - \lambda} \oint \left[\frac{dz}{z^{N+1}} \sum_{n=0}^{\infty} L_n^{\frac{m-2}{2}}(r^2 + r'^2) z^{2n} \right.$$

$$\left. \exp\left(\frac{2 r \cdot r' z}{1 - z^2} \right) \right] .$$

(D. 18)

Now making use of the translationally invariant ansatz the propagator defined in equation (5.2.11) can formally be written in the m-dimensional case,

$$\mathcal{G}_m(\underline{\rho}, 0, \lambda) = \frac{\pi^{-m}}{2\pi i} e^{-\rho^2/2} \sum_{n=0}^{\infty} L_n^{\frac{m-2}{2}}(\rho^2) \times$$

$$\times \sum_{N=0}^{\infty} \frac{1}{\lambda_N - \lambda} \oint \frac{dz}{z^{N+1}} z^{2n} \quad . \tag{D. 19}$$

After performing the contour integration the only terms which survive are those for which N = 2n. Thus equation (D. 19) reduces to

$$\mathcal{G}_m(\underset{\sim}{\rho}, 0, \lambda) = \pi^{-m} \exp\left(-\frac{\rho^2}{2}\right) \sum_{n=0}^{\infty} \frac{L_n^{\frac{m-2}{2}}(\rho^2)}{\lambda_{2n} - \lambda} \tag{D. 20}$$

From equation (D. 8) λ_{2n} value is substituted to get the final expression for the translationally invariant part of the m-dimensional harmonic oscillator propagator

$$\mathcal{G}_m(\underset{\sim}{\rho}, 0, \lambda) = \pi^{-m} \exp\left(-\frac{\rho^2}{2}\right) \sum_{n=0}^{\infty} \frac{L_n^{\frac{m-2}{2}}(\rho^2)}{4n + m - \lambda} \, . \tag{D. 21}$$

The final summation is carried out in Appendix E.

Appendix E

Compact Expression for $g_m(\underset{\sim}{\rho}, \lambda)$

The translationally invariant part of the propagator for the m-dimensional harmonic oscillator obtained in the above sections can further be simplified to a compact form by computing the infinite summation of the Lagaurre polynomial analytically. The simple poles are avoided by the choice of λ. The expression for $g_m(\underset{\sim}{\rho}, \lambda)$ is rewritten formally:

$$g_m(\underset{\sim}{\rho}, \lambda) = \frac{1}{\pi^m} \exp\left(-\frac{\rho^2}{2}\right) S(\alpha, \beta) \tag{E.1}$$

where

$$S(\alpha, \beta) = \sum_{n=0}^{\infty} \frac{L_n^{\alpha}(\rho^2)}{4n + 2\beta} \tag{E.2}$$

The variables α and β are

$$\alpha = \frac{m-2}{2} \tag{E.3}$$

and

$$\beta = \frac{m-\lambda}{2} . \tag{E.4}$$

It will be easy to perform the summation if the denominator could be expressed in terms of a finite integral. Thus replacing,

$$\frac{1}{4n+2\beta} = \frac{1}{2}\int_0^1 dz\, z^{2n+\beta-1} \tag{E.5}$$

with

$$2n+\beta \geqslant 1 \tag{E.6}$$

Then S(α , β) becomes,

$$S(\alpha,\beta) = \frac{1}{2}\int_0^1 dz\, z^{\beta-1}\sum_{n=0}^{\infty} L_n^{\alpha}(\rho^2) z^{2n} \tag{E.7}$$

The upper limit of the integration is changed infinitesimally to make use of the generating function of the Lagaurre polynomial. Thus by equation (D.17),

$$S(\alpha,\beta) = \lim_{\epsilon\to 0}\frac{1}{2}\int_0^{1-\epsilon} dz\, z^{\beta-1}(1-z^2)^{-\alpha-1} \times \exp -\frac{\rho^2 z^2}{1-z^2}. \tag{E.8}$$

Defining a new variable

$$1-z^2 = t \tag{E.9}$$

$$S(\alpha,\beta) = \lim_{\epsilon\to 0}\frac{1}{2} e^{+\rho^2}\int_\epsilon^1 dt\,(1-t)^{\frac{\beta-2}{2}} t^{-\alpha-1} e^{-\rho^2/t}. \tag{E.10}$$

This integral is evaluated using the standard integral given in terms of the Whittacker's function [118],

$$\int_0^u x^{\nu-1}(u-x)^{\mu-1}\, e^{-\alpha/x}\,dx = \alpha^{\frac{\nu-1}{2}}\, u^{\frac{2\mu+\nu-1}{2}}\, e^{-\alpha/2u}\,\Gamma(\mu)\, W_{\frac{1-2\mu-\nu}{2};\,\nu/2}(\alpha/u) \qquad \text{(E. 11)}$$

for Rel. $\mu > 0$; Rel $\alpha > 0$; $u > 0$.

Now the expression for $S(\alpha,\beta)$ reduces to

$$S(\alpha,\beta) = \frac{1}{4}\,\Gamma(\beta/2)\, e^{\rho^2/2}\, \rho^{-\alpha-1}\, W_{\frac{1-\beta+\alpha}{2};\,-\frac{\alpha}{2}}(\rho^2) \qquad \text{(E. 12)}$$

for Rel. $\beta/2 > 0$.

By substituting α and β in terms of m and λ, a closed analytical expression for $g_m(\underset{\sim}{\rho}, \lambda)$ can be written:

$$g_m(\underset{\sim}{\rho},\lambda) = \frac{\Gamma\left(\frac{m-\lambda}{4}\right)}{4\pi^m}\, \rho^{-m/2}\, W_{\frac{\lambda}{4};\,-\frac{(m-2)}{4}}(\rho^2) \qquad \text{(E. 13)}$$

for all values of $m > \lambda$.

Using the asymptotic expressions for the Whittacker's function [119], the corresponding asymptotic expression for the propagator can be obtained. Thus, as $\rho \to \infty$ i.e. the particles are well separated then the general form of the propagator is

$$g_m(\underset{\sim}{\rho} \to \infty, \lambda) = \frac{\Gamma\left(\frac{m-\lambda}{4}\right)}{4\pi^m}\, \rho^{\frac{\lambda-m}{2}}\, e^{-\rho^2/2} \qquad \text{(E. 14)}$$

and if they are very close to each other, i.e., as $\rho \to 0$

$$\mathcal{G}_m(\rho \to 0, \lambda) = \frac{\Gamma\left(\frac{m-2}{2}\right)}{4\pi^m}\, \rho^{2-m} \tag{E.15}$$

for m > 2.

For example, in the three-dimensional case,

$$\mathcal{G}_3(\underset{\sim}{\rho}, \lambda) = \frac{\Gamma\left(\frac{3-\lambda}{4}\right)}{4\pi^3}\, \rho^{-3/2}\, W_{\frac{\lambda}{4}; -\frac{1}{4}}(\rho^2) \tag{E.16}$$

and

$$\mathcal{G}_3(\underset{\sim}{\rho} \to \infty, \lambda) = \frac{\Gamma\left(\frac{3-\lambda}{4}\right)}{4\pi^3}\, \rho^{\frac{\lambda-3}{2}}\, e^{-\rho^2/2} \tag{E.17}$$

and

$$\mathcal{G}_3(\underset{\sim}{\rho} \to 0, \lambda) = \frac{\Gamma\left(\frac{3-2}{4}\right)}{4\pi^3}\, \rho^{-1} \tag{E.18}$$

Special Cases:

Table E.1 gives the final expressions for the propagator with the special choices of the value of λ in different dimensions. The asymptotic expressions are also written.

Table E.1

Dimensions: m	Choice of λ ($\lambda < m$)	$\mathcal{G}_m(\rho, \lambda)$	$\mathcal{G}_m(\rho \to \infty, \lambda)$	$\mathcal{G}_m(\rho \to 0, \lambda)$ $m > 2$
1	0	$\frac{\Gamma 1/4}{4\pi} \rho^{-1/2} W_{0;\frac{1}{4}}(\rho^2)$	$\frac{\Gamma 1/4}{4\pi} \rho^{-1/2} e^{-\rho^2/2}$	
2	0	$\frac{\Gamma 1/2}{4\pi^2} \rho^{-1} W_{0;0}(\rho^2)$	$\frac{\Gamma 1/2}{4\pi^2} \rho^{-1} e^{-\rho^2/2}$	
	1	$\frac{\Gamma 1/4}{4\pi^2} \rho^{-1} W_{\frac{1}{4};0}(\rho^2)$	$\frac{\Gamma 1/4}{4\pi^2} \rho^{-1/2} e^{-\rho^2/2}$	

m	λ	$G_m(\rho,\lambda)$	$G_m(\rho\to\infty,\lambda)$	$G_m(\rho\to 0,\lambda)$
	0	$\frac{\Gamma(3/4)}{4\pi^3}\,\rho^{-3/2}\,W_{0;-\frac{1}{4}}(\rho^2)$	$\frac{\Gamma(3/4)}{4\pi^3}\,\rho^{-3/2}\,e^{-\rho^2/2}$	$m>2$
3	1	$\frac{\Gamma(1/2)}{4\pi^3}\,\rho^{-3/2}\,W_{\frac{1}{4};-\frac{1}{4}}(\rho^2)$	$\frac{\Gamma(1/2)}{4\pi^3}\,\rho^{-1}\,e^{-\rho^2/2}$	$\frac{\Gamma(1/2)}{4\pi^3}\,\rho^{-1}$
	2	$\frac{\Gamma(1/4)}{4\pi^3}\,\rho^{-3/2}\,W_{\frac{1}{2};-\frac{1}{4}}(\rho^2)$	$\frac{\Gamma(1/4)}{4\pi^3}\,\rho^{-1/2}\,e^{-\rho^2/2}$	
	0	$\frac{\Gamma(1)}{4\pi^4}\,\rho^{-2}\,W_{0;-\frac{1}{2}}(\rho^2)$	$\frac{\Gamma(1)}{4\pi^4}\,\rho^{-2}\,e^{-\rho^2/2}$	
4	1	$\frac{\Gamma(3/4)}{4\pi^4}\,\rho^{-2}\,W_{\frac{1}{4};-\frac{1}{2}}(\rho^2)$	$\frac{\Gamma(3/4)}{4\pi^4}\,\rho^{-3/2}\,e^{-\rho^2/2}$	$\frac{\Gamma(1)}{4\pi^4}\,\rho^{-2}$
	2	$\frac{\Gamma(1/2)}{4\pi^4}\,\rho^{-2}\,W_{\frac{1}{2};-\frac{1}{2}}(\rho^2)$	$\frac{\Gamma(1/2)}{4\pi^4}\,\rho^{-1}\,e^{-\rho^2/2}$	
	3	$\frac{\Gamma(1/4)}{4\pi^4}\,\rho^{-2}\,W_{\frac{3}{4};-\frac{1}{2}}(\rho^2)$	$\frac{\Gamma(1/4)}{4\pi^4}\,\rho^{-1/2}\,e^{-\rho^2/2}$	

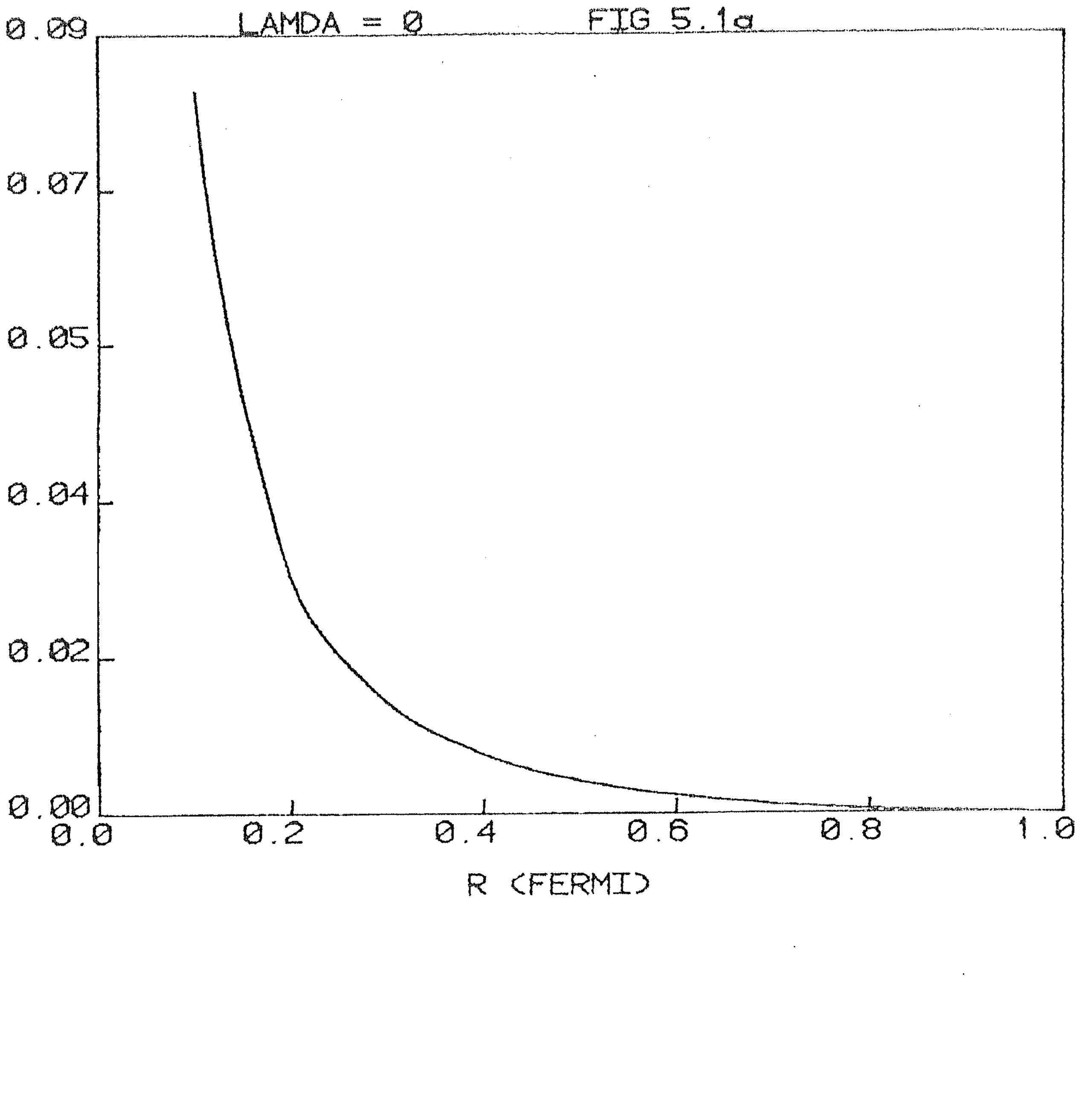
LAMDA = 0
FIG 5.1a
0.09
0.07
0.05
0.04
0.02
0.00
0.0
0.2
0.4
0.6
0.8
1.0
R (FERMI)

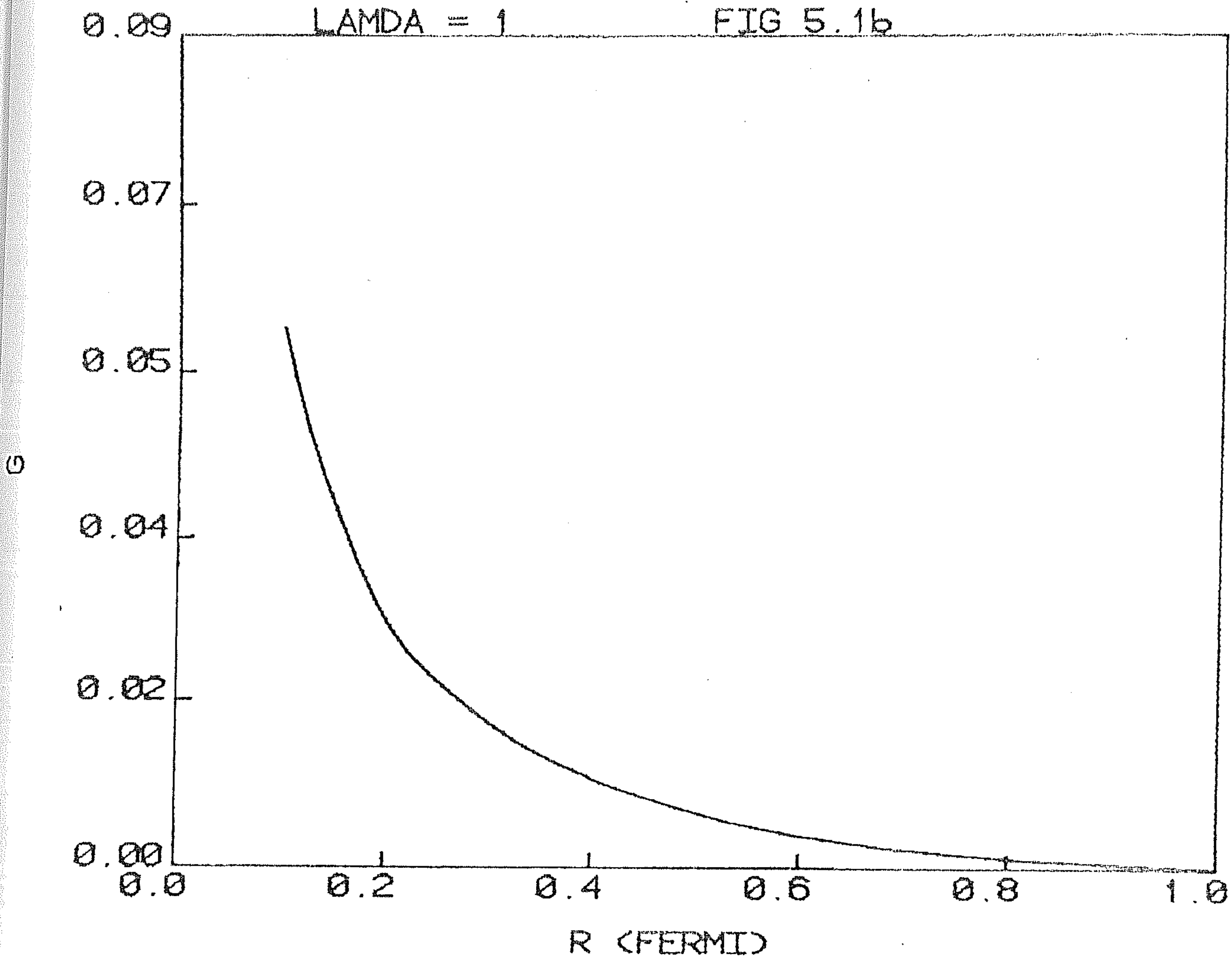
LAMDA = 1
FIG 5.1b
0.09
0.07
0.05
0.04
0.02
0.00
0.0
0.2
0.4
0.6
0.8
1.0
R (FERMI)
G

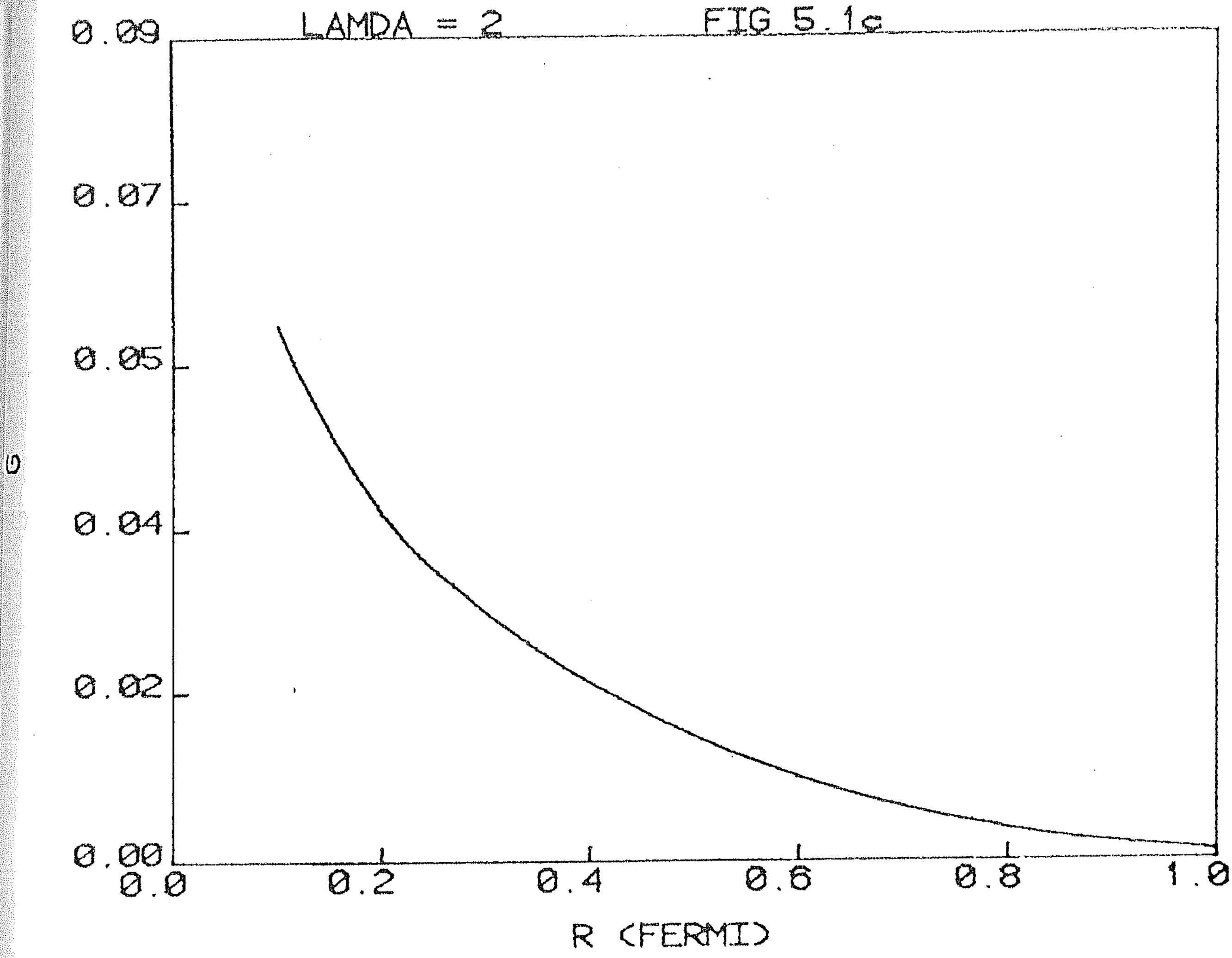
LAMDA = 2
FIG 5.1c
0.09
0.07
0.05
0.04
0.02
0.00
G
0.0
0.2
0.4
0.6
0.8
1.0
R (FERMI)

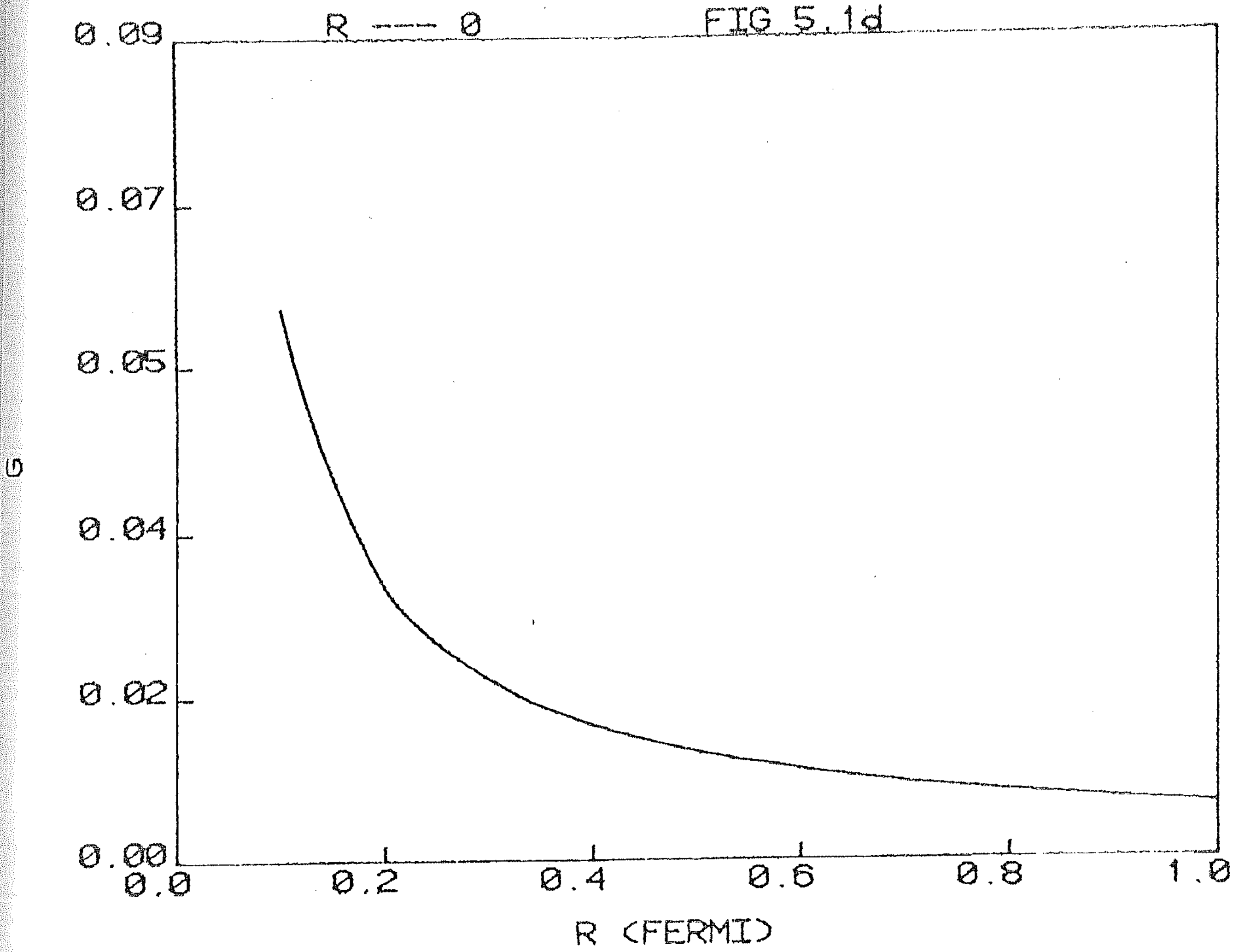

R --- 0
FIG 5.1d
G
0.09
0.07
0.05
0.04
0.02
0.00
0.0
0.2
0.4
0.6
0.8
1.0
R (FERMI)

CHAPTER VI

CONCLUSION

One of the evidences for Quantum Chromo Dynamics (QCD) is the existence of the glueballs [85-90]. The study of glueballs and their experimental confirmation is very crucial to the validity of QCD. In this thesis it has been our aim to study the confinement scheme for glueballs. Two different theoretical models are being studied for the confinement of gluons. They are (1) the current confinement model or CCM, and (2) the dielectric confinement model or DCM. A plausible link from the Yang-Mill's theory to these models is shown heuristically. The difficulty of the sharp boundary in bag-like models [76,78] is eliminated in these two models. The confined solutions of the gluons in CCM or DCM are very similar to the confined solutions of the quarks in RHM [23]. Thus a unified confinement basis for both the quarks and gluons is achieved though the present study.

Any massless vector particle exists only in two transverse physical modes [121]. Here the two physical transverse gluons are obtained in a general frame of Lorentz gauge. The secondary gauge condition which satisfies the two transverse solutions is the Coulomb gauge in DCM while that in CCM it is the oscillator gauge [72,80]. The choice of this oscillator gauge condition is a new feature of the present study which enables one to obtain the transverse gluon modes in the oscillator basis. The lowest confined gluon modes obtained in both the models are characterised by $J^P = 1^+$ (named as 'M'-gluon) and $J^P = 1^-$ (named as 'E'-gluon). The gluon fields are second quantized and the energies of the confined gluons are obtained.

Using these confined gluon modes the colour singlet di-gluon and tri-gluon bound states are constructed. The energies of these glueball states are calculated in both the models. The confinement model parameter is obtained by fitting iota (1440 MeV) 0^{-+} state as a di-gluon glueball state [88]. The results are quite encouraging. The spurious motion of the centre of the multi-gluon state in this study is taken into account exactly. The revised calculations for the low-lying glueball state shows excellent agreement with the existing experimental results. The CCM results are found to be more close to the experimental results than the DCM results. Thus as in the case of RHM (for quarks) [23,72] the success of CCM is also closely linked with the accounting for spurious motion of the centre of mass.

Having obtained the successful confinement scheme for glueballs, we have aimed at harmonizing the confinement schemes of quarks (RHM) and gluons (CCM). For this purpose we have obtained the confined gluon propagator. In CCM, the propagator is that of an oscillator propagator. A translationally invariant ansatz has been used to derive the relevant propagator in a closed analytical form. It is different from the oscillator. Green's function obtained by path integral formalism [114]. Derivation for such a propagator is generalized to m-dimensional case, the relevant propagator is in the Coulombic form when the particles are very close to each other and it falls in a Gaussian manner when the particles are away from each other. This behaviour of the confined gluon propagator is very promising in developing a bound state perturbation theory for quarks and gluons inside the hadrons.

The present study thus has laid a foundation by harmonising the confinement scheme of quarks and gluons to study the various properties of their bound systems like hadrons glueballs, meiktons etc. This study has got various applications. For example, calculation of Fermi-Breit like interactions between the confined quarks due to the exchange of the confined gluons will be an important result which has to be incorporated in the calculations of the nucleon-nucleon interaction using these models. The calculations of the 3-gluon and 4-gluon vertices can be done and may be important in the hyperfine splitting in glueball spectroscopy. It should be noted, however, that a certain amount of double counting may result in such calculations. In view of the excellent agreement with the naive confined models such corrections are expected to become negligible. It is very important to distinguish $q\bar{q}$, $q\bar{q}g$, gg and ggg states among the vast experimental data of the exotic states in the energy range 1-3 GeV for the identification of a true glueball state.

The momentum dependent inhomogeneous dielectric medium obtained in Chapter 3 has to be studied carefully when both the quarks and gluons are presented in such a medium. A perturbative analysis of the fields, its growth and propagation in such a medium is of importance from QCD point of view. Thus a detailed wave mode analysis of quark-gluon plasma [122] in such a medium might lead to the understanding of the QCD dynamics that leads to the deconfinement or phase transition. The effect of nonlinear interactions to the medium and the medium effects on the dynamics of the particles are to be studied to understand the phenomenological confinement models from the fundamental theory.

In the following, we list the various applications of the theory to highlight the future prospects.

1. The derivation of one gluon exchange potential using the confined gluons between the quarks.

2. The harmonious basis for the quarks (RHM) and gluons (CCM) can be exploited to develop the hadron-hadron interactions.

3. The three gluon and four gluon vertices of the confined gluons can be calculated to study the hyperfine splitting of the low-lying di-gluon and tri-gluon glueball states.

4. The spectroscopy of the hybrid i.e. $q\bar{q}g$ (or meiktons) can be studied.

5. The various decay processes of these exotic states (glueballs) to the lighter hadrons, its decay widths and the branching ratios have to be calculated.

6. In the light of current confinement for gluons the nonlinear QCD fields can be studied perturbatively by treating the confinement current in CCM as a part of the nonlinear interaction current averaged over all orders. The remaining portion of this nonlinear current can be treated perturbatively. This may lead one in obtaining the relationship between the model confinement parameter and the strong coupling constant.

REFERENCES

1. Gell-Mann M., Phys. Lett. 8 (1964) 2114.
2. Han M.Y. and Y. Nambu, Phys. Rev. B 139 (1965) 1006.
3. Greenberg O.W., Phys. Rev. Lett. 13 (1964) 598.
4. Donald H. Perkins "Introduction to High Energy Physics", (Addison-Wesley, 1972).
5. George S. La Rue, William M. Fairbank and James douglas Phillips, Phys. Rev. Lett. 42 (1979) 142.
6. Lamb R.C. et. al., Phys. Rev. Lett. 17 (1966) 1068.
7. Nambu Y., Sci. am. 235(5) (1976) 48.
8. Greenberg O.W. and C.A. Nelson, Phys. Rep. 32C (1977), 69.
9. Jaffe R.L., Nature 268 (1977) 201.
10. Kokkedee J.J.J. "The Quark Model" (Benjamin, New York, 1969).
11. Gross D. and Wilczek F., Phys. Rev. Lett. 30 (1973) 1343.

12. Weinberg S., Phys. Rev. Lett. 31 (1973) 494.

13. Politzer H.D., Phys. Rep. 14C (1974) 129.

14. Cheng and Li, "Gauge Theory of Elementary particle Physics" (Oxford University Press, Oxford, 1984).

15. Nambu Y., Phys. Rev. D 10 (1974) 4262.

16. Jaffe R.L. and Johnson K., Phys. lett. 60B (1976) 201.

17. Chodos A. et al., Phys. Rev. D9 (1974) 3471.

18. De Grand T. et al., Phys. Rev D12 (1975) 2060.

19. Johnson K., Acta Physica Polonia B6 (1975) 865.

20. Isgur N. and Carl G., Phys. lett. 72B (1977) 109.

21. Robson D., Nucl. Phys. A. 308 (1978) 308.

22. S. Rai Choudhary and A.N. Mitra, Phys. Rev. D 28 (1983) 2201.

23. Khadkikar S.B. and Gupta S.K., Phys. lett. 124B (1983) 523.

24. Feynman R.P., Phys. Rev. Lett. 23 (1969) 1415.

25. Feynman R.P. and Hibbs A.R., "Quantum Mechanics and Path Integrals", McGrow Hill, New York (1965).

26. Wilczek F., Ann. Rev. Nucl. and Part. Sci. 32 (1982) 177.

27. Muller A.H., Phys. Rep. 73 (1981) 237.

28. Fritzsch H. and Minkowski P., Phys. Rep. 73C (1981) 67.

29. Weyl H. "Space-Time-Matter" (1921) (Trans. by H.L. Brose), Dover, new York (1951).

30. Moryasu K. "An elementary primer for gauge theory", World Sci. Pub. Co., New York (1983).

31. Cheng Ta-Pei and Li, Ling-Fong, "Gauge Theory of Elementary Particle Physics", Oxford (1984) Reprints, 1986, (II).

32. Faddeev L.D. and Slavnov A.A. (1980) "Gauge Fields, Introduction to Quantum Theory", Benjamin Cummings, Massachusetts.

33. Salam A. (1968) (Nobel symp. No.8) (Ed. N. Svartholm) Almquist and Wilsell, Stockholm.

34. Taylors J.C. (1976) "Gauge Theories of Weak Interactions", Cambridge Uni. Press, Cambridge.

35. Abers E. and Lee B.W., Phys. Rep. 9C (1973) 1.

36. t'Hooft, Nucl. Phys. B33 (1971) 173.

37. Itzykson and Zuber (1985) McGraw Hill, Ch. 12.

38. Jackson J.D. (1974) "Classical Electro Dynamics", Wiley, New York.

39. Ramond P. (1981) "Field Theory : A Modern Primer", Benjamin Cummings.

40. Dirac, Can. Jnl. Math. 2 (1950) 129.

41. Yang and Mills, Phys. Rev. 96 (1954) 191.

42. Aitchison and Hey A.J.G. (1982) "Gauge Theories in Particle Physics", Hilger, Bristol.

43. Lee T.D. (1981) "Introduction to Field Theory", Harwood Academic, Ch.12.

44. Ramond and Gribod, Nucl. Phys. B 139 (1978) 1.

45. Feynman R.P., Acta Phys. Polonica 24 (1963) 697.

46. DeWitt B.S. Phys. Rev. 162 (1967) 1195, 1239.

47. Faddeev and Popov, Phys. Lett. B 25 (1967) 29.

48. Mandelstam, Phys. Rep. 23C (1976) 245; Phys. Rev. D 20 (1979) 3223.

49. Friedman J.T. and Kendall H.W., ann. Rev. Nucl. Sci. 22 (1972) 203.

50. Bjorken J.D., Phys. Rev. 163 (1967) 1767.

51. Gross and Wilczek, Phys. Rev. D 8 (1973) 3633.

52. Lee T.D., Phys. Rev. D 19 (1979) 1802.

53. Nielson H.B. and Patkos A., Nucl. Phys. B 195 (1982) 137.

54. George S. La rue, William M. Fairbank and Arthur F. Hebard, Phys. Rev. lett. 38 (1977) 1011.

55. Kinoshita T., Jnl. Math. Phys. 3 (1962) 650.

56. Lee T.D. and Nauenberg M., Phys. Rev. B 133 (1964) 1549.

57. Wilson K.g., Phys. Rev. D 10 (1974) 2445.

58. Parisi G. and Sourlas N., Nucl. Phys. B 206 (1982) 321.

59. Friedberg R. and Lee T.D., Nucl. Phys. B 225 (1983) 1.

60. Pagels H., Phys. Rep. 16 (1975) 219.

61. Phatak S.C. "Chiral Bag Model and Nuclear Physics", Proceedings of Recent Trends in theoretical Nuclear Physics" (1985), Madras, edited by K. Srinivasa Rao (MacMillan, 1987)

62. Jaffe R.L. and Johnson K., Phys. Lett. 60B (1976) 201.

63. Bogolioubov P.N., Ann. Inst. Henri Poincare 8 (1967) 163.

64. Close F.E. (1981) "Introduction to Quarks and Partons", Academic Press.

65. DeGrand and Jaffe R.L., Ann. Phys. 100 (1976) 425.

66. deRujula A., H. Georgi, Glashow S., Phys. Rev. D 12 (1975) 147.

67. Bardeen W.A., Chanowitz M.S., Drell S.D., Weinstein and Yan T.M., Phys. Rev. D 11 (1975) 1094.

68. Thomas A.W. (1982) "Chiral Symmetry and the Bag Model : A New Starting Point for Nuclear Physics", T.H. 3368-CERN-TRI-PP-82-29.

69. Rajat K. Bhaduri (1987) "Quark Bags and Chiral Symmetry", Lecture note at the Workshop on High Enegy Heavy Ion Quarks and Quark Degrees of Freedom in Nuclei, Puri, India.

70. Sakurai (1967) "Advanced Quantum Mechanics", Addison-Wesley, Ch.3.

71. Lipkin H.J., Phys. Rep. 8C (1973) 173.

72. Khadkikar S.B., Pramana 24 (1985) 63.
Khadkikar S.B. "Confinement of Quarks and Gluons", Proc. Recent Trends in Nuclear Physics (1985) Madras, edited by K. Srinivasa Rao (McMillian, 1987)

73. Furui S., Faessler A. and Khadkikar S.B., Nucl. Phys. A. 424 (1984) 495.

74. Wojceich Broniowski, Banerjee M.K. and Thomas D. Cohen, "Bag Formation in the Colour Dielectric Model", ORO 5126-298, University of Maryland pp 87-035 July 1986.

75. Wojceich Bronoiowski, Banerjee M.K. and Thomas D. Cohen (1986) "Absolute Confinement in a Mean Field Model with Glueballs", ORO 5126-273, University of Maryland.

76. Carlson C.E., Hanson T.H.,and Peterson C., Phys. Rev. D. 27 (1983) 1556.

77. Gomm H. and Schechter J., Phys. Lett. B 158 (1985) 449.

78. Kuti J. (1977) Proc. CERN-JINR School of Physics "Quarks Confinement and Quark Model", Sec. 2.

79. Daya Shankar Kulshreshtha, "Glue Balls as the Bound States of Massive Gluons" (1983) Fewbody X, Karlsruhe, Germany, Aug. 21-27 (1983), edited B. Zeitnitz, K. Karlsruhe.

80. Khadkikar S.B. and Vinodkumar P.C., Pramana 29 (1987) 39.

81. Fetter and Walecka (1971) "Quantum theory of Many Particle Systems", McGraw Hill, New York, Sec. 50.

82. Celenza L.S., and Shakin C.M., Phys. Rev. D 34 (1986) 1591.

83. Moshinsky M. (1969) "the Harmonic Oscillator in Modern Physics : From Atoms to Quarks", Gordon and Breach Science Publishers.

84. Fritsch and Minkowski P., Nuovo Cim. 30A (1975) 393.

85. Freund P.G.O. and Nambu Y., Phys. Lett. 34 (1975) 1645.

86. Barnes T., Zeit Phys. C 10 (1981) 275.

87. Carlson C.E., J.J. Coyne, Fishbane P.M., Gross F., and Meshkov S., Phys. Lett. 99B (1981) 353.

88. Sharre D.L. et al., Phys. Lett. 97B 329.

89. Edwards C. et al., Phys. Rev. Lett. 48 (1982) 458; 49 (1982) 259; 51 (1983) 859.

90. Linden Baum S.J. et al., Phys. Lett. 165B (1985) 202.

91. Okubo S., Phys. Lett. 5 (1963) 165.

92. Zweig G., CERN-TH-401,402 (1964).

93. Iizuka J., Prog. Theor. Phys. Suppl. 37-38 (1966) 21.

94. Chanowit and Sharpe S., Nucl. Phys. B 222 (1983) 211.

95. Ishikawa K., Teper M. and Scherholz G., Phys. Lett. 116B (1982) 429.

96. Yang C.N., Phys. Rev. 77 (1950) 242.

97. Lee T.D. (1987) ERICE Lectures Aug. 3-14, edited by Zichichi (1983).

98. Lindenbaum S.J. (1983) ERICE Lectures Aug. 3-14, edited by Zichichi (1983).

99. Aubert J.J. et al., Phys. Rev. Lett. 38 (1974) 1404.

100. Augustin J.E. et al., Phys. Rev. Lett. 37 (1976) 1406.

101. Konigsmann K. (1986) DESY 86-009, January 1986.

102. Usha Mallick (1987) SLAC Pub. 4238, February 1987.

103. Appelquist and Politzer H.D., Phys. Rev. Lett. 34 (1975) 43.

104. Billoire A. et al., Phys. Lett. 80B (1979) 381.

105. Korner J.G. et al., Nucl. Phys. B 229 (1983) 115.

106. Richman J.D. (1985), Ph.D. Thesis, CALT-68-1231 (1985).

107. Edwards C. (1984), Ph.D. Thesis, CALT-68-1165 (1984).

108. Cooper S. (1985), SLAC-PUB-3819 (1985).

109. Fishbane and Meshkov, Comm. Nucl. Part. Sci. 13 (1984) 325.

110. Ishikawa K. et al., Phys. Lett. 120B (1983) 387.

111. Senba K. and Tanimoto M. (1984) Preprint, Ehime Uni., EHU-84-01.

112. Rudolf Peierls (1979) "Surprises in Nuclear Physics", Princeton University Press, section 7.2.

113. Celenza L.S. and Shakin C.M. (1987) Preprint BCC NT87/111/172.

114. Bjorn Felsager (1981) "Geometry, Particles and Fields", Odense University Press, 4th edition (1987) Ch.5.

115. Titchmarsh E.C. (1958) "Eigenfunction Expansions Associated with Second Order Differential Equations", vol.II, Oxford clarendon, Sec.5.13.5.

116. Mathew and Walker (1964) "Math. Methods of Physics", Benjamin, 2nd edition, Chap.9.

117. Magnus w., Oberhettinger F. and Soni R.P. (1966) "Formulae and Theorems for the Special Functions of Mathematical Physics", Heidelberg, New York, Secs. 5.5.2 and 5.6.2.

118. Gradshteyn and Ryzhik (1980) "Table of Integrals, Series and Products", Academic Press, 3.471.

119. Abramowitz (1972) "Hand Book of Mathematical Functions", Dover Publications, New York, 13.1.8, 13.1.33.

120. Feynman R.P., Kislinger M. and Ravndal F., Phys. Rev. D 3 (1971) 2706.

121. Landau and Lifshitseries vol.4 "Quantum Electrodynamics" (1979) Pergman Press.

122. Larry McLerran, Rev. Mod. Phys. 58 (1986) 1021.

123. Rose M.E. (1955) "Multipole Fields", John Wiley, New York.

List of Publications

1. S.B. Khadkikar and P.C. Vinodkumar, "Glueballs in Current Confinement Scheme", Int. Conf. on Nucl. Phys., BARC, Bombay, India (1984), 128.

2. S.B. Khadkikar and P.C. Vinodkumar, "Quantized Gluon Fields in Harmonic Current Confinement", Proc. Int. Nucl. Phys. Conf., Harrogate, U.K. (1986) Vol.1, E22.

3. S.B. Khadkikar and P.C. Vinodkumar, "Confinement Models for Gluons", Pramana Journal of Physics 29 (1987) 39.

4. Vinodkumar P.C. and Khadkikar S.B., "Confined Gluon Propagators in a Translationally Invariant Ansatz" (in preparation)